

Electronic Thesis and Dissertation Repository

9-13-2016 12:00 AM

Investigating mycotoxins and secondary metabolites in Canadian agricultural commodities using high-resolution mass spectrometry

Megan J. Kelman
The University of Western Ontario

Supervisor
Dr. Mark Sumarah
The University of Western Ontario Joint Supervisor
Dr. Ken Yeung
The University of Western Ontario

Graduate Program in Chemistry
A thesis submitted in partial fulfillment of the requirements for the degree in Master of Science
© Megan J. Kelman 2016

Follow this and additional works at: <https://ir.lib.uwo.ca/etd>

 Part of the [Analytical Chemistry Commons](#)

Recommended Citation

Kelman, Megan J., "Investigating mycotoxins and secondary metabolites in Canadian agricultural commodities using high-resolution mass spectrometry" (2016). *Electronic Thesis and Dissertation Repository*. 4144.
<https://ir.lib.uwo.ca/etd/4144>

This Dissertation/Thesis is brought to you for free and open access by Scholarship@Western. It has been accepted for inclusion in Electronic Thesis and Dissertation Repository by an authorized administrator of Scholarship@Western. For more information, please contact wlsadmin@uwo.ca.

Thesis abstract

Mycotoxins are secondary metabolites produced by fungi, which are harmful to humans and/or animals. *Alternaria* is a common fungal plant pathogen that can produce mycotoxins in agricultural commodities, such as processed wheat products, and fruit juices. Liquid chromatography mass spectrometry (LC-MS) is commonly used for the detection, characterization and quantitation of mycotoxins in agricultural products. Canadian *Alternaria* species were assessed to provide a risk assessment of their secondary metabolites in agricultural products by describing their global metabolome data obtained from the Orbitrap LC-MS instrument. Combination of this high mass accuracy data with post data-acquisition analysis techniques resulted in the discovery of new conjugated mycotoxins and secondary metabolites produced by Canadian species of *Alternaria*.

Data independent acquisition-digital archiving (DIA-DA) was applied as a non-targeted approach for metabolomic profiling of naturally-contaminated silage. DIA-DA allowed for high quality retrospective sample analysis of high resolution LC-MS data with high analyte selectivity.

Keywords: emerging mycotoxins, Orbitrap, high resolution mass spectrometry, *Alternaria*, metabolomics

Co-authorship Statement

Chapter 2- Non-targeted Metabolomics of *Alternaria* spp. in Canada

All generations and subsequent analyses of PCA plots, K-means clustering and generation of p values with metabolite data was generated by the author. Amy McMillan (PhD candidate, Microbiology and Immunology) and Dr. Greg Gloor (Department of Biochemistry) provided technical assistance, and provided script generation for R using xcms, MetabolAnalyze, and FactoMineR. Cultures were provided by Dr. Keith Seifert from the Canadian Collection of Fungal Cultures, (Ottawa, Ontario).

Chapter 3- Semi-targeted detection of new mycotoxins and secondary metabolites in Canadian agricultural commodities

Identification of six new Alternaria sulfoconjugated metabolites by high resolution neutral loss filtering

All experiments and data analyses were conducted by the author. Dr. Justin Renaud (Agriculture Canada, London) assisted with method development, training and technical assistance for the mass spectrometer. Dr. Keith Seifert, Jonathan Mack (Agriculture and Agri-Food Canada, Ottawa) and Dr. Kumaran Sivagnanam (Canadian Grain Commission) provided mycology assistance and *Alternaria* strains.

Semi-targeted detection of total AAL-toxins and enniatins using product ion filtering

Dr. Justin Renaud (Agriculture Canada, London) developed the method and experimental protocol for product ion filtering of new fumonisins, and the method was subsequently applied to AAL-toxins and enniatins. Experiments and data analyses of AAL-toxins and enniatins were conducted by the author.

Chapter 4- Combining data independent acquisition-digital archiving (DIA-DA) with next-generation sequencing for profiling of fungal contaminated silage

All fungal isolation, DNA sequencing, next-generation sequencing (NGS) and metabolomic analyses was conducted by the author. The DIA-DA method is applied from previous work using contaminated maize, which was developed and conducted by Dr. Justin Renaud and Dr. Mark Sumarah (Agriculture Canada, London). Nimalka Weerasuriya (M.Sc candidate, Department of Biology) provided training and NGS primers. Amy McMillan (PhD candidate, Microbiology and Immunology) and Dr. Greg Gloor (Department of Biochemistry) provided assistance with NGS

data generation and analysis. Samples were provided by Dr. Danica Baines, (Agriculture Canada, Lethbridge).

Acknowledgements

During the past five years in Dr. Sumarah's lab (my last two years as a M.Sc. student) at Agriculture Canada, I've had the pleasure of learning from several incredibly talented and knowledgeable technicians: Aga Pajak, Lyne Sabourin, Betty Singh and Tim McDowell. In addition, I have been very lucky to have met Dr. Kevin Burgess during his post-doctoral research, whose enthusiasm for NMR and organic chemistry was infectious, but thankfully was not contagious. Dr. Justin Renaud was my mentor during my graduate studies, predominantly in the field of mass spectrometry. Dr. Renaud's passion for mass spectrometry and chemistry truly inspires me to be a better scientist. I never would have accomplished what I did without his valuable knowledge and expertise.

I was fortunate to have worked alongside Tianyu Qi, who was incredibly supportive and understanding as we both worked towards our M.Sc. degrees together. I was privileged to work alongside Janet Schapurga, who is one of the best lab mates you could have. Whether it was helping to set up an experiment, offering to pour media, or helping to keep my scatterbrain grounded, Janet was an asset. I'd also like to thank Dr. Ken Yeung, who I was very lucky to have as a co-supervisor. Dr. Yeung always provided meticulous appraisals for developing new research objectives, and encouraged critical out-of-the-box thinking to address problems. Having two supervisors ensured that research objectives were always polished prior to peer review. I also need to thank members from Dr. Yeung's research laboratory at Western University: Shirley Fan, Jasmine Wang, Chao Chao Chen, and Kristina Jurcic.

As my research was incredibly multi-disciplinary, I was fortunate enough to be connected to extremely knowledgeable and world renowned scientists in several fields. This included several mycologists, including Dr. Jim Traquair, who first introduced me to the field of mycology, and Dr. Keith Seifert at Agriculture Canada in Ottawa, Ontario. I'd also like to express my gratitude to Professor Miller at Carleton University for providing unparalleled expertise in mycotoxins and

fungal secondary metabolites. Thank you to Nimalka Weerasuriya and Dr. Greg Thorn's research laboratory at the University of Western Ontario for their help in generating NGS data. I'd like to thank Amy McMillan for her immense patience, and her tireless efforts in helping with the interpretation of the NGS data and teaching me how to use R. In addition, thank you to Dr. Greg Gloor and his laboratory for facilitating the NGS data interpretation, and other bioinformatics expertise.

Thank you to my committee members and examiners: Dr. Martin Stillman, Dr. Lars Konermann and Dr. Greg Thorn, and the committee chair, Dr. Charles Xu.

But perhaps most of all, I need to thank Dr. Mark Sumarah. When I was initially hired five years ago, I never had any intentions of pursuing a career in chemistry. However, I soon became enthusiastic about working with natural products research, and combining it with the field of mycology. After starting my chemistry degree at Western, Dr. Sumarah became keen on convincing me to pursue a graduate degree. Though I was initially hesitant, his daily persistence eventually convinced me to apply for graduate school. Dr. Sumarah was a wonderful supervisor, who was supportive in every aspect of my degree, and open-minded towards new research objectives. He believed in my potential, even though I did not.

I need to thank my overly patient and long-suffering friends and family who I neglected in the name of science. It made me realize the immense guilt stemming from the research profession; the guilt of not writing papers, coupled with the guilt of not ever spending time with your friends and family. The process reminded me of what was truly important in life, and thus, I dedicate this work to you.

Table of Contents

Thesis abstract.....	i
Co-authorship Statement.....	ii
Acknowledgements.....	iii
Table of Contents.....	v
List of Tables.....	ix
List of Figures.....	x
List of Symbols and Abbreviations.....	xiii
List of Appendices.....	xiv
Chapter 1- Introduction.....	1
1.1 Mycotoxins in Agricultural Commodities.....	2
1.1.1 Fungi.....	2
1.1.2 Mycotoxins and secondary metabolites.....	3
1.1.3 <i>Alternaria</i>	5
1.1.4 Silage co-contamination.....	6
1.2 High resolution mass spectrometry-based metabolomics.....	7
1.2.1 Molecular qualification.....	9
1.2.2 Statistical analysis.....	10
1.3 Analytical techniques.....	12
1.3.1 High-performance liquid chromatography (HPLC).....	12
1.3.2 Mass spectrometry.....	15
1.3.2.1 <i>Heated Electrospray Ionization (HESI) Ion source</i>	15
1.3.2.2 <i>Quadrupole mass filter</i>	16
1.3.2.3 <i>The C-trap</i>	17
1.3.2.4 <i>Higher-energy collisional dissociation (HCD) cell</i>	17
1.3.2.5 <i>Orbitrap mass analyzer</i>	18
1.3 Molecular analyses.....	19
1.3.1 Deoxyribonucleic acid (DNA) sequencing.....	19
1.3.2 Next-generation sequencing (NGS).....	19
1.4 Thesis objectives.....	21

Chapter 2- Non-targeted Metabolomics of <i>Alternaria</i> spp. in Canada.....	22
2.1 Chapter 2 objectives	22
2.2 Introduction	22
2.3 Experimental	24
2.3.1 Fungal material and identification	24
2.3.2 Plug extraction	24
2.3.3 LC-HRMS Analysis	24
2.3.4 Global metabolomic analyses	25
2.3.4.1 Principal component analysis (PCA) and K means clustering	25
2.3.4.2 Metabolomic analysis	26
2.4 Results and Discussion.....	26
2.4.1 Global metabolomic chemotyping of Canadian species of <i>Alternaria</i> using PCA and K means clustering	26
2.4.2 Metabolomic analyses and chemotaxonomy	34
2.4.2.1 Group 1 differentiation	36
2.4.2.2 Group 2 differentiation	40
2.4.2.3 Group 1 subgroups.....	43
2.4.2.4 Group 2 subgroups.....	49
2.5 Conclusions and future work.....	54
Chapter 3- Semi-targeted detection of new mycotoxins and secondary metabolites in Canadian agricultural commodities	55
3.1 Chapter 3 objectives	56
Identification of six new <i>Alternaria</i> sulfoconjugated metabolites by high-resolution neutral loss filtering.....	56
3.2- Introduction.....	56
3.2.1 Fungal material and identification	58
3.2.2 Plug extraction and fermentation in liquid media, on Cheerios and rice	58
3.2.3 LC-HRMS and MS ² analysis.....	59
3.3 Results and Discussion.....	60
3.4 Conclusions and Future Work.....	66
Semi-targeted detection of total AAL-toxins and enniatins using product ion filtering.....	67
3.5 Introduction	67

3.5.1 <i>Alternaria arborescens</i> and AAL-toxins	67
3.5.2 <i>Fusarium</i> and enniatins	68
3.6 Experimental	71
3.6.1 Fungal material	71
3.6.2 <i>Alternaria arborescens</i> fermentation in tomatoes and extraction	71
3.6.3 General conditions, ddMS ² and rapid polarity switching- AAL-toxins from <i>Alternaria arborescens</i>	71
3.6.4 <i>Fusarium</i> spp. fermentation and extraction in liquid media and corn.....	72
3.6.5 Extraction of naturally-contaminated flour for enniatin analysis	73
3.6.6 HRMS and MS ² analysis of total enniatins	73
3.7 Results and Discussion.....	74
3.7.1 Total AAL toxins in artificially inoculated tomatoes	74
3.7.2 Method validation for total enniatin analysis in artificially inoculated liquid media and corn	77
3.7.3 Product ion filtering for the detection of total enniatins in naturally-contaminated flour	80
3.8 Conclusions and Future Work.....	82
Chapter 4- Combining data independent acquisition-digital archiving mass spectrometry (DIA-DA) with next-generation sequencing to profile fungal contaminated silage	83
4.1 Chapter 4 objectives	83
4.2 Introduction	83
4.3- Experimental	86
4.3.1 Silage material	86
4.3.2.1 PCR Conditions	87
4.3.2.2 Sequencing analysis.....	87
4.3.3 Next-generation sequencing of total silage DNA.....	88
4.3.4 Plug extraction of isolated fungal cultures	89
4.3.5 Metabolite extraction of silage	89
4.3.6 LC-HRMS, ddMS ² analysis for isolated cultures.....	90
4.3.7 LC-HRMS DIA analysis for isolated cultures and contaminated silage	90
4.4 Results and Discussion.....	92
4.4.1 Isolated fungal cultures.....	92

4.4.2 Secondary metabolites from isolated cultures	93
4.4.3 Secondary metabolites from contaminated silage and retrospective analysis	94
4.4.4 Next-generation sequencing of fungi for the community profiling of contaminated silage	97
4.4.5 Next-generation sequencing of bacteria for the community profiling of contaminated silage	100
4.5 Conclusions and Future Work.....	101
Chapter 5- Conclusions.....	103
5.1 Conclusions	103
References.....	105
Appendix A1- Chapter 2 Supplementary.....	118
Appendix A2- Chapter 3 Supplementary.....	123
Appendix A3- Chapter 4 Supplementary.....	128
Megan Kelman Curriculum Vitae.....	137

List of Tables

Table 1-Peak list generation conditions using xcms in R.[40–42]	25
Table 2- Group 1 metabolites generated by the Wilcoxon test with FDR correction from data generated in negative ionization mode	36
Table 3- Group 1 metabolites generated by the Wilcoxon test with FDR correction from data generated in positive ionization mode	39
Table 4- Significant metabolites ($p < 0.01$) in group 2 from metabolomics data generated in negative ionization mode	40
Table 5- Significant metabolites ($p < 0.01$) in group 2 generated by the Wilcoxon test with FDR correction from metabolomics data generated in positive ionization mode	41
Table 6- Subgroup 1A metabolites generated by the Wilcoxon test with FDR correction in negative ionization mode	44
Table 7- Significant metabolites in subgroup 1B as determined by the Wilcoxon test with FDR correction in negative ionization mode.....	48
Table 8- Showing subgroup 2B metabolites generated by the Wilcoxon test with FDR correction	50
Table 9- Showing subgroup 2A metabolites from group 2 generated by the Wilcoxon test using FDR correction.....	52
Table 10- Summary of significant metabolites detected in negative ionization mode, and evaluated by the Wilcox test for significance	53
Table 11- Accurate mass precursors of the conjugated <i>Alternaria</i> spp. metabolites, found by NLF of SO ₃ observed in ddMS ² spectra generated in negative mode	65
Table 12- Total AAL toxins and molecules detected by the TCE product anion in tomato artificially inoculated with <i>A. arborescens</i>	75
Table 13- Total enniatins detected in artificially inoculated liquid enniatin media and maize using product ion filtering in positive ionization mode	77
Table 14- Optimized LC-DIA conditions for 3 separate LC runs	91
Table 15- Fungal species isolated from contaminated silage. *Indicates that the fungus has been previously isolated from silage (Alonso, V.A et al., 2013). Bolded species were commonly isolated from the contaminated sites.....	93
Table 16- Mycotoxins and secondary metabolites detected in the plug isolates and extracted silage	95

List of Figures

Figure 1- A typical growth phase curve for fungal fermentations using a finite amount of nutrients	3
Figure 2A) A cherry tomato which has been artificially contaminated by <i>Alternaria</i> sp. B) Concatenated conidia of <i>Alternaria</i> as shown under the microscope.....	5
Figure 3- Grass and corn silage that has been naturally contaminated by fungi.....	7
Figure 4- Measuring resolution at full-width half maximum (FWHM)	10
Figure 5A- Agilent 1290 HPLC. B) Agilent 1290 coupled to the Thermo Q-Exactive mass spectrometer	12
Figure 6- C18 column connected to the ESI source of the mass spectrometer	13
Figure 7- Showing the typical output from the HPLC, as detected by the mass spectrometer as a TIC, or a base peak chromatogram.....	14
Figure 8- Next-generation sequencing for the profiling of fungal DNA from extracted genomic DNA....	20
Figure 9- Designed barcoded primers with adapter regions (left), and bridge amplification procedure (right) for target DNA amplification [81]	21
Figure 10- A) PCA (scoreplot) of 150 strains of <i>Alternaria</i> , showing HRMS data in negative ionization mode B) Associated loadings plot from PCA, showing numbered metabolites	28
Figure 11- PCA (scoreplot) of 150 strains of <i>Alternaria</i> , showing HRMS data in positive ionization mode, coloured by Group 1 (black) and Group 2 (red) from Figure 5A	29
Figure 12- K means clustering of 150 strains of <i>Alternaria</i> using full MS data generated in positive ionization mode. PCA, where groups are coloured by unique clusters calculated using the K means clustering algorithm of centroided data points.....	30
Figure 13- K means clustering of 150 strains of <i>Alternaria</i> using full MS data generated in negative ionization mode. PCA, where groups are coloured by unique clusters calculated using the K means algorithm of centroided data points	30
Figure 14- PCA of 148 <i>Alternaria</i> strains (excluding type strains) of full MS data acquired in negative ionization mode. Samples are coloured by the substrate from which the fungus was originally isolated ..	31
Figure 15- PCA plots of metabolomics data generated in negative ionization mode (A) and positive ionization mode (B) for 20 randomly selected samples. Samples are coloured by their previous K-means clustering assignment (Figures 13 and 14)	33
Figure 16- Volcano plots generated from the Wilcoxon test with corrected p-values between groups 1 and 2 for data generated in negative ionization mode. A) Fold changes in metabolite peak area with respect to their p-value significance. B) Fold changes in metabolite peak area with respect to their actual peak area	35
Figure 17- PCA plot from metabolomics data generated in negative ionization mode coloured by logged peak areas of TeA. Samples in red show larger peak areas detected	37
Figure 18- PCAs of metabolomics data generated in negative ionization mode, coloured by significant metabolites detected in group 1. Samples coloured darker red had larger peak areas	38
Figure 19- PCA plot from data generated in negative ionization mode coloured by infectopyrone peak area. The darker red areas indicate larger peak areas detected in the samples	42
Figure 20- PCA plot from data generated in negative ionization mode coloured by 219 peak area. The darker red areas indicate larger peak areas detected in the samples	42

Figure 21- PCA of metabolomics data within group 1 generated in negative ionization mode. Samples are coloured by their K means clustering assignment.....	43
Figure 22- PCA of metabolomics data generated in negative ionization mode. Samples are coloured by the peak area of altenuisol. Darker red areas indicate larger peak areas detected	45
Figure 23- Extracted ion chromatogram for C ₁₅ H ₁₂ O ₆ , which was significant in subgroup 1A	46
Figure 24- ddMS ² spectra for the isobaric compounds dehydroaltenuisin (top) and 3-hydroxyalternariol 5-O-methyl ether (bottom)	47
Figure 25- PCA of metabolomics of group 1 data generated in negative ionization mode, coloured by peak area intensity of dehydroaltenuisin.....	47
Figure 26- PCA showing separation within group 2 in negative ionization mode. Samples are coloured by the K means clustering algorithm	49
Figure 27- PCA of group 2 coloured by host substrate.....	51
Figure 28- PCA of group 2 metabolomics data generated in negative ionization mode. Samples are coloured by the peak area of altenuisol. Darker red areas indicate larger peak areas detected	52
Figure 29- 'In source' generated fragment ions for pseudo MS ³ of sulfoconjugated metabolites[64]	60
Figure 30- Constructed neutral loss plot of an <i>Alternaria</i> sp. extract, showing the precursor metabolite m/z and the observed neutral mass loss (Da). The neutral mass loss of SO ₃ (79.957 Da) is highlighted with a dashed line, with each 'x' corresponding to a sulfoconjugated parent metabolite along the x-axis.	61
Figure 31- A) MS spectra including isotope pattern at high resolution showing the fully resolved 34S peak as evidence for sulfoconjugation of the known metabolite AME and the new metabolite ALU-SO ₃ . B) MS ² spectra for each metabolite confirming the neutral loss of SO ₃ C) MS ³ spectra for the sulfoconjugated version of each metabolite showing the fragment ions of the in source generated 'free' metabolite. D) MS ² spectra for 'free' versions of both metabolites showing the same fragmentation patterns as the MS ³ of the sulfoconjugated metabolites.....	62
Figure 32- Production of the four predominant free and sulfoconjugated metabolites (AOH, AME, ALU and DHA) by the 148 Canadian <i>Alternaria</i> sp. isolates from the plug screening method.....	64
Figure 33- Chemical structures of the known free <i>Alternaria</i> metabolites: Alternariol (AOH), Alternariol monomethyl ether (AME), Altenuene (ALT), Dehydroaltenuisin (DHA), Altenuisin (ALU), Desmethylaltenuisin (DMA), Altersetin (ALS) and Maculosin (MAC).....	65
Figure 34- Commonly detected AAL toxins of current agricultural importance, with highlighted TCE functional group	67
Figure 35- Cyclohexadepsispeptide skeleton, and commonly detected enniatins in agricultural products	69
Figure 36- MS ² spectrum of enniatin B in positive ionization mode, showing the common 196.13321 product ion	70
Figure 37- <i>Fusarium</i> isolates inoculated into liquid enniatin media (left) and maize (right).....	73
Figure 38- Product ion filter plot in negative ionization mode from artificially-infected tomatoes. The plot shows all MS ² spectra which contain the TCE fragment, and the retention time that they were detected .	75
Figure 39- Characterization of AAL toxins by MS ² spectra of acetyl-TA and the new acetyl-TA ketone AAL toxins in positive ionization mode [158]	76
Figure 40- Product ion filter plots showing MS ² spectra containing the 196 and 210 fragments. A) Extract from <i>F. avenaceum</i> inoculated into liquid artificial enniatin media B) Extract from <i>F. avenaceum</i> inoculated into maize	77

Figure 41- MS² spectra of the unknown enniatin (top) and enniatin B (bottom) in positive ionization mode 79

Figure 42- Product ion filter plots in positive ionization mode showing MS² spectra containing the 196 product ion. Extracts were obtained from commercial flour samples..... 81

Figure 43- Barplot of Ascomycetes by proportion in contaminated silage, showing the most abundant 26 fungal species. The commonly detected species between sites are listed in highest abundance to lowest abundance from bottom to top 99

Figure 44- Barplot of bacteria by proportion in contaminated silage, showing the most abundant 27 bacterial species. The commonly detected species between sites are listed in highest abundance to lowest abundance from bottom to top 101

List of Symbols and Abbreviations

AAFC	<i>Agriculture and Agri-Food Canada</i>	MAC	<i>Maculosin</i>
AAL	<i>Alternaria alternata f.sp. lycopersici</i>	MAFFT	<i>Multiple Alignment Fast Fourier</i>
AC	<i>Alternating current</i>	MS ²	<i>Tandem Mass Spectrometry</i>
ACN	<i>Acetonitrile</i>	m/z	<i>Mass-to-charge ratio</i>
ALS	<i>Altersetin</i>	NLF	<i>Neutral loss filtering</i>
ALT	<i>Altenuene</i>	NGS	<i>Next-Generation Sequencing</i>
ALU	<i>Altenuisin</i>	OTU	<i>Operational taxonomic unit</i>
AME	<i>Alternariol Monomethyl Ether</i>	PC	<i>Principal Component</i>
AOH	<i>Alternariol</i>	PCA	<i>Principal Component Analysis</i>
BLAST	<i>Basic Local Alignment Search Tool</i>	PCR	<i>Polymerase Chain Reaction</i>
CFIA	<i>Canadian Food Inspection Agency</i>	PDA	<i>Potato Dextrose Agar</i>
CID	<i>Collision-induced Dissociation</i>	PIF	<i>Product ion filtering</i>
CYA	<i>Czapek Yeast Autolysate</i>	RF	<i>Radiofrequency</i>
DC	<i>Direct current</i>	RT	<i>Retention time</i>
DHA	<i>Dehydroaltenuisin</i>	sp.	<i>Species (singular)</i>
DIA-DA	<i>Data independent acquisition-digital</i>	spp.	<i>Species (plural)</i>
DNA	<i>Deoxyribonucleic acid</i>	TCE	<i>Tricarballic Ester</i>
DMA	<i>Desmethylaltenuisin</i>	TeA	<i>Tenuazonic acid</i>
EFSA	<i>European Food Safety Authority</i>	TEN	<i>Tentoxin</i>
EtOAc	<i>Ethyl acetate</i>	TIC	<i>Total Ion Current</i>
EtOH	<i>Ethanol</i>		
FAO	<i>Food and Agriculture Organization (of</i>		
FHB	<i>Fusarium Head Blight</i>		
FWHM	<i>Full width half maximum</i>		
H ₂ O	<i>Water</i>		
HAc	<i>Acetic acid</i>		
HCD	<i>Higher Collision Energy Dissociation</i>		
HESI	<i>Heated Electrospray Ionization</i>		
HPLC	<i>High Performance Liquid</i>		
HRMS	<i>High-Resolution Mass Spectrometry</i>		
IT	<i>Injection Time</i>		
ITS	<i>Internal transcribed spacer</i>		
kV	<i>Kilovolts (10³ volts)</i>		
LC	<i>Liquid Chromatography</i>		
LoRDC	<i>London Ontario Research and</i>		

List of Appendices

Appendix A1- Chapter 2 Supplementary.....	118
Appendix A2- Chapter 3 Supplementary.....	123
Appendix A3- Chapter 4 Supplementary.....	128

Chapter 1- Introduction

Fungi grow ubiquitously worldwide in many different environments and substrates. There are millions of different fungal species, with a number of them capable of infecting agricultural crops and commodities.^[1] In the early 1990's, it was estimated that plant pathogens caused annual losses to the Canadian economy of approximately \$172 million; roughly 15.5% of the country's total agricultural production at the time.^[2] In 2015, Agri-Food exports equated to \$55 billion, or approximately 10% of the total merchandise exports.^[3] Worldwide, approximately \$1 billion is spent annually on fungicides to control fungal pathogens.^[4]

Crop losses caused by fungi, and their effects on production yields not only result in an associated loss of income for the farmers, but they also have consequences for the consumer; higher production costs result in higher retail prices, global food shortages, and malnutrition. There are over 7 billion people in the world, with 36 million people living in Canada^[5] and it has been projected that the world needs to double its current agricultural production in order to feed the estimated rise in population by 2050.^[6]

Fungal pathogens not only result in a decrease in crop yield and quality, but may also produce harmful secondary metabolites in food and animal feed. The FAO estimates that 25% of the worldwide crop production is contaminated by mycotoxins, while the United Nations has stated that more than 30% of the world's mortality rate is caused by consumption of food which has been contaminated by harmful microorganisms or parasites.^[6,7] Mycotoxin exposure in Canada is limited when compared to developing countries, primarily through implementing proper crop management and storage.^[8] However, even in developed countries, exposure to particular classes of mycotoxins, such as trichothecenes, fumonisins and ergot alkaloids, still occurs.

Secondary metabolite analyses are predominantly performed by liquid chromatography mass spectrometry (LC-MS) due to the robustness of the instrument in complex biological matrices. There are numerous challenges to detection of mycotoxins, especially for new, emerging and conjugated mycotoxins, and the continued monitoring of those toxins in food and feed. By combining statistical analysis methods with high resolution mass spectrometry (HRMS), we can describe the global metabolomics of pathogenic and potentially mycotoxigenic fungal species in

Canadian agricultural commodities and provide a risk assessment. In addition, through the development of semi-targeted LC-MS experiments, we can describe new but structurally related mycotoxins and secondary metabolites of potential toxicological concern.

1.1 Mycotoxins in Agricultural Commodities

1.1.1 Fungi

Fungi are eukaryotic organisms that belong to their own kingdom, (Kingdom Fungi), which includes yeasts, molds and mushrooms. There are approximately 70,000 identified fungal species on Earth, though it has been estimated that there may be between 1.5 - 8 million species, which suggests many fungi have not yet been discovered or described.^[1] Fungi are globally distributed, and can thrive on a diverse variety of substrates in many different environments, including extreme temperatures, acidic or anaerobic conditions.

Fungi are heterotrophic organisms, and obtain their metabolizable energy by extracellularly digesting decomposing organic matter.^[9] Due to the diversity of the digestive enzymes produced, fungi are often used industrially as food additives to promote digestion, and to culture fine cheeses, such as Roquefort and Camembert. The saprobic capabilities of fungi, combined with their ability to digest a wide variety of substrates, makes them ideal plant pathogens. Plant pathogens consist of infectious organisms that colonize and cause disease within plants.

While preharvest pathogens affect the plant as it is growing, there are also a number of postharvest fungal pathogens responsible for crop spoilage. Postharvest fungal pathogens occur during the transportation of harvested agricultural crops, or during their storage.^[10] The contaminant fungi are often present at the time of harvest, but remain dormant; most contaminated crops initially go unnoticed at the time of harvest. The fungi then accelerate their growth during ripening, or by the introduction of wounds caused accidentally during harvesting or by insect pests.^[10]

In addition to crop loss caused by persistent fungal plant pathogens, many plant pathogens also produce secondary metabolites, known as phytotoxins, to invade the immune system of the plant.

1.1.2 Mycotoxins and secondary metabolites

Fungi produce a variety of natural products through secondary metabolism, and are subsequently characterized as fungal secondary metabolites.^[11] Unlike primary metabolites, secondary metabolites are not directly involved in the growth, development or reproduction of the organism, and are produced in the stationary growth phase of fungal fermentation, (Figure 1).^[9,12] Primary metabolism occurs during the exponential growth phase, while secondary metabolism is predominant during the stationary growth phase. Secondary metabolites are produced through intermediates or precursor metabolites formed during primary metabolism, such as acetate or amino acids.^[9] There are different structural classes of fungal secondary metabolites which are classified based on the precursor primary metabolite used during secondary metabolism; some of these secondary metabolites may be antimicrobial (bacteria and other fungi), toxic towards plants (phytotoxins), or humans and animals (mycotoxins). The production of mycotoxins is largely dependent on the fungal species, and may differ by isolate, the surrounding microbial community, abiotic conditions, and the source of carbon and nitrogen, though favourable fungal growth is not essential for mycotoxin production.^[13-17]

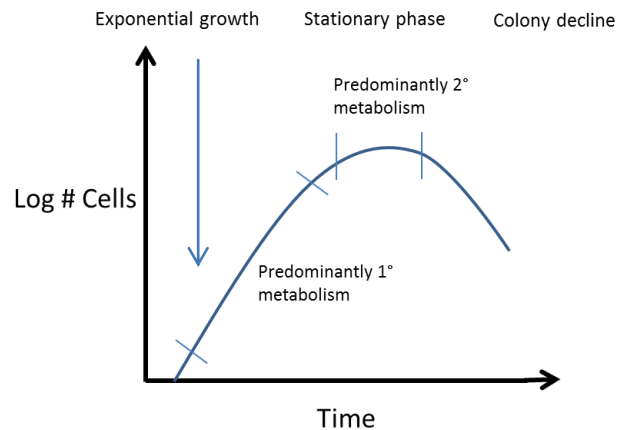


Figure 1- A typical growth phase curve for fungal fermentations using a finite amount of nutrients

Some secondary metabolites may also be referred to as virulence factors, as their production contributes to the pathogenicity and rate of colonization of the host organism.^[18] Many fungal plant pathogens produce virulence factors as a means of invading the immune system of the plant. Many phytotoxins produced are non-host specific, and can cause disease in many different

hosts independent of whether or not they are a common host of the plant pathogen.^[19] Tentoxin for example, is a non-host specific phytotoxin produced by species of *Alternaria*, which has been shown to inhibit chloroplast synthesis in pea shoots.^[20] There are numerous studies on saprobic fungal plant pathogens that produce host-specific toxins (HSTs), which are virulence factors capable of enhancing toxicity only in the specific plant host species.^[21] AAL-toxin is a HST produced by the pathogenic fungus *Alternaria alternata*, and is specific only to certain tomato cultivars (*Lycopersicon esculentum*).^[22] Non-susceptible or resistant tomato cultivars are 1000-fold less sensitive than susceptible cultivars to AAL-toxin.^[22] Some phytotoxins, such as AAL-toxin, are also mycotoxins as they cause harm within humans and animals. AAL-toxin contains a tricarballic ester moiety which interferes with sphingolipid metabolism in plants, but also similarly interferes with membrane function in humans and animals.^[23] As mycotoxigenic fungi contaminate agricultural crops, their mycotoxins accumulate in the feedstock. There are numerous mycotoxin-producing fungi that may be introduced during preharvest or postharvest conditions, so it is possible for agricultural products to have co-contamination from several fungi. Currently, human and animal exposure to mycotoxins and secondary metabolites is limited due to their monitoring in food, which adheres to strict government regulations from reported toxicological data. Canada has strict regulations for toxicologically relevant concentrations of mycotoxins, such as deoxynivalenol (DON), patulin and ochratoxin A (OTA), in agricultural crops.^[24] The European Union, under the European Food Safety Authority (EFSA), has suggested guidelines for many emerging mycotoxins and secondary metabolites for which toxicological data does not yet exist; recommendations are primarily based on the Threshold of Toxic Concern (TTC) value using simulated structure activity relationships.

Known mycotoxins are also produced in conjugated forms by the fungus, in which the known mycotoxin is bound to another molecule such as sulfate, or acetyl groups.^[25] Similar to conjugation, it has been demonstrated that plants can create masked mycotoxins as a detoxification mechanism, where the plant links a polar molecule (such as a glucoside molecule) to the mycotoxin to increase its rate of excretion.^[25] Known conjugated and masked mycotoxins are commonly detected in foodstuffs, however unknown conjugated and masked toxins may be missed by traditional screening methods due to a shift in retention time and an altered molecular formula.^[25,26] This creates challenges for their detection and discovery in agricultural products, which is especially important as the mycotoxins may retain their biological activity and toxicity

as the conjugated or masked groups are enzymatically cleaved off during digestion. Many regulatory agencies are factoring in concentrations of both the conjugated and parent mycotoxins to account for the potential total toxicity.

Newly described mycotoxins that have not been widely studied or regulated are termed ‘emerging mycotoxins.’ As such, routine screening for mycotoxins in agricultural commodities often overlooks emerging mycotoxins due to a lack of toxicological information and need for monitoring.^[27] The impact of climate change may also affect the relative geographic distributions of mycotoxigenic fungi, which may alter the mycotoxins and secondary metabolites subsequently detected in agricultural commodities.^[28] Thus, unexpected mycotoxins typically associated with warmer climates, which are unlikely to be screened for, may be present in Canadian crops.

1.1.3 *Alternaria*

Alternaria is a ubiquitous fungal genus that can grow in a wide variety of substrates and environments. The genus consists of both pathogenic and saprobic species, and the 300 described species are currently divided into 26 sections based on molecular sequencing.^[29–31] Some species are major preharvest plant pathogens of a number of agriculturally-relevant crops, including wheat and other grains, canola, tomatoes (Figure 2A), apples, and citrus fruits.^[31–34] Pathogenic species are capable of overwintering on dried infected crop material and within surrounding weeds, which perpetuates the disease cycle.^[33] Management of *Alternaria* consists of a combination of fungicide applications with crop rotation and tillage practices.

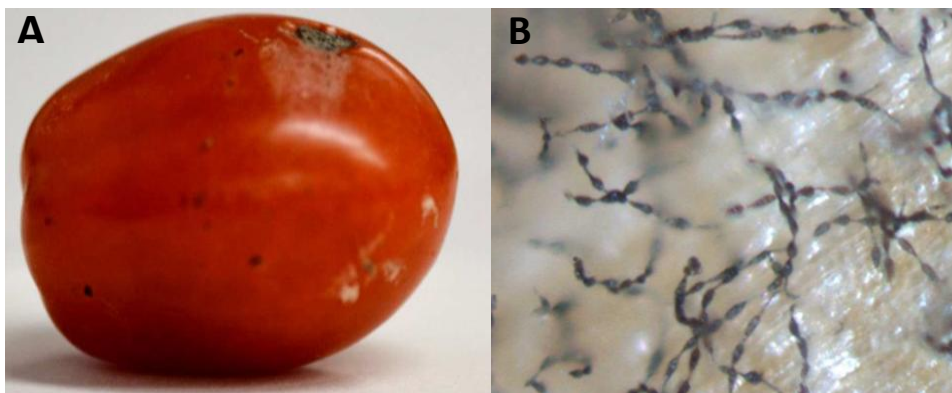


Figure 2A) A cherry tomato which has been artificially contaminated by *Alternaria* sp. **B)** Concatenated conidia of *Alternaria* as shown under the microscope

More than 70 phytotoxins produced by species of *Alternaria* have been characterized, and include virulence factors that have both nonspecific and specific host interactions, (HSTs). Several *Alternaria* secondary metabolites have been evaluated by the European Food Safety Authority (EFSA) as potentially causing risks to human health, including alternariol (AOH), alternariol monomethyl ether (AME), tenuazonic acid (TeA), altenuene (ALT), and tentoxin (TEN).^[35,36]

1.1.4 Silage co-contamination

Silage, which consists of blends of corn, wheat, barley and haylage, is an important stored feedstock for livestock. Silage production has steadily increased in agricultural areas since the 1960s, and consists of approximately 50-75% of the total livestock diet; many ruminants consume kilograms of silage daily.^[37,38] Farmers in many European countries store the majority of their forage material as silage due to its cost-effectiveness as a daily food source to provide fibre and digestible carbohydrates and proteins.^[39] To increase the storage lifetime for yearlong feeding, the forage material is stored under anaerobic conditions, and is combined with lactic acid-producing bacteria (*Lactobacilli*) to prevent nutrient spoilage and potential microbial contamination by reducing the pH.^[40] However, silage can become contaminated with filamentous fungi (Figure 3) that are tolerant to acidic environments, as well as other extreme conditions. Conditions become favourable for fungal growth due to improper harvesting, transportation and storage conditions, or by introducing moisture or oxygen to the ensiled material. As moisture conditions become more favourable, opportunistic contaminant fungi, such as *Penicillium* and *Aspergillus* can rapidly spread within the silage. The rise in metabolic activity also results in an increase in silage temperature, which makes it conducive to growth for other dormant fungi.



Figure 3- Grass and corn silage that has been naturally contaminated by fungi

Fungal contaminated silage results in a loss of nutritional quality, and a subsequent loss of palatability, leading to an overall decline in livestock health. Ruminants are typically resilient to acute mycotoxin exposure due to the effectiveness of rumen microbiota at inactivating secondary metabolites.^[41] However, livestock mycotoxicity can still occur after chronic toxin exposure, or after exposure to immunocompromising toxins such as enniatins, or antimicrobial metabolites, such as patulin, mycophenolic acid, citrinin and roquefortine C.^[42–46] In the 1960's, maize silage predominantly contaminated with *P. roqueforti* in Wisconsin led to observed mycotoxicosis in pigs, resulting in abortion and placental retention.^[47] There is also a high risk for farmers to develop respiratory infections or other illnesses when improperly handling the contaminated forage material. There is a danger for mycotoxin co-contamination of many different classes of mycotoxins in silage, which are produced by both the preharvest and postharvest fungal populations. Mycotoxin co-contamination occurs when either the same species of fungi produces multiple mycotoxins, when several mycotoxin-producing fungi are present, or when multiple contaminated forage materials are blended together as feedstock. The differences in chemical structures among the mycotoxin classes caused by co-contamination make silage extraction and multi-toxin analysis difficult.

1.2 High resolution mass spectrometry-based metabolomics

Fungal metabolomics

Metabolomics is the complete profiling of the total set of metabolites produced by a biological organism.^[48,49] Fungal primary metabolites, such as citrate, lactic acid and amino acids, are

biological precursors directly involved in their growth and reproduction, and have associated physiological functions. Fungal secondary metabolites have additional functions not related to growth or development, but may assist in defense, microbial community competition, or evading plant immune systems. The set of small molecules produced through primary and secondary metabolism for a given species of fungus comprises its metabolome. In understanding and perhaps redefining fungal species, metabolomics has numerous advantages over transcriptomics or proteomics in that the metabolites detected are directly related to the phenotype and the current level of genetic expression; all changes in the small molecule fungal metabolism are reflected by the metabolites observed.^[50]

The preferred analysis of metabolomics data is through liquid chromatography mass spectrometry (LC-MS), due to the substantial number of metabolites detected by using softer ionization techniques, but also due to its robustness in complex biological matrices, and its selectivity and sensitivity towards sample analytes.^[48] However, it has been approximated that 90% of the total metabolomics data are either artifacts, or completely unknown metabolites.^[51] For instance, Iijima et al., (2008) described over 860 metabolites in tomatoes, and 494 of the metabolites were unknown.^[52] Without published metabolomics databases to identify unknown metabolites, sample analysis is limited to targeted analyses by comparison to commercial standards, and isolation and characterization by NMR for unknown compounds- this is unfeasible for the potentially large number of unknown metabolites. In addition, other limitations of LC-MS for metabolomics are based on analysis in complex matrices resulting in ion suppression, and the resolution and mass accuracy of the instrument. Though lower resolution MS instruments (<10,000 resolution) such as triple quadrupole mass spectrometers are extremely sensitive instruments used for quantification, they are not widely employed for metabolite discovery and metabolomics. Lower resolution instruments cannot differentiate between closely-related masses, which may obscure potentially important metabolites, and are often operated at nominal mass. High resolution mass spectrometry (HRMS) instruments, such as time-of-flight (TOF) and Orbitrap mass spectrometry, can not only obtain the exact mass and thus molecular formula, but they can also distinguish between closely related masses, resulting in a higher mass accuracy.

1.2.1 Molecular qualification

Determining the mass accuracy is an important feature in molecular qualification, as a more accurate mass is more indicative of exact molecular formula.^[53,54] Mass accuracy is defined as the experimental mass measurement in relation to its exact (theoretical) mass, or its error, (Equation 1).

$$(1) \quad \text{mass accuracy (ppm)} = \frac{\text{Experimental mass} - \text{Exact mass}}{\text{Exact mass}} \times 10^6$$

Ideally, mass accuracy needs to be sufficient enough to provide reasonable molecular formula(e), where 5 ppm is said to be a limit for formula selection.^[53] Triple quadrupole mass spectrometry instruments can achieve between 17 – 30 ppm mass accuracy, which can provide the likely molecular formula for smaller mass ranges, however, when operated in reaction monitoring mode, they generally achieve 500 mDa mass accuracy. The Q-Exactive Orbitrap is capable of achieving mass accuracy ± 2 ppm, which is capable of providing the exact molecular formula. The known molecular formula can be used to narrow the possibilities of the identity of the analyte. The exact mass can also provide useful information regarding the presence of chlorine, bromine or sulfur atoms attached due to their negative mass defects.^[55] The mass defect is the difference between the experimental mass and its nominal mass, (the whole number before the decimal). The presence of sulfur, bromine and chlorine can also be further confirmed by comparison to their isotopic peaks with sufficient resolution.

Resolution, or resolving power, as defined by IUPAC is defined as its experimental mass divided by the change in mass between the chromatographic peak (Equation 2, Figure 4) at full-width half maximum (FWHM).

$$(2) \quad \text{Resolution (R)} = \frac{\text{Experimental mass}}{m_2 - m_1}$$

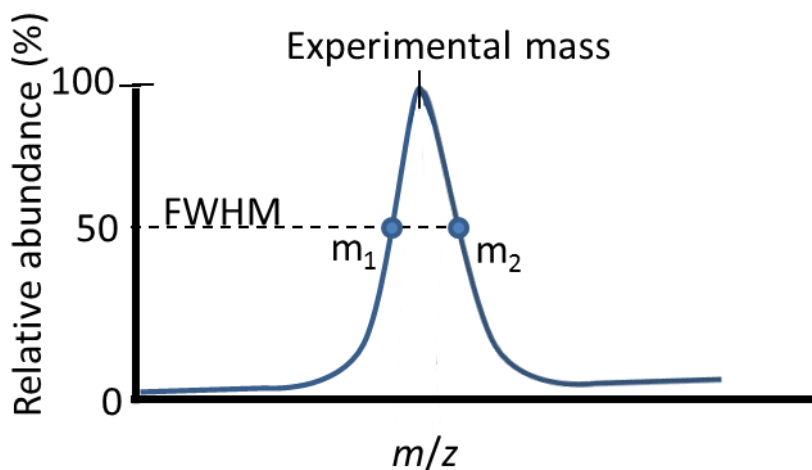


Figure 4- Measuring resolution at full-width half maximum (FWHM)

Triple quadrupole MS can achieve resolutions of approximately 1000, which is appropriate for resolving the nominal mass of the parent molecular ion. However, the Q-Exactive Orbitrap is capable of 140,000, which can fully resolve the M+1 and M+2 peaks, as well as isotopic patterns from the presence of other polyisotopic elements, such as sulfur and selenium. However, in addition to the accurate mass and molecular formula, the confidence in molecular qualification increases with comparison to known characteristic MS² fragments and matching retention time (RT) obtained either from commercial standards, or from literature values. Each MS variable, (RT, precursor mass, five fragments) is a defining feature for each known metabolite. The confidence in identifying the correct analyte increases with each matching feature as defined by individual validation procedures for each analyte and matrix from the LC-MS spectra and chromatograms. For instance, European Commission (SANCO) guidelines for identifying pesticides in food and feed consists of matching three known features using high-resolution mass spectrometry (HRMS).^[56] Complex matrices may require a larger number of matching unique features to increase the confidence level in analyte detection.

1.2.2 Statistical analysis

Principal Component Analysis (PCA) is an untargeted and unbiased statistical approach to visualize individual variation, and to describe patterns within large sets of data. PCA takes values that are strongly correlated in x and y coordinates, and plots it in possibly related components as

dimensions that describe variability.^[57] Dimensions on a PCA plot have no physical independent or dependent variables such as x and y, but rather describe a sample in 3D space in a new coordinate system, known as principal components. The first principal component describes the highest variability in the dataset, and is plotted against the second principal component, or the next-highest variability.

Non-targeted statistical analysis is commonly described by principal component analysis (PCA). PCA is an unbiased statistical tool for exploratory data analyses of raw metabolite data. Important information from a generated metabolite peak list table, which contains *m/z* values, retention times and peak areas, can be extracted as sets of principal components.^{[58][59]} The principal component that describes the highest variability is plot on the x-axis, against the component with the second highest variability on the y-axis; the generation of the associated PCA plot is termed a score plot, where each sample is represented as a point in the plot. Various patterns begin to emerge on the score plot as the metabolites present in each sample begin to influence the location of the sample point.^[58] Samples that group together represent a particular chemotype, in which the samples share similar secondary metabolites, and therefore share a similar metabolism. Despite the observation of particular groups in a PCA, the groups may not be true groups in 3D space, and the data must be statistically validated to become meaningful; even applying a group by eye introduces potential sample bias. Thus to remove bias and still determine if there are groups in the data, K-means clustering can be utilized prior to further statistical analysis. K-means clustering analysis uses an algorithm that assigns groups based on a number of randomly selected samples, and indicates the group that it is closest to in 3D space.

Related to PCA plots are loading plots, which describe the metabolites responsible for the variation in the total dataset. The loading plots are described as arrows, with each arrow indicating an individual metabolite. The direction and length of the arrow indicates the direction and degree of variation observed in the samples respectively. The metabolites responsible for variation can be investigated using p-values for their true impact on the dataset.

P-values are calculated probabilities to test the hypothesis that there are significant differences in datasets. The significance level is set by the researcher, and describes the p-value cut-off which is deemed to be significant, (commonly $P < 0.01$). Extremely low probabilities that are less than

the set p-value cut-off are deemed statistically significant, while values above the cut-off value are not significant. The most common test for significance is a t-test, which tests the hypothesis that the two datasets are different from one another. However, for most metabolomics datasets, the data cannot be assumed to be normally distributed. Thus, significance for metabolomics datasets is calculated by using the Wilcoxon test.^[60] However, in metabolomics, testing multiple hypotheses (significant metabolites) can lead to a number of accidental false positives. For instance, setting the P-value at 0.01 when there are 4000 metabolite features, 40 metabolites will be false positives. Benjamini-Hochberg False discovery rate (FDR) correction addresses the large number of false positives by increasing the p-value cut-off based on the number of metabolites being tested.^[61] Thus by applying the FDR correction to a metabolomics dataset, fewer false positives will be accepted as significant metabolites.

1.3 Analytical techniques

1.3.1 High-performance liquid chromatography (HPLC)

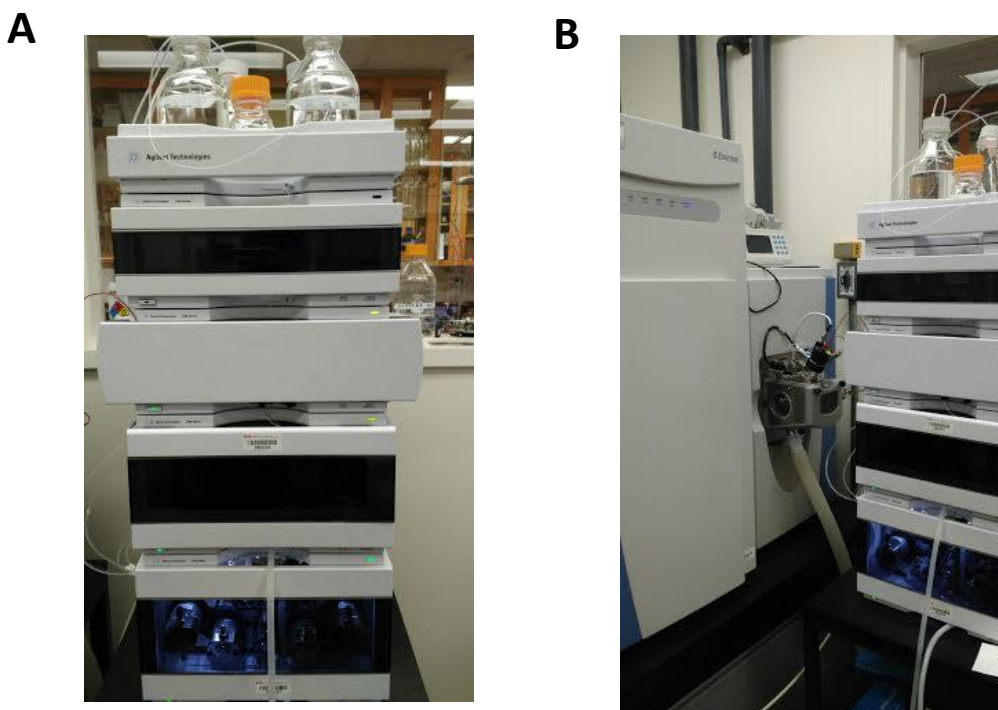


Figure 5A- Agilent 1290 HPLC. B) Agilent 1290 coupled to the Thermo Q-Exactive mass spectrometer

Reverse phase HPLC (Figure 5A) aids in the separation of a complex mixture of analytes based on their polarity.^[62] Solvent mixtures, known as the mobile phase, are pumped through a packed column under high pressure. Secondary metabolite data generation and analysis was performed through separation by HPLC and detection by high resolution mass spectrometry, (LC-MS, Figure 5B).

Analyte separation

As the sample is injected, analytes in the sample matrix interact with the stationary phase of the column, which is comprised of nonpolar (such as C18) or polar (silica-based) material. Molecules with strong interactions with the stationary phase of the column will be retained longer on than molecules that have less affinity; this changes the retention time of each particular analyte as they elute from the column and pass through to the detector, (Figure 6).



Figure 6- C18 column connected to the ESI source of the mass spectrometer

In Orbitrap mass analyzers, ions do not physically strike a detector, but instead induce a charge image on a sensor as they move around the central electrode of an Orbitrap. The mass-to-charge ratio (m/z) of an ion is determined following a Fast Fourier transform as a signal, which is caused by the presence of a particular analyte and converted by Fourier transform of the time domain into a frequency domain which can be related to mass and charge. The m/z signals as a function of LC retention time are visualized as total ion current (TIC) chromatograms, or base peak chromatograms (Figure 7). The TIC represents the total intensity of all of the m/z units detected in each scan over the course of the analysis run. Similar to the TIC, detected m/z units can be

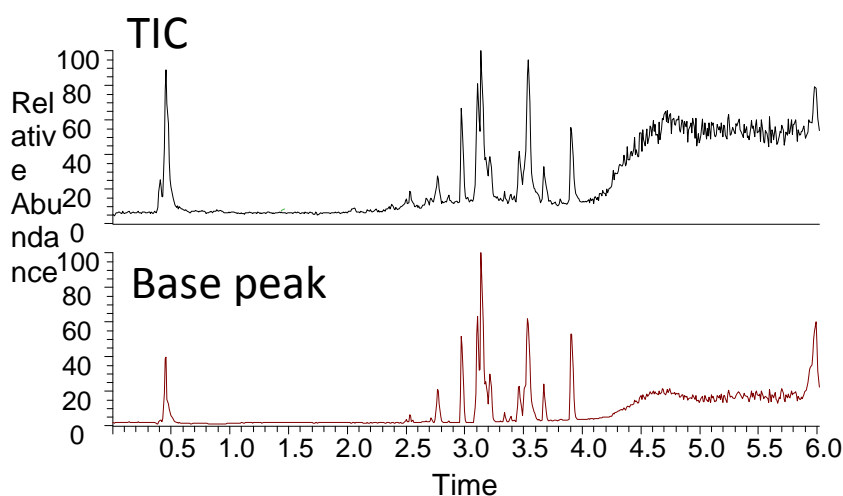


Figure 7- Showing the typical output from the HPLC, as detected by the mass spectrometer as a TIC, or a base peak chromatogram

visualized as base peak chromatograms, however only the most intense m/z peaks from analytes in each spectrum contribute to the visualized plot.

LC columns can be modified to suit the analytes for particular analyses, either by changing the column length, altering the functional groups on the packed material or changing the pore size of the packing material. The mobile phase may elute either by isocratic flow, where the mobile phase proportions remain constant over the sample run, or by gradient flow, where the mobile phase changes over the course of the run. Using nonpolar columns with polar mobile phases is termed reversed phase chromatography, and is the most common form used for the separation of nonpolar analytes such as mycotoxins and secondary metabolites.

1.3.2 Mass spectrometry

Mass is measured in daltons, (Da), which is the standardized unified atomic mass unit (amu).^[63] One amu is 1/12th the mass of the carbon 12 atom (1g/mol) equal to 1.66×10^{-27} kg. Mass spectrometry instruments are typically combined with HPLC instruments (LC-MS), and are commonplace in metabolomic analysis and characterization of small molecules. Mass spectrometry (MS) is an analytical detection technique for determining masses of analytes within a sample, more specifically by determining the mass-to-charge ratio (m/z) of gas phase ions. The chemical species are ionized in the source, and qualified by their mass-to-charge ratios (m/z). In a Q-Exactive instrument, ions are filtered by their mass-to-charge ratios by the quadrupole mass analyzer, which uses alternating current (AC) using radiofrequency (RF) with direct current (DC) to scan over the desired mass windows; any ions that do not fall within the scan ranges do not pass through the quadrupole. After mass selection, ions are stored in the C-trap and can be selected for MS² analysis in the HCD cell, or continue to the Orbitrap mass analyzer for full MS analysis. Relevant terms are discussed below as they pertain to the Q-Exactive Orbitrap (Thermo Fisher Scientific) mass spectrometer, which was used for the generation of all high resolution MS (HRMS) data.^[64]

1.3.2.1 Heated Electrospray Ionization (HESI) Ion source

Traditional MS instruments relied on 'hard' ionization techniques, such as electron impact (EI) for analysis of volatile organic compounds, (GC-MS). The higher internal energy produced from hard ionization techniques reduces many molecules into low molecular weight characteristic reproducible fragments. The caveat of EI ionization is that many molecules and biological specimens cannot be readily introduced into the gas phase without first causing extensive thermal decomposition of the analyte molecules.^[65] More recently, the mass spectrometry trends for both small and large molecule study, as well as metabolome analysis have shifted towards softer ionization techniques, such as electrospray ionization (ESI). This is predominantly due in part to ground breaking work accomplished by Drs. Malcolm Dole and John Bennett Fenn for their work towards ESI.^[66,67] There are many benefits of ESI over harder ionization techniques, including preservation of parent ions and fragments for structural elucidation and quantification, increased analyte sensitivity, a wider range of ionisable compounds, and the direct combination

of mass spectrometry with liquid chromatography for rapid analysis. Samples in a liquid matrix are aerosolized from a charged needle (capillary) into a heated chamber *in vacuo*.^[68,69] The tip of the charged capillary passes a large electric potential between the needle and a counter-electrode onto the surface of the droplet, which in turn generates a mist of similarly charged droplets called a Taylor Cone. The capillary tip can impart either positive or negative potential onto the droplet surface.

There are two predominant theories for gas phase ion production at the surface of the droplet for both small and large molecules: the ion evaporation model (IEM), and the charge residue model (CRM), however the chain ejection model (CEM) has been proposed specifically for large unfolded proteins.^[66,70,71] The ion evaporation model (IEM) proposed by Iribarne and Thompson (1976) suggests the ion evaporates directly from the droplet when the electric field strength at the droplet surface increases resulting in an energy gain (ΔG) by expelling the solvated ions.^[71] In the CRM, inert nebulizing gas, such as nitrogen gas, and increased temperature of the chamber causes droplets to become smaller, and evaporate much faster, creating an increased surface charge density on the droplets.^[68,69] As the solvent from the droplet evaporates (desolvation) in the heated chamber, the electrostatic repulsion builds on the surface until it exceeds the surface tension, called the Rayleigh Limit. The droplet then undergoes a ‘Coulombic explosion,’ generating smaller charged droplets which themselves repeat the cycle.^[68,70] After repeated cycles, the solvent evaporates away, leaving behind a charged analyte. Most molecules are detected as either a protonated or deprotonated form, however some molecules can be ionized as non-covalent adduct complexes such as NH_4^+ , Na^+ and K^+ . There are many reviews that support both models co-occurring, though the prevailing theory is likely molecule-specific.

1.3.2.2 Quadrupole mass filter

In mass spectrometry, the quadrupole is a mass analyzer used for the filtering of charged ions by their mass-to-charge ratios (m/z). The quadrupole consists of four parallel electrode rods, and causes charged particles passing through the center of the rods to be filtered based on the stability of their trajectories in an applied electric field across the electrodes. Thus, only ions of a particular m/z can pass through the quadrupole.

Ions are filtered in the quadrupole due to the force of the electric fields after applying time-dependent alternating current (AC) using radiofrequency (RF) voltages, and time-independent direct current (DC), to the electrodes.^[72] Electrodes will be given the same voltage as the one directly opposite; two will be given positive AC and DC voltages and two will be given negative AC and DC voltages. Therefore, m/z values are either repelled or attracted to the positive or negative electrodes dependent on its charge, and results in the ions either crashing on the electrode surface, or passing through the quadrupole. In positive ionization mode, and when the DC is positive, there is a stabilizing effect to positive charges of high m/z particles in the quadrupole, as larger molecules have a slower acceleration and have a stronger repulsion against the electrodes compared to lower masses. In contrast, when the DC is negative, smaller m/z particles are stabilized, as the larger m/z molecules are strongly attracted to the negative electrodes. Thus, only ions within a small m/z window will have a stable trajectory from the AC and DC over a scan. Over the course of the run, both the AC and DC are amplified and manipulated to create a mass spectrum over a wide scan range.

1.3.2.3 The C-trap

After mass filtering, the ions are stored in an ion trap controlled by radiofrequency (RF) voltages.^[73] The trap accumulates ions and cools them under a stream of inert nitrogen to prevent internal collisions prior to collision-induced dissociation (CID) in the HCD cell.

1.3.2.4 Higher-energy collisional dissociation (HCD) cell

Mass-selected ions pass from the C-trap to the higher-energy collisional dissociation (HCD) cell for fragmentation, or MS^2 . Directly related to Orbitrap technology, HCD is a type of collision-induced dissociation (CID), where ions are fragmented in the gas phase, but collision occurs external to the ion trap. The ions are accelerated into the HCD cell, where they collide with an inert gas, (typically nitrogen). The collision converts the kinetic energy from the acceleration into internal energy, which causes fragmentation of the parent or precursor ion into smaller fragments. The characteristic fragments, in addition to the precursor mass are used for the identification of the analyte. Each molecule receives a normalized amount of collision energy, (normalized collision energy, NCE) relative to its mass; larger masses receive more energy, as

they require more energy to fragment. The fragments are then accelerated back to the C-trap for injection onto the Orbitrap mass analyzer.

1.3.2.5 Orbitrap mass analyzer

The ion trap was developed based on the principles from the 1920's, when Kingdon passed a charge over a long wire, which was enclosed by a metal can.^[74] The charged wire became an electrode, which produced an electric field within the can, and trapped the charged particles within the can. Additional experiments performed by Knight applied the ion trap technique to obtain crude mass-to-charge ratios, though the mass accuracy was limited.^[75]

The Orbitrap, which is an ion trap mass analyzer, was developed by Alexander Makarov.^[76] Similar to the thin wire electrode, a central spindle-shaped electrode is encased by complemented outer electrodes. As ions are ejected into the Orbitrap from the C-trap, charged particles begin to oscillate axially across the central spindle-shaped electrode, which is confined by the outer electrodes.^[77] After ion injection, a small voltage ramp is applied to the central electrode, causing circular (radial) oscillation around the electrode. As the voltage increases across the central electrode, the radial oscillation decreases, which results in the packet of ions spreading across the electrode into thin rotating rings. The oscillation of the ions in the trap induces an image current which is detected by a differential amplifier on the outer electrode. The differential amplifier converts the time domain signal into a frequency domain using Fourier Transform for each m/z detected to generate a mass spectrum. The signal detected in the differential amplifier is proportional to the number of ions detected for that particular m/z value. The sensitivity of a particular analyte is related to the number of ions detected relating to its m/z under the applied conditions, and is a function of its concentration.^[78]

1.3 Molecular analyses

1.3.1 Deoxyribonucleic acid (DNA) sequencing

DNA contains specialized genetic information for all living species crucial for their growth, development and reproduction. In fungi, their metabolome is largely dependent on the genes present at the generic or even species level, which are responsible for encoding the production of mycotoxins and certain secondary metabolites.^[79] In addition to morphological and colony characterization, fungal species may be differentiated based on differing regions in their DNA.

Fungal genera and species are differentiated on a molecular basis by the variability of their nucleotide sequences in known regions in their DNA. Primers are used as DNA targets, and are designed as short nucleotide sequences complementary to the known nucleotide sequences in the DNA. Primers designed based on the internal transcribed spacer (ITS) region are the most commonly used general fungal primers, as nucleotide variability in the region relates to differing fungal genera and species. The ITS region has also been suggested as a possible fungal DNA barcode due to its broad range of differentiating fungal genera.^[80] However, there are some fungal genera, such as *Penicillium* and *Aspergilli*, that cannot be defined to the species level based on the sequencing of the ITS region, as their ITS regions are more conserved.^[81] Additional fungal primers based on the β -tubulin and calmodulin regions are used in the differentiation of both *Penicillium* and *Aspergilli* respectively. Similarly, the RBP2 primer has been proposed by Woudenberg (2013) for the differentiation of *Alternaria* species.^[30]

1.3.2 Next-generation sequencing (NGS)

Similar to standard sequencing reactions, there is a primer nucleotide set corresponding to specific regions in the DNA that differentiate between particular species. Rather than one amplification product for one sample, next-generation sequencing (NGS) provides differing sequences profiles pertaining to different species present in each sample (Figure 8).

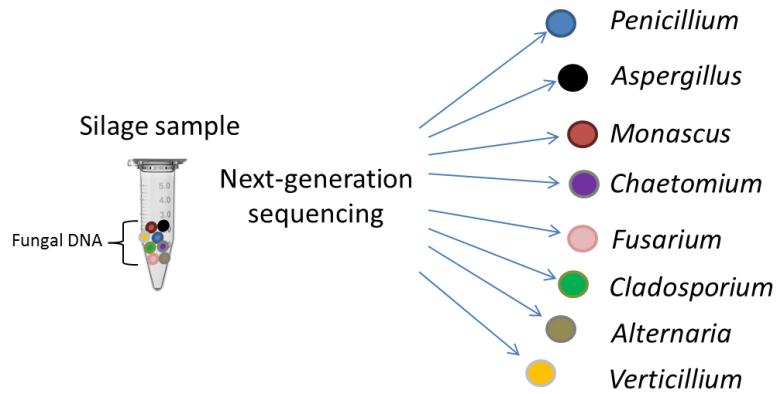


Figure 8- Next-generation sequencing for the profiling of fungal DNA from extracted genomic DNA

NGS is a newly developed method for high-throughput DNA sequencing, which was developed to aid in total genome analysis.^[82] NGS is now commonly used for both identifying and detecting members of mixed microbial communities.^[83] The Illumina MiSeq, which is a commonly used platform, utilizes specialized barcoded primers (Figure 9) to process a large number of sequences present from total extracted DNA.^[82]

Total genomic DNA from each sample is extracted, and each sample is PCR-amplified with a unique combination of forward and reverse barcoded primers (Supplementary Table 5S). Each amplified DNA from the original sample forms a cluster within the flow cell, and each cluster is sequenced using fluorescently labelled nucleotides, which are detected by a camera located within the MiSeq unit. Using bioinformatics software, the differing sequences in the sample can be assigned to the appropriate sample based on the associated barcode, and all the sequences are aligned and analyzed to profile the diversity from each sample.^[82] NGS data processing using the developed pipeline is discussed further in 4.3.3.

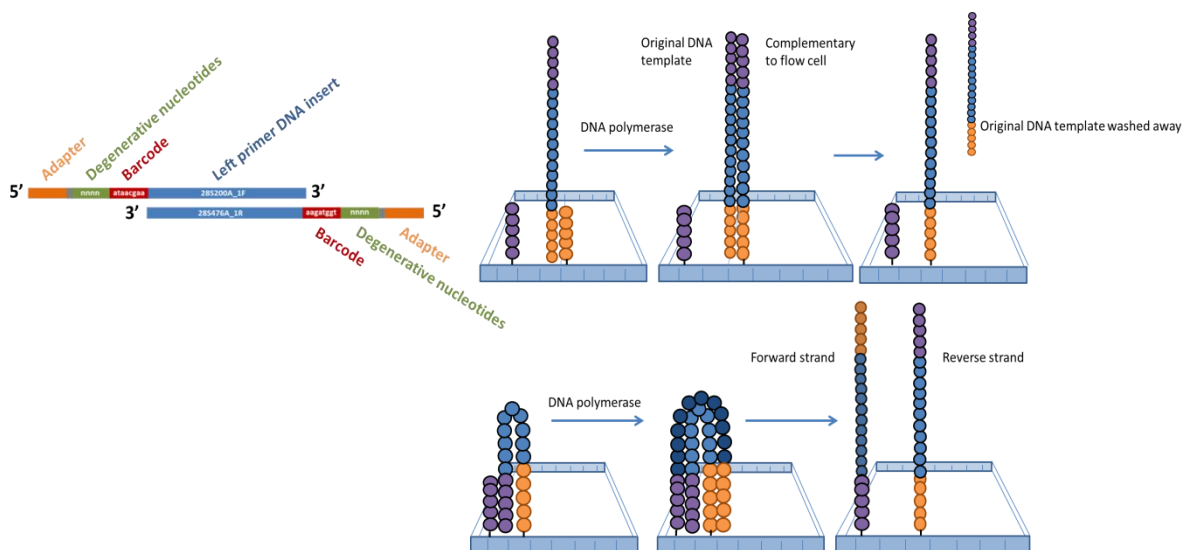


Figure 9- Designed barcoded primers with adapter regions (left), and bridge amplification procedure (right) for target DNA amplification [81]

1.4 Thesis objectives

Advances in analytical instrumentation and screening methods have resulted in an improved ability to detect mycotoxins and secondary metabolites in trace quantities. Statistical analysis of total metabolomics data, and the use of semi-targeted and non-targeted screening methods were similarly validated for their use in tandem with targeted mass spectrometry. The overall objective is to detect and characterize potentially new and emerging mycotoxins and secondary metabolites using high resolution mass spectrometry to provide data for risk assessors on their occurrence in Canadian agricultural commodities.

Chapter 2- Non-targeted Metabolomics of *Alternaria* spp. in Canada

2.1 Chapter 2 objectives

As part of the ongoing emerging mycotoxin risk assessment for Canadian species of *Alternaria*, the objective is to ascertain the distribution of isolated *Alternaria* species in Canada by chemotaxonomy, and to characterize their secondary metabolite production as a risk assessment for agriculturally-relevant crops.

2.2 Introduction

Alternaria is a cosmopolitan and globally distributed fungal genus, though the exact species and host range in major Canadian agricultural commodities are relatively unknown. The major problem with identifying the host range, and thus identifying the risk for toxicologically-relevant secondary metabolites, is the difficulty in distinguishing between species. Traditionally, the majority of isolated *Alternaria* species have been identified as the more common *A. alternata* species, many of which are often misidentified.^[84-87] Substantial attempts have been made towards organizing the taxa of *Alternaria* into more appropriate species-groups or formae-speciales, but many species are practically identical on a genetic basis.^[88] General fungal primers (ITS) and even *Alternaria*-specific primers, (RBP2) have been developed, but they cannot accurately distinguish between *A. alternata* or the *A. arborescens* species complex during DNA sequencing.^[30,31] The lack of specificity from the designed primers also explains the predominance of reported *A. alternata* in the literature. By comparing whole genomes of *Alternaria*, Woudenberg (2013) combined *A. alternata*, *A. tenuissima* and *A. arborescens* into one section (section *Alternaria*) due to the inability to separate the individual species genetically.^[30] Many described species of *Alternaria* within the 26 sections are solely based on morphology, thus many species do not differ molecularly, making DNA sequencing problematic.^[31]

By morphology, *Alternaria* species are identified based on their sporulation patterns as reported by Simmons.^[88] However, even morphological identification is often difficult, as inducing conidial production typical of the particular species is a challenge on artificial media.^[89]

Chemotaxonomy has been previously successful in differentiating between filamentous fungi.^[13] *A. infectoria* was previously identified on the basis of chemotaxonomy due to its production of infectopyrone and novaezelandins, which is also in congruence with molecular methods.^[90] Therefore, the metabolomics data may assist mycologists in species-level assignments through chemotaxonomy of *Alternaria* isolates. Global metabolomics studies have been successful in differentiating between large-spored species, (*A. dauci*, *A. porri*) using chemotaxonomy, and previous attempts at differentiating between small-spored *Alternaria* strains have been similarly investigated using strains from Argentina and Greece.^[34,90-93] The predominant species previously reported in food-relevant crops have been *A. alternata*, *A. arborescens*, *A. tenuissima*, and *A. infectoria*, though the species and secondary metabolite distribution in cool climate Canadian food crops is relatively unknown. The production of fungal secondary metabolites is largely influenced by environmental and genetic factors.^[11] In addition, different substrates where the fungi may be isolated act as different sources of carbon and nitrogen which may further alter the metabolism. To further complicate *Alternaria* chemotaxonomy, there are seven reported *A. alternata* species pathotypes based on their production of host-specific toxins due to the presence of specific toxin encoding genes contained within a common superfluous chromosome.^[94] Thus, secondary metabolites may differ in other climates and crops. Regardless of the naming convention in *Alternaria*, these studies highlight the urgency to analyze the metabolome of Canadian species specific to agricultural products by chemotaxonomy.

To investigate the global metabolomics and potential chemotypes of Canadian species of *Alternaria*, 148 strains isolated from wheat, apples, blueberries, tomatoes and various perennial shrubs, in addition to two type strains, were examined using statistical analysis of non-targeted high-resolution mass spectrometry (HRMS) data. Individual extracts from each strain were analyzed by principal component analysis (PCA) using data generated by untargeted LC-HRMS (liquid chromatography high resolution mass spectrometry) data. In addition to non-targeted screening, all strains were assessed for their potential production of AAL-toxins. Chemotypes were investigated as possible chemotaxonomy assignments, however proper identifications of

each individual species need to be further established to accompany the metabolomics data in order to accurately predict the potential for secondary metabolite production in agricultural products for a particular species of *Alternaria*.^[31]

2.3 Experimental

2.3.1 Fungal material and identification

148 Canadian strains of *Alternaria* spp. were isolated from plant material or were obtained from the Canadian Collection of Fungal Cultures (CCFC) in Ottawa, Ontario. The majority of these strains were isolated from grain, with additional strains isolated from tomato, apple, grape, and various perennial shrubs. Individual strains were initially identified to the genus level based on morphology. Further morphological identifications were performed at Agriculture and Agri-food Canada (AAFC) in Ottawa, Ontario. 81 representative strains were sent to Dr. Joyce Woudenberg at Centraalbureau voor Schimmelcultures (CBS, Utrecht, Netherlands) and sequenced using the RPB2 primer.^[30] Strains were transferred onto potato dextrose agar (PDA) plates (Sigma Aldrich) as 3-point inoculations and incubated at 25°C in the darkness for 7 days, or until the colonies reached approximately 4 cm in diameter. PDA was selected for metabolite screening media as it produced the largest variety of metabolites detected in comparison to the other agar media screened. Additional information regarding the strains is provided in Appendix A1, Table 1.

2.3.2 Plug extraction

Initial metabolomic screening of the 148 *Alternaria* spp. strains was performed by removing six agar plugs from each three-point inoculum using a 6 mm cork borer and extracting the plugs with ethyl acetate containing 1% formic acid (Sigma, St. Louis, MO) prior to LC-MS screening.^[91,95]

2.3.3 LC-HRMS Analysis

HRMS data were obtained using a Thermo Q-Exactive Quadrupole Orbitrap Mass Spectrometer, coupled to an Agilent 1290 HPLC. A Zorbax Eclipse Plus RRHD C18 column (2.1 x 50 mm, 1.8 µm; Agilent) was maintained at 35 °C. The mobile phase was comprised of water with 0.1% formic acid (A), and acetonitrile with 0.1% formic acid (B) (Optima grade, Fisher Scientific, Lawn, NJ). Mobile phase B was held at 0% for 30 seconds, before increasing to 100% over three

and a half minutes. B was held at 100% for 1 and a half minutes, before returning to 0% B in 30 seconds. 2 μL injections were used at a flow rate of 0.3 mL/min. The following conditions were used for negative HESI for full MS: capillary voltage, 3.7 kV; capillary temperature, 400°C; sheath gas, 17.00 units; auxiliary gas, 8.00 units; probe heater temperature, 450 °C; S-Lens RF level, 45.00; AGC target, 1e6; maximum IT, 512 ms; scan range, 100 – 1200 m/z . Similar conditions were used for positive HESI, but with a capillary voltage of 3.9 kV. HRMS data for both positive and negative full MS data were acquired at a resolution of 140 000 and max IT of 500 ms.

2.3.4 Global metabolomic analyses

2.3.4.1 Principal component analysis (PCA) and K means clustering

Centroided raw HRMS data generated by the Q-Exactive Orbitrap from the 148 isolates and two type strains were processed using xcms with R (r-project.org) to generate a peak list.^[96–98] xcms detects every metabolite m/z value for a given set of conditions supplied, such as the noise level, and the minimum peak area intensity required to be considered for analysis. A subset of a sample peak list is provided in Appendix A2. The following conditions listed in Table 1 were used to generate peak lists:

Table 1-Peak list generation conditions using xcms in R.[40–42]

Condition	Setting	Explanation
prefilter=c(k,I)	k = 3, I = 5000	To be considered a peak, must have 3 peaks with intensity > 5000
ppm	2	Maximum tolerated m/z deviation in consecutive scans
snthresh	5	Signal to noise ratio
peakwidth=c(min,max)	min = 5, max = 20	Chromatographic peak width in seconds
noise	100000	Anything < 100000 intensity is noise
retcor	method=orbiwarp	Calculates retention time deviations from each sample
bw	5	Bandwidth setting, using half width half maximum
minfrac	0.25	Minimum fraction of samples in at least one sample to be considered a group
mzwid	0.015	Width of overlapping slices of m/z values

Data from the peak list were pretreated to correct for heteroscedasticity by first replacing zero values with 2/3 of the minimum peak area value of all of the metabolites detected.^[99] This was followed by performing a log transformation of the peak areas.^[59] To adjust for fold differences between the metabolites, pareto scaling^[59] was performed on the transformed data prior to PCA

generation using MetabolAnalyze and FactoMineR. Unsupervised groups in the PCA were assigned using K means clustering analysis using scripts adapted for R.^[100]

2.3.4.2 Metabolomic analysis

Individual metabolites responsible for the large variation between groups examined in the PCA were investigated using the Wilcoxon test using the Benjamini Hochberg False Discovery Rate (FDR) correction for multiple testing.^[60] Corrected p-values < 0.01 were investigated within each group. Results were visualized as volcano plots, which were generated by plotting the log₂ fold change (ratio of average peak area in group 1: average peak area in group 2) against metabolite intensity and FDR-corrected p-value. Metabolites which were zero-replaced by 2/3 of the minimum peak area value, (2.3.4.1) were still detected as a ‘fold change’ difference by the Wilcoxon test with FDR correction, even though the metabolites were either present or absent. Thus, each metabolite was confirmed through inspection of the MS spectra between groups to confirm presence/absence, or mere concentration differences. Metabolites were confirmed by comparing their MS² spectra to authentic standards, or to reported literature transitions. Unknown metabolites were compared in both SciFinder and Antibase 2013.

2.4 Results and Discussion

2.4.1 Global metabolomic chemotyping of Canadian species of *Alternaria* using PCA and K means clustering

It is imperative to screen for any potential emerging mycotoxins produced by *Alternaria* species as a risk assessment for their presence in Canadian agricultural commodities. The same species of *Alternaria* may still produce different secondary metabolites (different chemotypes) due to genetic or epigenetic differences. Therefore, it becomes important to monitor the current distribution of *Alternaria* species in Canada, and to characterize their secondary metabolite production. To assess the global metabolomics and specific chemotypes of *Alternaria* species in Canada, 150 strains (148 strains and 2 type strains) were analyzed using PCA of data generated by LC-HRMS in negative ion mode, (Figure 10).

Each metabolite number corresponds to a particular m/z value in the peak list. The arrows attached to each metabolite number indicate the directions that each individual metabolite is 'pulling' or influencing the samples on the PCA plot. Potential correlations or patterns between the samples and variables were determined by comparing the score and loading plots. The generated score plot (Figure 10A) shows the separation of individual samples, which are represented by spots in the PCA chart. Each sample separates based on the set of metabolites that it contains, and samples containing similar metabolites group together; groups of samples can be described as chemotypes. Figure 10A clearly suggests a separation of the metabolomics data into two distinct chemotypes in negative ionization mode, with 33.78% of the variability being explained by dimension 1.

The direction in which every distinct metabolite influences the position of a sample is described by the loading plot (Figure 10B). Comparing between the PCA plot and the loading plot ensures a non-biased approach to defining relationships between the samples and variables, (such as metabolites). The loadings plot as shown in Figure 10B describes the distribution of the metabolites within the samples, with each arrow representing a metabolite in the peak list. The figure further supports the separation of metabolites into two groups, with the longer overlapping arrows describing the metabolite distribution between the groups. Arrows pointing in different directions, which correspond to other metabolites, are the metabolites responsible for the variation observed within the groups.

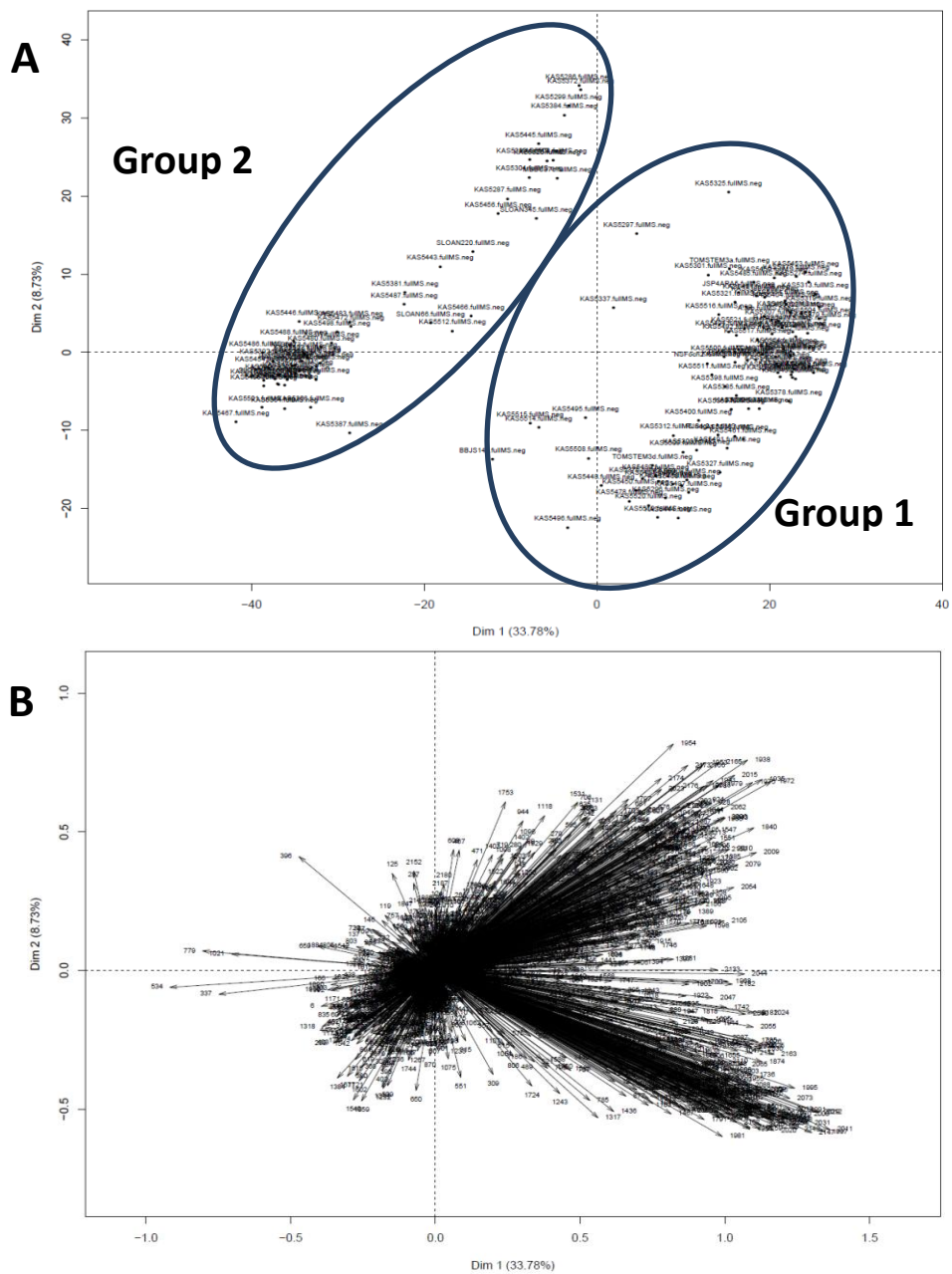


Figure 10- A) PCA (scoreplot) of 150 strains of *Alternaria* , showing HRMS data in negative ionization mode
 B) Associated loadings plot from PCA, showing numbered metabolites

While individual metabolites can be analyzed from the loading plots, large sets of metabolites are investigated for their significance (p-values) using statistical analyses, such as the Wilcoxon test with False Discovery Rate (FDR) correction.

To further assess the two groups observed in the PCA, coordinates from each group in the scoreplot (Figure 10A) were exported and described as metadata in a PCA for the positive ionization mode data, (Figure 11). While the data appears to spread further across the first dimension (Dim 1) in the positive mode PCA data, the data group similarly in both positive and negative mode, which would suggest that there are two chemotypes for the 150 strains of *Alternaria* spp. that were screened. As the data are better separated in Figure 10A than Figure 11, the groupings were further investigated using the negative ionization mode dataset.

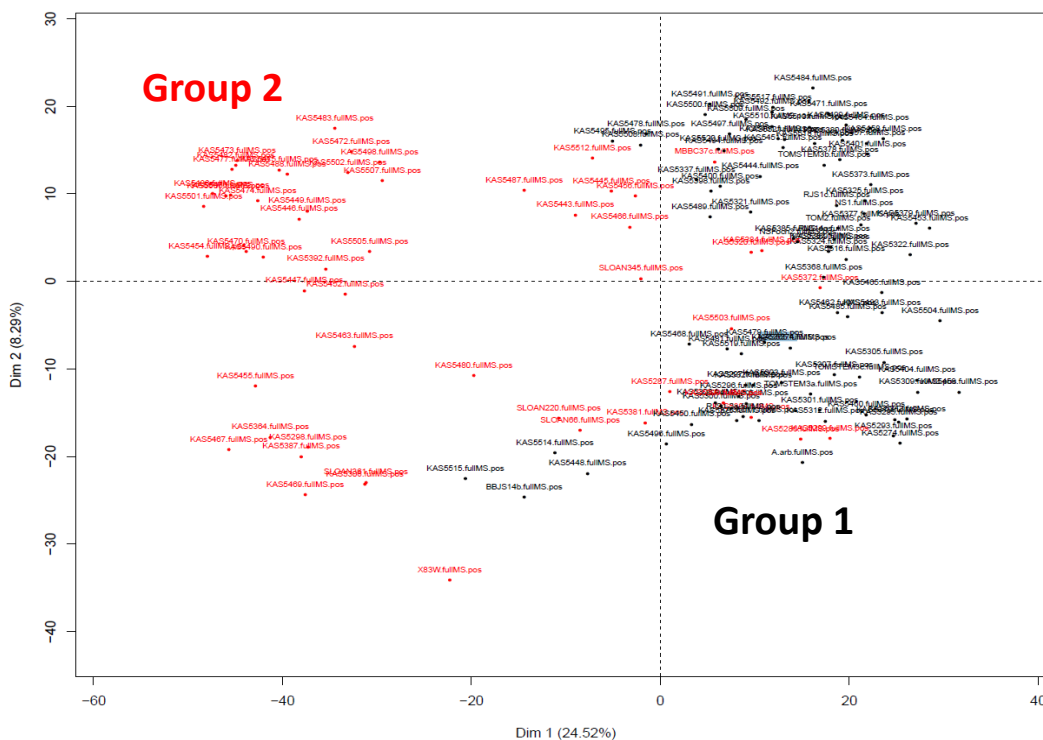


Figure 11- PCA (scoreplot) of 150 strains of *Alternaria*, showing HRMS data in positive ionization mode, coloured by Group 1 (black) and Group 2 (red) from Figure 5A

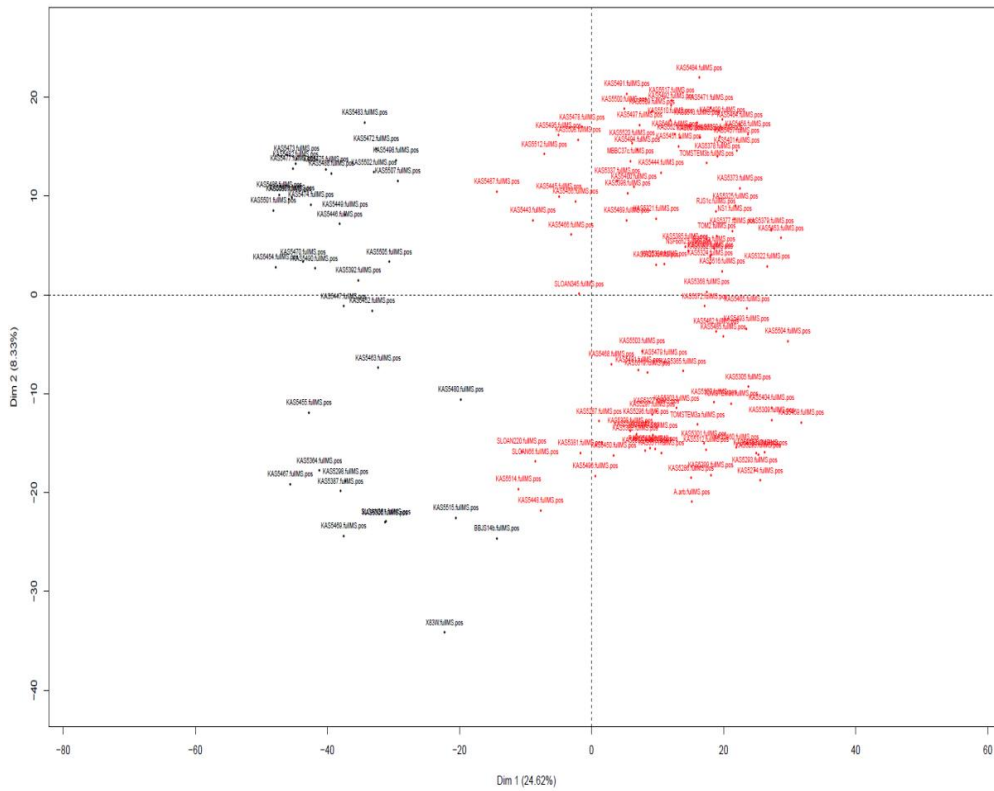


Figure 12- K means clustering of 150 strains of *Alternaria* using full MS data generated in positive ionization mode. PCA, where groups are coloured by unique clusters calculated using the K means clustering algorithm of centroided data points

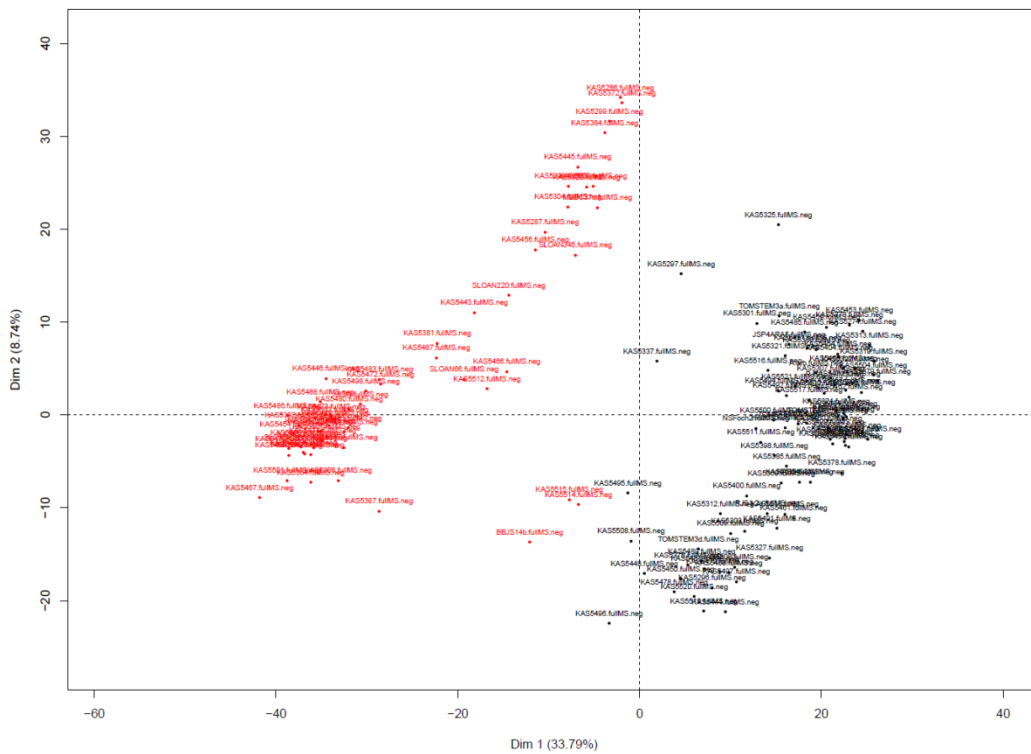


Figure 13- K means clustering of 150 strains of *Alternaria* using full MS data generated in negative ionization mode. PCA, where groups are coloured by unique clusters calculated using the K means algorithm of centroided data points

Manually assigning groups, or creating ‘supervised’ groups on a PCA is statistically unfounded, and not always accurate. To avoid statistically biasing the PCA by imposing supervised groups, K-means clustering was used to describe unbiased, or ‘unsupervised’ clusters in the dataset to confirm the presence of two groups. K-means clustering further confirmed the presence of two unique groups within the *Alternaria* strains in both positive (Figure 12) and negative (Figure 13) ionization modes.

Before concluding that these are chemotypes are unique to Canadian species of *Alternaria*, the data was investigated for other potential reasons that could cause the data to split into two groups. Information about the individual strains was imported as metadata into the PCA, and strains were coloured by the metadata information such as the material from which the fungus was isolated, (Figure 14), isolation date and isolation location.

Though several wheat samples grouped together in (-)Dimension 1, there were no other clear associations between the metadata and the groups in the PCA.

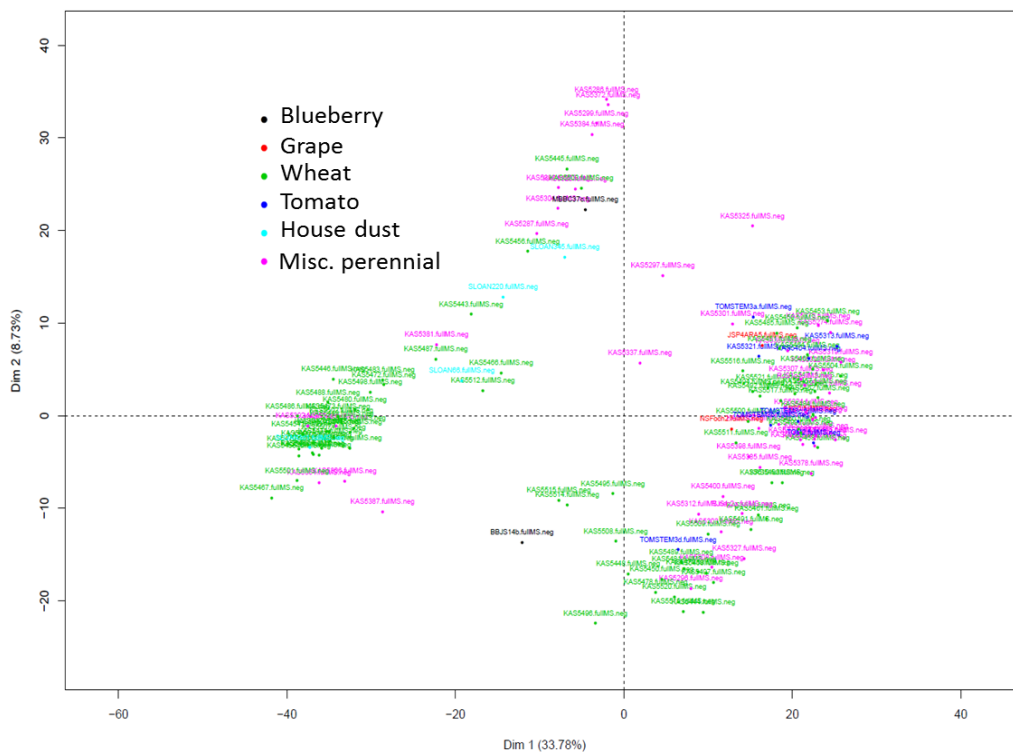


Figure 14- PCA of 148 *Alternaria* strains (excluding type strains) of full MS data acquired in negative ionization mode. Samples are coloured by the substrate from which the fungus was originally isolated

To ensure the data were reproducible, 20 strains of *Alternaria* (10 from each group, Figure 13) were randomly selected for regrowth and re-extraction for HRMS analysis. This also ensured that any potential fluctuations in metabolite production due to colony growth differences between the 150 strains were not responsible for the differentiation of the groups; generated PCAs for both negative and positive ionization mode are shown in Figure 15. PCA plots generated were coloured by their group assignment from K-means clustering (Figures 13 & 14) to investigate whether samples were grouping together as before. Datasets were run approximately 1 year apart from each other.

Despite the small sample size, the randomly selected samples (Figures 15A & B) still cluster into two groups, as coloured by the metadata. Similar to Figure 10A, clusters are more evident within the negative ionization mode data, likely due to the larger variability being explained by dimension 1 (37.55%). It is also possible that the metabolites that are responsible for the separation may have better ionization efficiencies in negative ionization mode, or there are additional metabolites in positive ionization mode affecting the separation. The data appear to be grouping into two chemotypes, and this large variability observed is reproducible.

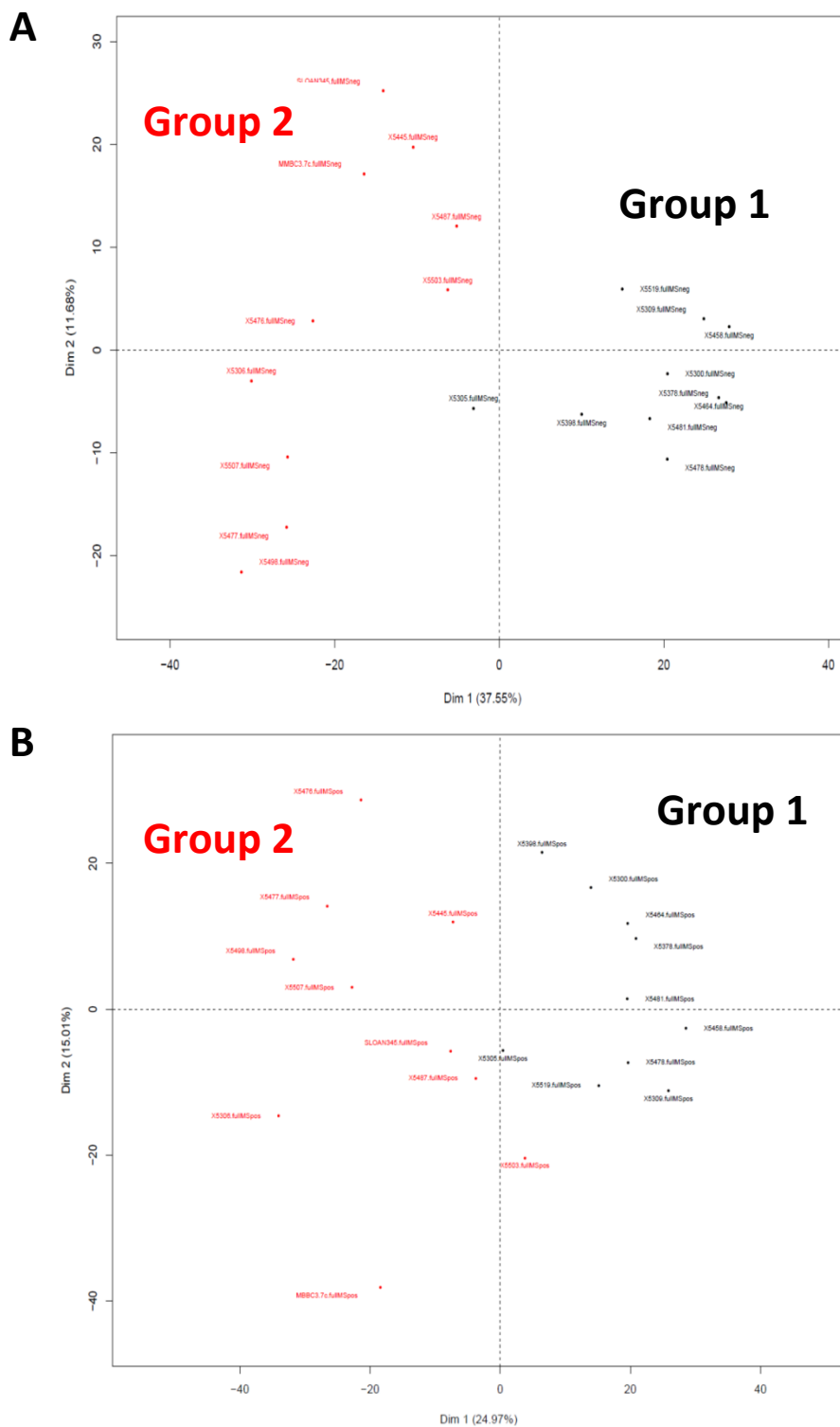


Figure 15- PCA plots of metabolomics data generated in negative ionization mode (A) and positive ionization mode (B) for 20 randomly selected samples. Samples are coloured by their previous K-means clustering assignment (Figures 13 and 14)

2.4.2 Metabolomic analyses and chemotaxonomy

As species level differentiation between *Alternaria* species is difficult, it becomes important to be able to find metabolite markers within the observed chemotypes to assist with determining appropriate taxonomy.^[30,31] The 148 Canadian strains of *Alternaria* that were screened grouped into two major chemotypes, and the result was reproducible (Figure 15). However, the metabolites responsible for the differences between the groups need to be investigated.

To better understand why the data are grouping in this manner, a Wilcoxon test with Benjamini Hochberg False Discovery Rate (FDR) correction was performed between the two groups for HRMS data generated in both positive and negative ionization modes.^[60,61] Due to the propensity for metabolites to have variable ionization efficiencies between positive and negative mode, metabolites from both modes were investigated using HRMS to ensure adequate metabolome coverage. As the chemotypes were more defined in the negative mode data, (Figure 10A, Figure 13), their ‘group’ assignments were applied to positive mode data. A table of m/z values were prepared with P-values (Wilcoxon test), corrected P-values (Benjamini Hochberg FDR correction), and calculated fold changes (ratios) of metabolite peak areas between groups; this allowed for examination of metabolites responsible for the differentiation between the two groups. The generation of volcano plots (Figure 16) allowed for easy visualization of significant metabolites between groups (Wilcoxon, FDR correction, $p < 0.01$) in order to select metabolites to investigate within both groups. Due to the large number of significant metabolites, only those with a \log_2 value (average peak area ratio group 1: group 2) greater than 1 were investigated.

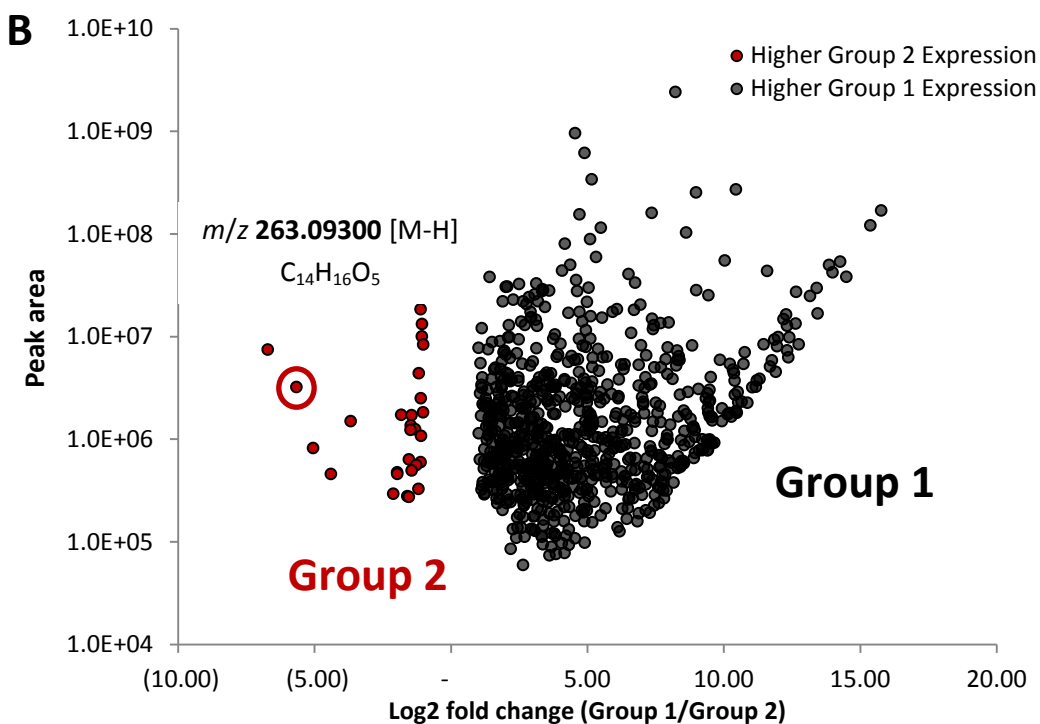
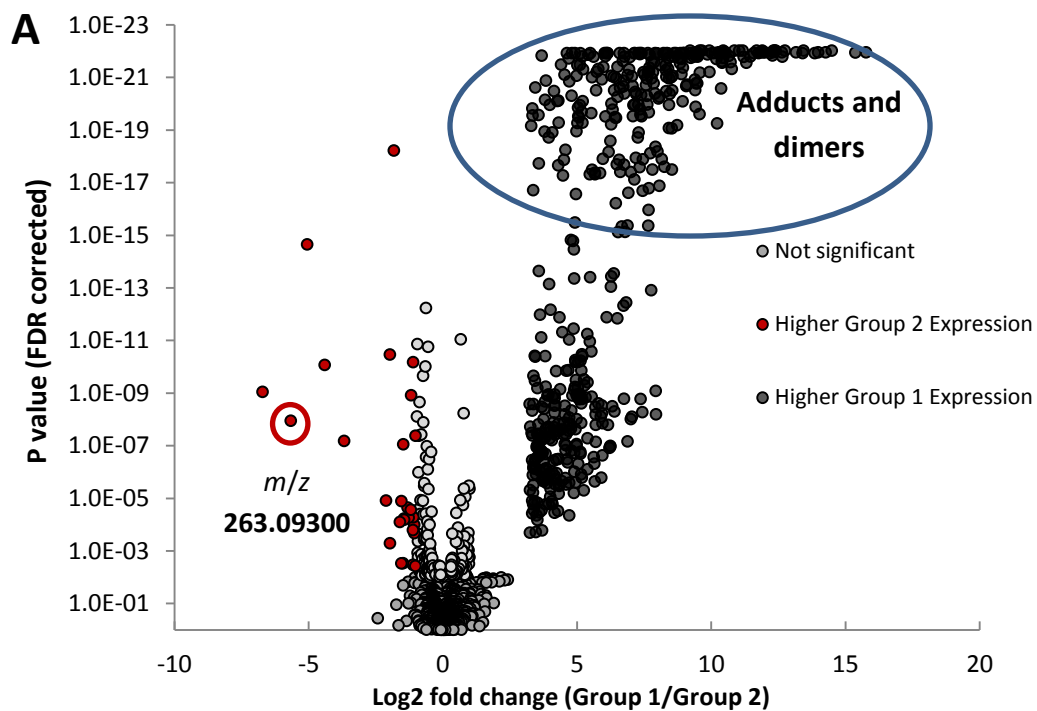


Figure 16- Volcano plots generated from the Wilcoxon test with corrected p-values between groups 1 and 2 for data generated in negative ionization mode. A) Fold changes in metabolite peak area with respect to their p-value significance. B) Fold changes in metabolite peak area with respect to their actual peak area

Both volcano plots visualize the significant metabolites, not only in regards to their significance (Figure 16A, p-values), but also in regards to their intensity in the full MS (Figure 16B, peak area). Both significance and intensity are imperative when designating potential differentiating metabolites between species; this allowed for rapid selection of both statistically significant ($p < 0.01$) and abundant peaks. For instance, the metabolite with a m/z of 263.09300 [M-H] in group 2 was initially investigated due to its significance (Figure 16A, $p = 1.12 \times 10^{-8}$), and its abundance (Figure 16B, 3.22×10^6). Many metabolites within group 1 had p-values less than 1.0×10^{-13} . However, upon investigation, the significant metabolites were adducts or dimers of abundant, (but still significant) metabolites. Future analysis included pre-filtering and sorting of the generated peaklist m/z values by mass defect.^[101] Significant metabolites responsible are in Table 2 (group 1) and Tables 3 and 4 (group 2), and discussed below.

2.4.2.1 Group 1 differentiation

The volcano plots illustrated in Figure 16 illustrated the predominance of significant metabolites in group 1, rather than in group 2. This suggests that the differences between the two groups are marked by the presence of some metabolites in group 1, but the absence of many of these metabolites in group 2. Tenuazonic acid (TeA), which is a commonly described secondary metabolite produced by species of *Alternaria*, was almost 300-fold more abundant in group 1 than in group 2 (Table 2) as calculated by the Wilcox test.

Table 2- Group 1 metabolites generated by the Wilcoxon test with FDR correction from data generated in negative ionization mode

m/z [M-H]	Molecular formula	Confirmed as	p-value (FDR corrected)	Fold change (peak area 1/2)
196.09697	C ₁₀ H ₁₅ NO ₃	Tenuazonic acid (TeA)	1.18×10^{-22}	298.15*
289.07159	C ₁₅ H ₁₄ O ₆	Altenusin	1.35×10^{-8}	35.56
257.04524	C ₁₄ H ₁₀ O ₅	Alternariol	7.67×10^{-10}	29.65
271.06105	C ₁₅ H ₁₂ O ₅	Alternariol monomethyl ether (AME)	6.37×10^{-9}	23.31
277.07153	C ₁₄ H ₁₄ O ₆	Alternarienoic acid	7.11×10^{-10}	20.63
413.21912	C ₂₂ H ₃₀ N ₄ O ₄	Tentoxin	2.25×10^{-8}	8.978

*Later determined to be based on presence/absence, rather than a fold change difference

Samples from both groups were investigated for the secondary metabolite, and it was determined that TeA was only present in group 1, while absent in group 2, rather than a fold change difference in concentration between the groups. Figure 17 illustrates detected peak areas of TeA in the PCA. *A. alternata*, *A. arborescens*, and *A. tenuissima*, which are all common isolates from North America, have been reported to produce TeA.^[102] However, Andersen (2002) reported that type strain isolates of *A. alternata* and *A. infectoria* did not produce TeA, suggesting tentative potential species identifications for group 2.^[103]

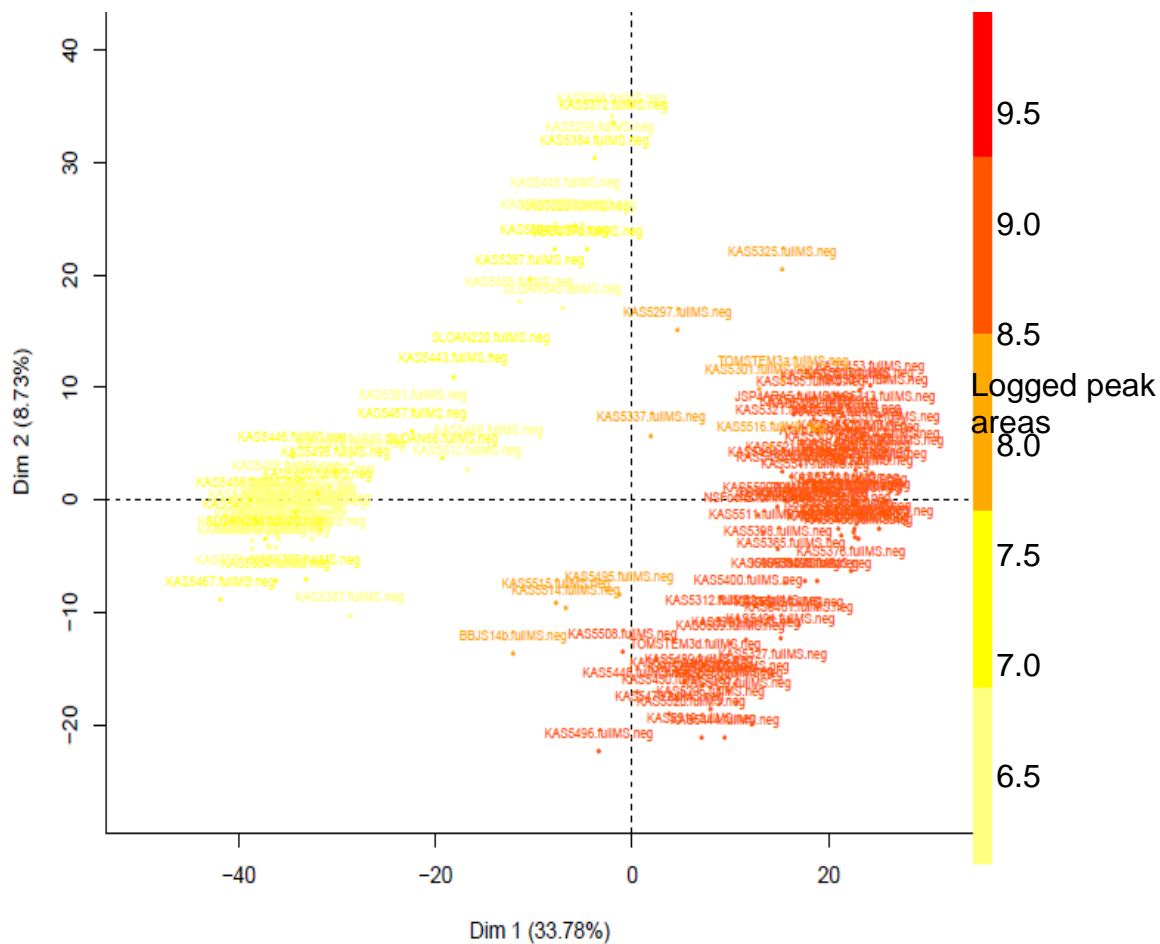


Figure 17- PCA plot from metabolomics data generated in negative ionization mode coloured by logged peak areas of TeA. Samples in red show larger peak areas detected

Other significant metabolites (Tables 2 and 3) responsible for the separation between the two groups were similarly investigated for their intensities within the groups, (Figure 18).

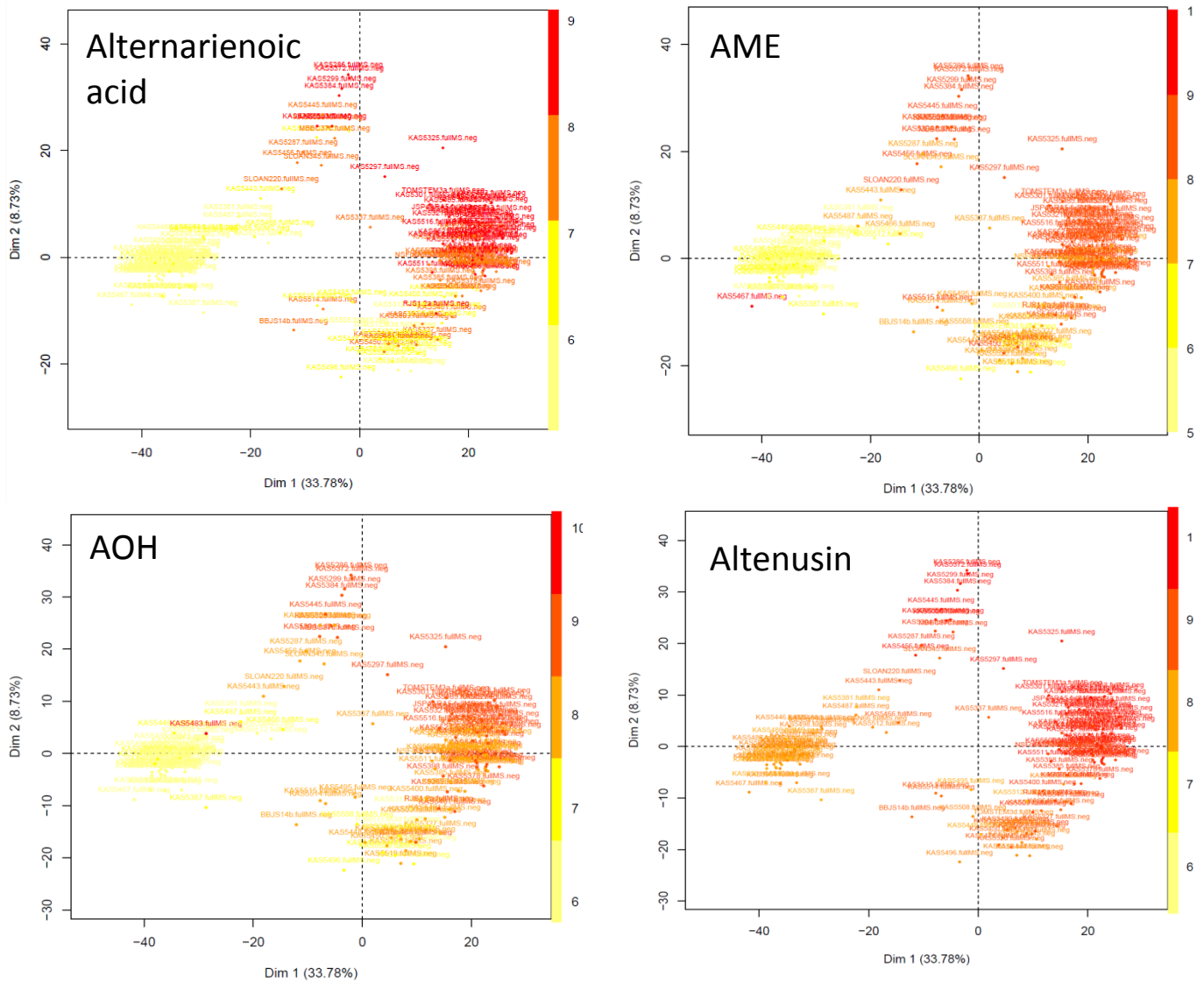


Figure 18- PCAs of metabolomics data generated in negative ionization mode, coloured by significant metabolites detected in group 1. Samples coloured darker red had larger peak areas

Table 3- Group 1 metabolites generated by the Wilcoxon test with FDR correction from data generated in positive ionization mode

m/z [M+H]	Molecular formula	Confirmed as	p-value (FDR corrected)	Fold change (peak area 1/2)
400.24842	C ₂₄ H ₃₃ NO ₄	Altersetin	1.65x10 ⁻¹³	155.94
273.07576	C ₁₅ H ₁₂ O ₅	AME	3.59x10 ⁻¹⁵	156.74
363.21663	C ₂₁ H ₃₀ O ₅	ACTG toxin F	4.98x10 ⁻¹⁷	142.00
349.23739	C ₂₁ H ₃₂ O ₄	ACTG toxin B or tricycloalternarene 1 (TCA 1)	4.98x10 ⁻¹⁷	141.69
259.06025	C ₁₄ H ₁₀ O ₅	Alternariol (AOH)	1.31x10 ⁻¹⁵	79.42
365.23239	C ₂₁ H ₃₂ O ₅	ACTG toxin C or TCA E	9.85x10 ⁻¹¹	43.24
347.22172	C ₂₁ H ₃₀ O ₄	ACTG toxin D or TCA 2a	6.21x10 ⁻¹⁵	21.41

Figure 18 demonstrates the peak areas (larger peak areas are dark red) detected for alternarienoic acid, alternariol (AOH), alternariol monomethyl ether (AME), and altenusin (ALU). These metabolites are largely absent (yellow) from some regions of the PCA, and abundant (red) in other regions within both groups, suggesting that there is additional separation within the two groups themselves. TeA was most responsible (Figure 17, Table 2) for the initial dimension 1 separation of the samples into two major groups, while alternarienoic acid, AOH, AME, and ALU (Table 2) caused separation within the groups themselves. The separation within the groups is important, as it may lead towards a more definitive species-level characterization based solely on metabolomics data.

Additional significant metabolites ($p < 0.01$) detected solely in positive ionization mode (Table 3) were altersetin, tricycloalternarenes (TCAs) and ACTG toxins. Altersetin, which was reported as a novel antibiotic, as also previously reported to be produced by both the *A. arborescens* and *A. tenuissima* species groups.^[34,104] TCAs and ACTG toxins are structurally-related secondary metabolites, but TCAs have been reported as host non-specific toxins, while ACTG toxins are host-specific toxins (HST).^[105] The occurrences of TCAs and ACTG toxins in Canadian agricultural commodities has not been described, and it is unclear which of the metabolites are present without paired nuclear magnetic resonance data for full structural characterization.

The separation within group 1 is described in 2.4.2.3.

2.4.2.2 Group 2 differentiation

One of the significant metabolites in group 2 corresponded to a m/z of 263.09300 [M-H], which was both statistically significant, ($p = 1.12 \times 10^{-8}$) and abundant (3.22×10^6), (Table 4). Comparing full MS to Antibase 2013 and MS² data (Supplementary Figure 1S) to published literature MS transitions both confirmed that it was the known *Alternaria* metabolite infectopyrone, which is solely produced by *Alternaria infectoria*. The secondary metabolite was previously reported as a novel biomarker for *A. infectoria*, and has since been detected along with phomapyrone and novaezelandins.^[34,103] A m/z 219 compound was also significant ($p = 8.92 \times 10^{-10}$) and abundant (3.22×10^6), (Tables 4 and 5) though it has not yet been reported in the literature. However, Andersen (2002) previously reported Unknown X with retention index of 907 as another potential biomarker along with infectopyrone, which may represent the 219 metabolite.^[34,103,106]

Table 4- Significant metabolites ($p < 0.01$) in group 2 from metabolomics data generated in negative ionization mode

m/z [M-H]	Molecular formula	Confirmed as	p-value (FDR corrected)	Peak area fold change (2/1)
263.09230	C ₁₄ H ₁₆ O ₅	Infectopyrone	1.12×10^{-8}	50.868
219.10199	C ₁₃ H ₁₆ O ₃	Unknown 1	8.92×10^{-10}	105.508
179.07030	C ₁₀ H ₁₂ O ₃	Unknown 2*	8.44×10^{-11}	21.203

Both metabolites were detected as being significantly different between groups 1 and 2 within negative and positive ionization modes, (Tables 4 and 5). Phomapyrones were also significantly different ($p < 0.01$) between the groups, but were detected solely in positive ionization mode (Table 4). Phomapyrones, in addition to novaezelandins (which were not detected) have all been reported as common secondary metabolites of *A. infectoria* from European isolates. *A. infectoria* and *A. alternata* have been previously analyzed by PCA through both morphological analysis of the conidial size and sporulation patterns, as well as through metabolite profiles.^[103,106] *A. infectoria* differs in both morphological and metabolite profiles, and is easily identified based on PCA.

Table 5- Significant metabolites ($p < 0.01$) in group 2 generated by the Wilcoxon test with FDR correction from metabolomics data generated in positive ionization mode

m/z [M+H]	Molecular formula	Confirmed as	p-value (FDR corrected)	Peak area fold change (2/1)
265.10710	C ₁₄ H ₁₆ O ₅	Infectopyrone	2.01x10 ⁻¹³	312.814
221.11729	C ₁₃ H ₁₆ O ₃	'219' Unknown 1	2.49x10 ⁻⁷	21.853
235.13285	C ₁₄ H ₁₈ O ₃	Phomapyrone A	1.67x10 ⁻⁷	98.059
233.11731	C ₁₄ H ₁₆ O ₃	Phomapyrone F	2.55x10 ⁻¹¹	30.662
251.12785	C ₁₄ H ₁₈ O ₄	Phomapyrone E/G	1.12x10 ⁻¹²	258.102
253.14346	C ₁₄ H ₂₀ O ₄	Unknown	9.50x10 ⁻¹⁶	71.978
203.17945	C ₁₁ H ₂₄ NO ₂	Unknown	1.68x10 ⁻¹²	57.238
233.11729	C ₁₄ H ₁₆ O ₃	Unknown	2.55x10 ⁻¹¹	30.662
269.13838	C ₁₄ H ₂₀ O ₅	Unknown	1.67x10 ⁻¹⁰	21.919
223.09649	C ₁₂ H ₁₄ O ₄	Phomapyrone D	1.48x10 ⁻¹⁴	8.424

Samples that produced both infectopyrone (Figure 19) and 219 (Figure 20) are similarly grouping together in the PCA, and appear to have larger peak areas localized within group 2 compared to other samples. The localized concentration of infectopyrone and the 219 peak, in addition to the presence of other significant group 1 metabolites investigated in Figure 19, also seem to suggest that there are subgroups within group 2. *A. infectoria* does not produce many of the common *Alternaria* metabolites, such as tenuazonic acid (TEA), alternariol (AOH), or alternariol monomethyl ether (AME), so the localized production of infectopyrone and the 219 peak by certain samples may suggest their tentative identification as *A. infectoria*. The only other reported species of *Alternaria* known to not produce TeA is *A. alternata*, suggesting a potential species-level identification for the other subgroup within group 2. Group 2 subgroups are discussed in 2.4.2.4.

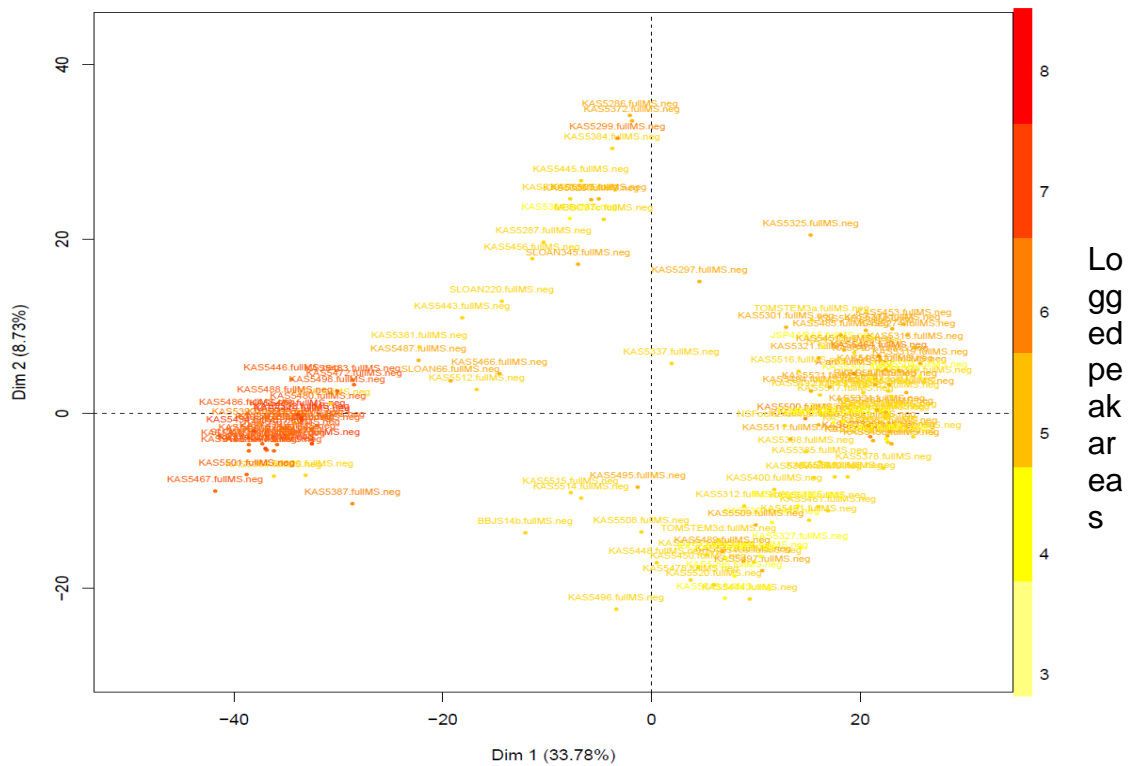


Figure 19- PCA plot from data generated in negative ionization mode coloured by infectopyrone peak area. The darker red areas indicate larger peak areas detected in the samples

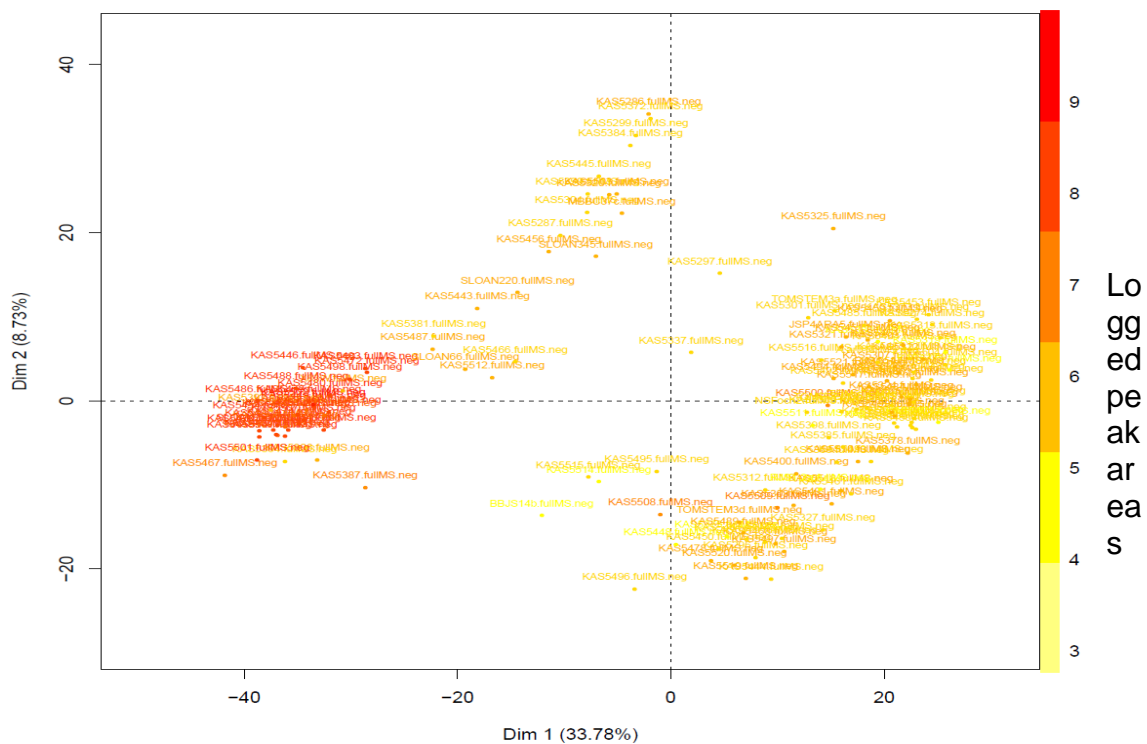
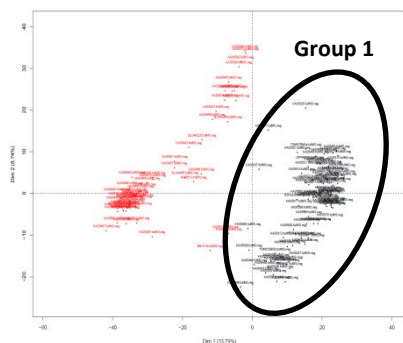


Figure 20- PCA plot from data generated in negative ionization mode coloured by 219 peak area. The darker red areas indicate larger peak areas detected in the samples

2.4.2.3 Group 1 subgroups



The metabolite differences within group 1 (Figure 18) were investigated for potential subgroups through K means clustering analysis, (Figure 21). All samples in group 1 were re-analyzed separately to avoid potential carry-over from other groups from the global metabolomics analysis. Figure 21 confirms the clustering of the samples into two separate subgroups, (1A and 1B). Similar to the global metabolomics, significant metabolites between the subgroups were investigated using the Wilcoxon test, (Table 6).

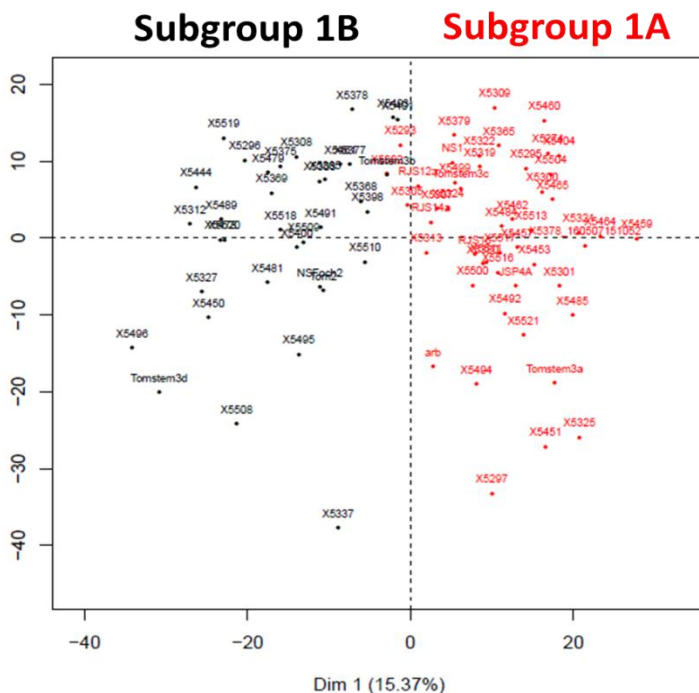


Figure 21- PCA of metabolomics data within group 1 generated in negative ionization mode. Samples are coloured by their K means clustering assignment

Table 6- Subgroup 1A metabolites generated by the Wilcoxon test with FDR correction in negative ionization mode

<i>m/z</i> [M-H]	Molecular formula	Confirmed as	Corrected p-value	Fold change (Area A/Area B)
189.05472	C ₁₁ H ₁₀ O ₃	2,5-dimethyl-7-hydroxychromone	6.02x10 ⁻¹⁵	44.289
231.06567	C ₁₃ H ₁₂ O ₄	Altechromone B	4.37x10 ⁻¹⁶	87.803
319.04568	C ₁₅ H ₁₂ O ₈	Alternarian acid	4.72x10 ⁻¹⁰	93.478
289.07159	C ₁₅ H ₁₄ O ₆	Altenuisin	2.04x10 ⁻¹⁹	80.078
273.04032	C ₁₄ H ₁₀ O ₆	Altenuisol	1.62x10 ⁻¹¹	50.167
287.05596	C ₁₅ H ₁₂ O ₆	3-hydroxyalternariol 5-O-methyl ether (I)	2.75x10 ⁻¹⁸	48.218
287.05581	C ₁₅ H ₁₂ O ₆	3-hydroxyalternariol 5-O-methyl ether (II)	8.03x10 ⁻¹⁴	12.807
287.05587	C ₁₅ H ₁₂ O ₆	Dehydroaltenuisin (DHA)	2.04x10 ⁻¹⁹	33.422
321.06130	C ₁₅ H ₁₄ O ₈	Altenuic acid II	2.04x10 ⁻¹⁹	40.616

It was initially assumed that the two subgroups within group 1 were to be *A. arborescens* and *A. tenuissima* due to their abundance in food crops, such as wheat, blueberries and apples.^[34,92,107] Both species have very similar genomes, and reported metabolites with the exception of dehydroaltenuisin, (produced by *A. arborescens*) and altertoxin III (produced by some isolates of *A. tenuissima*).^[31,34] This trend seemed to be in agreeance with the observed metabolites within the two subgroups, as there were not any metabolites that were present or absent from either group; many metabolites were in higher abundance, (subgroup 1A) but still shared between the two groups. Andersen (2015) reported that altenuisol was not detected in the *A. arborescens* or *A. tenuissima* isolates.^[34] As altenuisol was reported to be a significant metabolite ($p = 1.62 \times 10^{-11}$), and was approximately 50 fold higher in subgroup 1A, it can be inferred that a species-level definition for subgroup 1A cannot be confidently identified from the current metabolomics data at this time.

Altenuisol was investigated in the PCA of group 1, (Figure 22) which is predominantly produced by samples in subgroup 1A. There is overlap between subgroups for altenuisol, suggesting that

while the metabolite is absent in the majority of the samples from subgroup 1B, it may still be produced by several individual isolates.

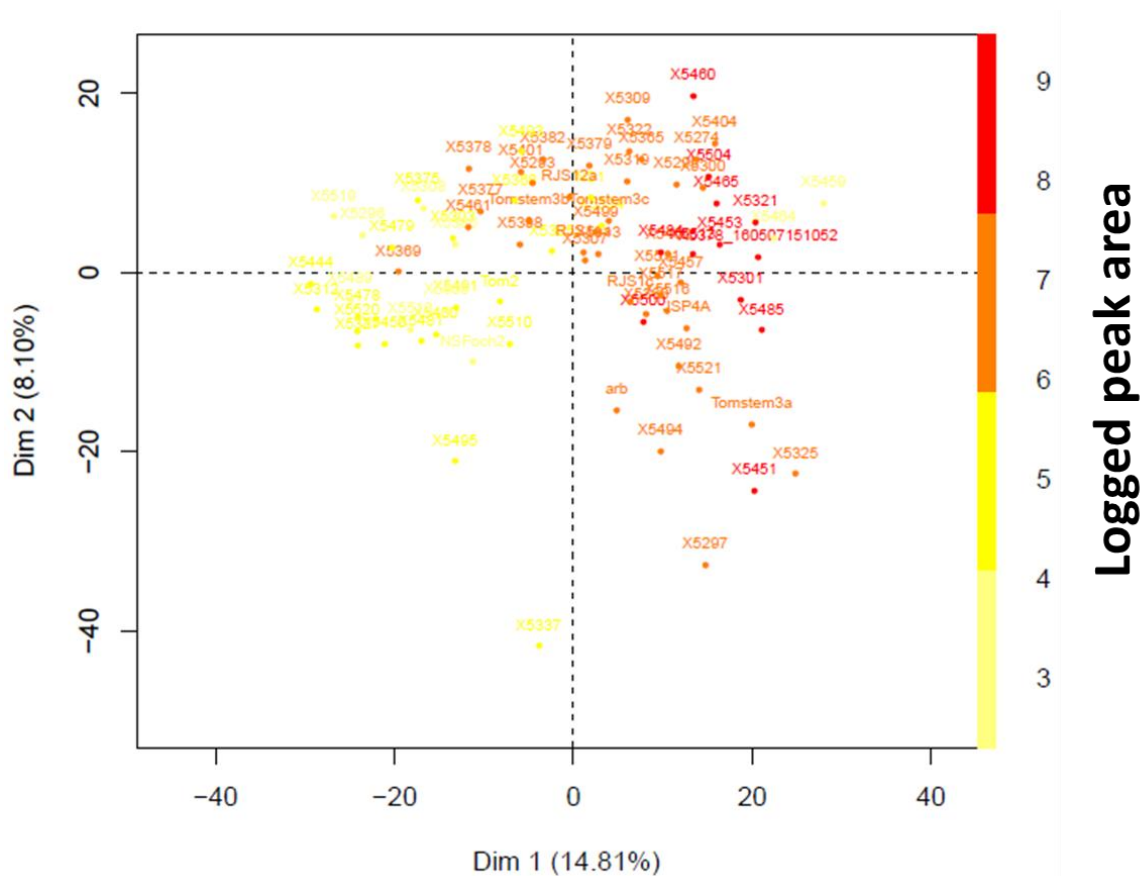


Figure 22- PCA of metabolomics data generated in negative ionization mode. Samples are coloured by the peak area of altenuisol. Darker red areas indicate larger peak areas detected

On examination of the chromatograms in subgroups 1A and 1B for dehydroaltenusin (significant in subgroup 1A, $p= 2.04 \times 10^{-19}$, $C_{15}H_{12}O_6$, RT: 3.06), it was noted that there were 3 individual peaks in the chromatogram, separated by different retention times, suggesting possible isobaric secondary metabolites (Figure 23). One of those peaks corresponded to the known secondary metabolite of *Alternaria*, 4-hydroxyalternariol 5-O methyl ether (RT: 3.34). The metabolite was approximately 50 fold higher in subgroup 1A, and its identity was confirmed by MS² spectra (Figure 24). Similarly, dehydroaltenusin (RT 3.06) was approximately 30 fold higher in subgroup 1A than subgroup 1B (Figure 25). Smaller peaks at RT: 3.38 and 3.64 suggest possible structural isomers of 3-hydroxyalternariol 5-O methyl ether, where the methyl ether may be linked through another carbon.

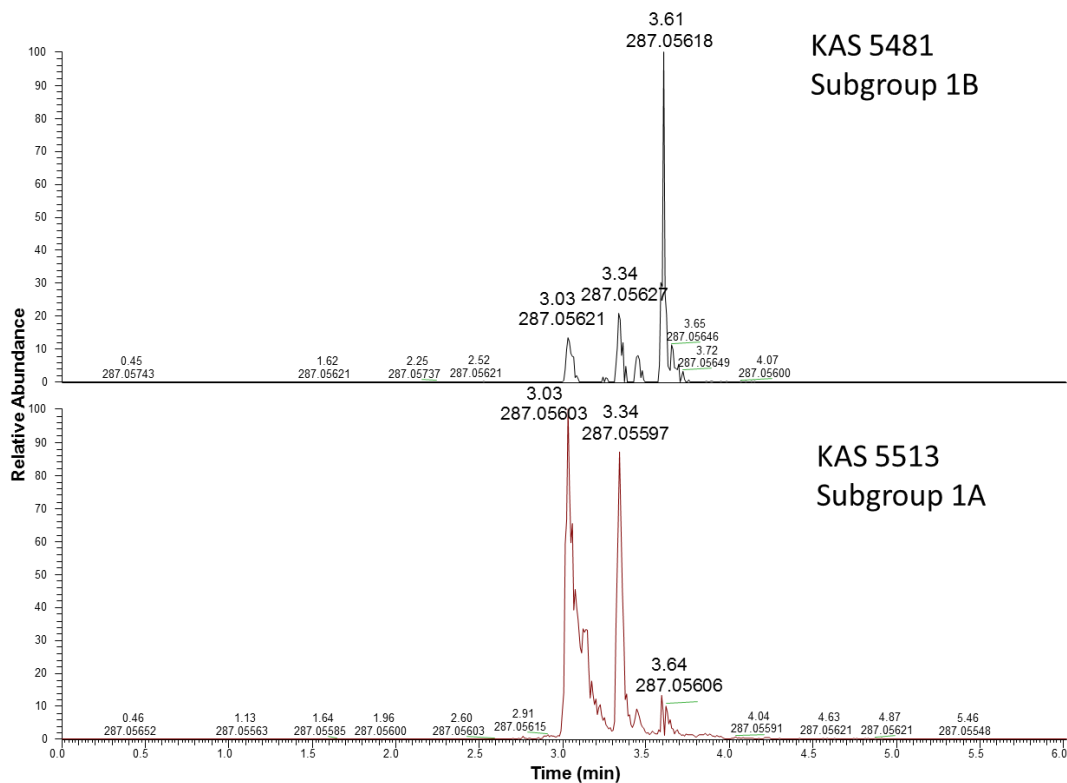


Figure 23- Extracted ion chromatogram for $C_{15}H_{12}O_6$, which was significant in subgroup 1A

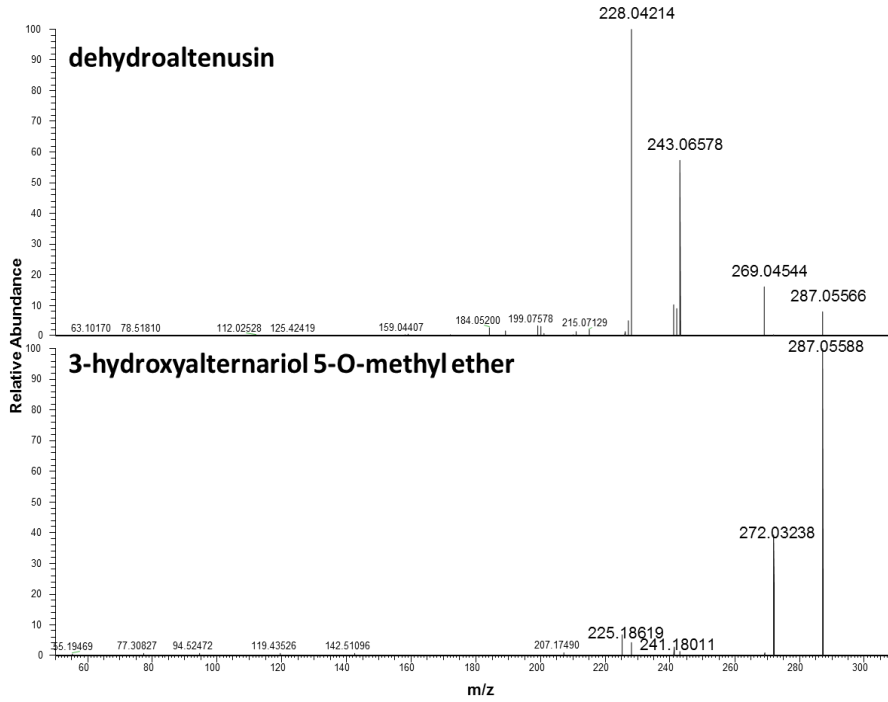


Figure 24- ddMS² spectra for the isobaric compounds dehydroaltenusin (top) and 3-hydroxyaltenariol 5-O-methyl ether (bottom)

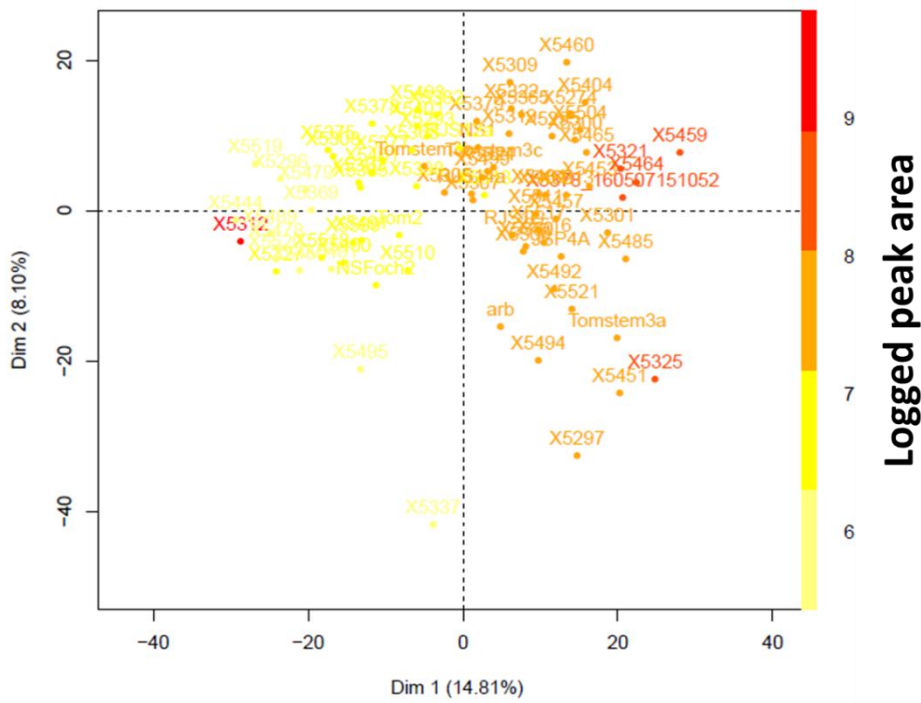


Figure 25- PCA of metabolomics of group 1 data generated in negative ionization mode, coloured by peak area intensity of dehydroaltenusin

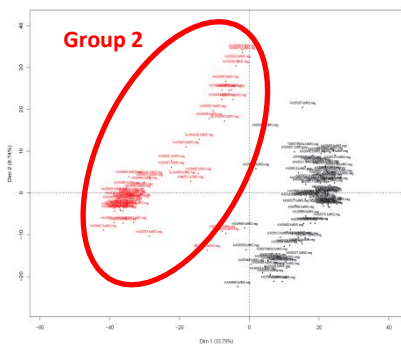
There were only a few significant metabolites that were different within subgroup 1B (Table 7), with the majority of metabolites existing as unknowns. While the subgroups of 1A and 1B could be differentiated, 5 to 10 x fold changes in metabolite peak area are not helpful for positive identification- especially when the sample size has decreased. Subgroup 1B produces similar metabolites to subgroup 1A, but the metabolites are less abundant. Whether this is variation within the same species, or variation between two closely related species remains unclear.

Another suggestion was that the two subgroups consisted of differing genotypes of *A. alternata*, due the presence of a superfluous chromosome influencing its secondary metabolome.^[94] There are at least ten species pathotypes of *Alternaria* which can produce HSTs, and seven of them are reported to be distinct pathotypes of *A. alternata*.^[108] To potentially identify species within the *Alternaria* subgroups, the sporulation patterns may need to be determined as per Simmons, 2007, and then combined with the metabolomics data for a more confident answer.^[88]

Table 7- Significant metabolites in subgroup 1B as determined by the Wilcoxon test with FDR correction in negative ionization mode

<i>m/z</i> [M-H]	Molecular formula	Confirmed as	Corrected p- value	Fold change (Area B/Area A)
319.15502	C ₁₈ H ₂₄ O ₅	Tricycloalternarene A (TCA A)	5.28x10 ⁻³	5.587
170.11752	C ₉ H ₁₇ NO ₂	Unknown 1	3.78x10 ⁻⁴	10.968
427.17925	C ₂₃ H ₄₀ O ₇	Unknown 2	9.69x10 ⁻³	7.846
276.12389	C ₁₅ H ₁₉ NO ₄	Unknown 3	1.05x10 ⁻³	5.966
214.14413	C ₁₁ H ₂₁ NO ₃	Unknown 4	1.19x10 ⁻⁹	4.520
266.13961	C ₁₄ H ₂₁ NO ₄	Unknown 5	3.35x10 ⁻³	9.158

2.4.2.4 Group 2 subgroups



To investigate potential separations within group 2, the data were plotted separately as a PCA using K-means clustering analysis to determine any potential groups. All samples from group 2 were also re-run to reduce carry-over and to confirm the accuracy of the clustering, and the secondary metabolite analysis. Due to the smaller subset of data, minor differences observed in the PCA, such as slight differences in intensity, may be exaggerated; therefore, only large fold changes of metabolites are reported.

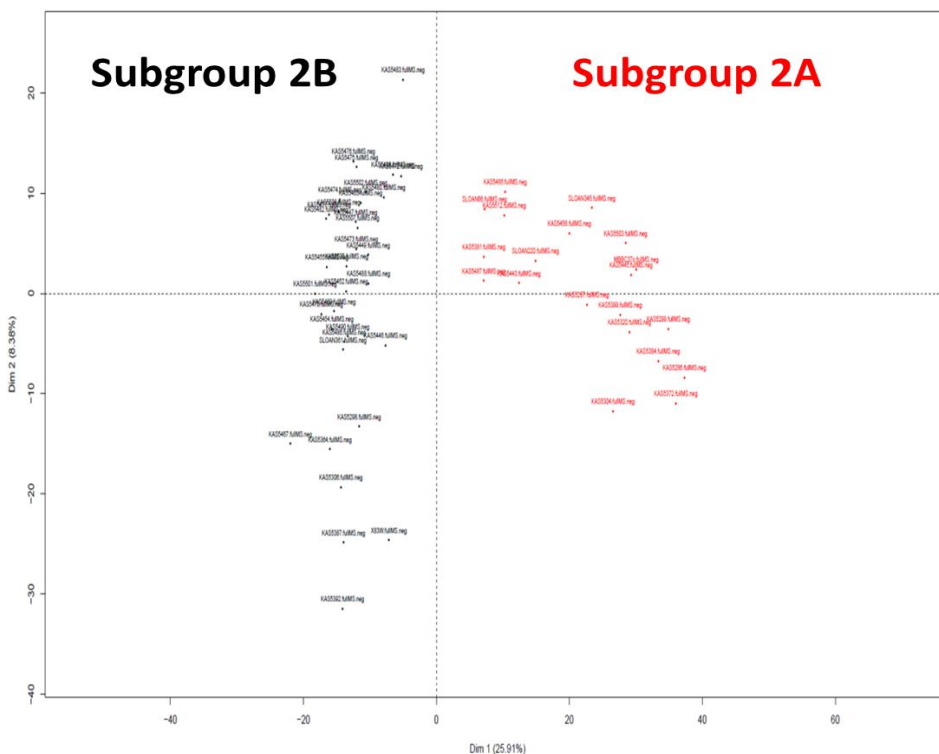


Figure 26- PCA showing separation within group 2 in negative ionization mode. Samples are coloured by the K means clustering algorithm

K-means clustering analysis within the group supports the further separation of group 2 into two smaller subgroups, 2A (red) and 2B (black), (Figure 26). Metabolites responsible for the separation were investigated using Wilcox test with FDR correction, and are reported in Tables 6 (subgroup B) and 7 (subgroup A).

Table 8- Showing subgroup 2B metabolites generated by the Wilcoxon test with FDR correction

<i>m/z</i> [M-H]	Molecular formula	Confirmed as	Corrected p-value	Fold change (area B/A)
219.10191	C ₁₃ H ₁₆ O ₃	Unknown	3.03x10 ⁻⁶	3615.0810
263.09221	C ₁₄ H ₁₆ O ₅	Infectopyrone	1.88x10 ⁻⁷	694.1310
299.05920	C ₁₃ H ₁₆ SO ₆	SO ₃ of 219 unknown	5.53x10 ⁻⁶	191.0908
263.12848	C ₁₅ H ₂₀ O ₄	Absciscic acid	5.40x10 ⁻⁵	66.4779
251.09212	C ₁₃ H ₁₆ O ₅	3-methoxy-3-epiradicinol	4.71x10 ⁻⁶	48.1581

The unknown 219 peak and infectopyrone are both reported as significant metabolites, ($p = 3.03 \times 10^{-6}$ and 1.88×10^{-7} respectively) which are responsible for the variation between subgroups A and B, (Table 6). Figure 27 shows group 2 with metadata showing the substrate from which the species were isolated. Subgroup B appears to be predominantly being isolated from wheat with the minor exception of some various perennial species. This further supports the tentative identification of *A. infectoria* for subgroup B, as *A. infectoria* predominantly, (though not solely) infects wheat.^[109,110] There is minor variation within the subgroup from perennial species due caused by small fluctuations in intensity for some of the shared secondary metabolites. On inspection, both sets still reported similar peak areas for both the 219 unknown metabolite, and infectopyrone suggesting that they are still *A. infectoria*. While these samples were included for calculation of p-values and significant metabolites, they were removed for subsequent PCA analyses. 3-methoxy-3-epiradicinol, ($p = 4.71 \times 10^{-6}$) was also detected, and was previously reported to be a secondary metabolite solely produced by *A. infectoria*.^[34]

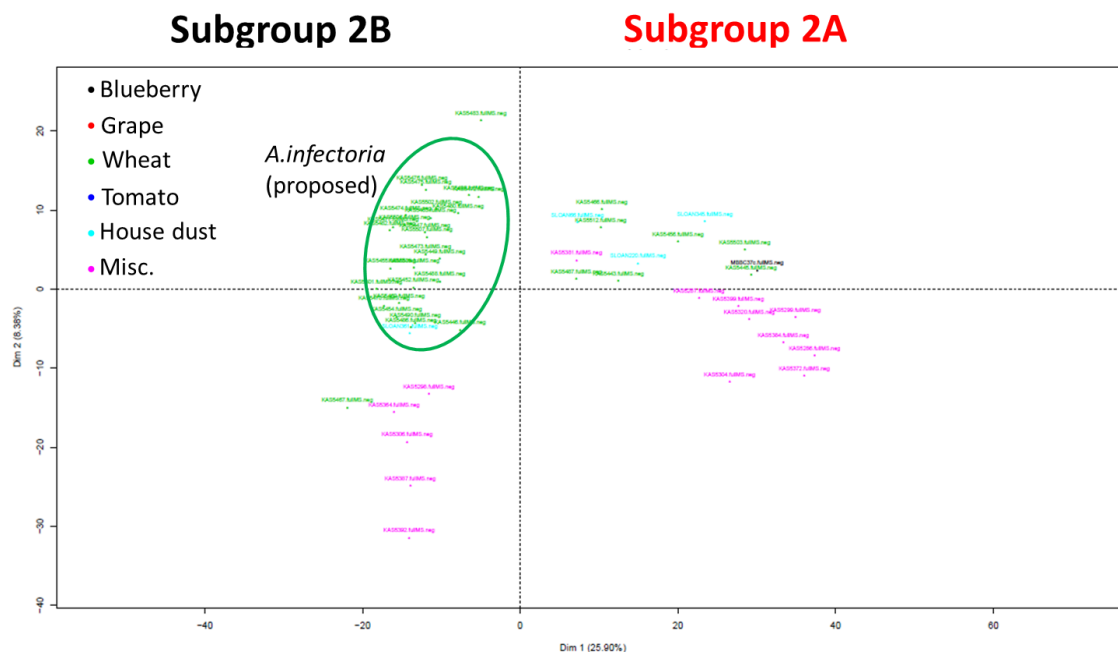


Figure 27- PCA of group 2 coloured by host substrate

The secondary metabolites responsible for the variation in the subgroup 2A PCA (Figure 26) are due to the large upregulation of the common *Alternaria* metabolites, such as alternariol (AOH), alternariol monomethyl ether (AME) and its sulfoconjugate, dehydroaltenusin and its sulfoconjugate, and altersetin (Table 7).^[111] It has been previously reported that *A. infectoria* does not produce these common metabolites, further supporting that subgroup 2B is *A. infectoria*.^[34,103] Additionally, it was demonstrated that altenuisol was detected approximately 3300 fold higher in subgroup 2A than in subgroup 2B, (Table 7). Andersen (2015) also reported that the *A. alternata* strains, which also did not produce TeA or tentoxin (TEN), produced altenuisol (altertenuol), while *A. infectoria*, *A. arborescens* and *A. tenuissima* did not.^[34] To confirm, the PCA was coloured by altenuisol peak area for the group 2 samples, (Figure 28). The largest peak areas detected for altenuisol are concentrated in subgroup 2A for the majority of the samples. In addition to the lack of production of TeA and TEN, and the production of the common *Alternaria* secondary metabolites (Table 7), the production of altenuisol is further confirmation that subgroup 2A is *A. alternata*. There are conflicting reports of the predominance

of *A. alternata* isolates from agriculture sources in the literature; many suggest *A. alternata* is the predominant species, however that may be related to the misclassification of *A. tenuissima* and *A. arborescens*.^[107] Significant secondary metabolites as evaluated by the Wilcoxon test are summarized below in Table 10.

Table 9- Showing subgroup 2A metabolites from group 2 generated by the Wilcoxon test using FDR correction

<i>m/z</i> [M-H]	Molecular formula	Confirmed as	p-value (FDR corrected)	Fold change (area A/B)
257.04520	C14H10O5	Alternariol (AOH)	5.08x10 ⁻⁹	416.0430
271.06102	C15H12O5	Alternariol monomethyl ether (AME)	4.40x10 ⁻⁷	216.2170
273.04029	C14H10O6	Altenuisol (altertenuol)	2.87x10 ⁻⁶	3227.7020
275.05596	C14H12O6	Talaroflavone	5.53x10 ⁻⁶	237.0023
277.07147	C14H14O6	Alternarienoic acid	2.16x10 ⁻⁷	89.2513
287.05588	C15H12O6	Dehydroaltenuisin (DHA)	6.91x10 ⁻⁶	272.6997
289.07159	C15H14O6	Altenuisin	7.38x10 ⁻⁷	298.3280
351.01775	C15H12SO8	AME-SO3	2.72x10 ⁻⁵	1482.1320
363.21755	C21H32O5	Brassicicene F	7.67x10 ⁻⁷	149.6401
367.01259	C15H12SO9	DHA-SO3	6.91x10 ⁻⁶	304.2002
398.23356	C24H33NO4	Altersetin	5.05x10 ⁻⁴	172.7359

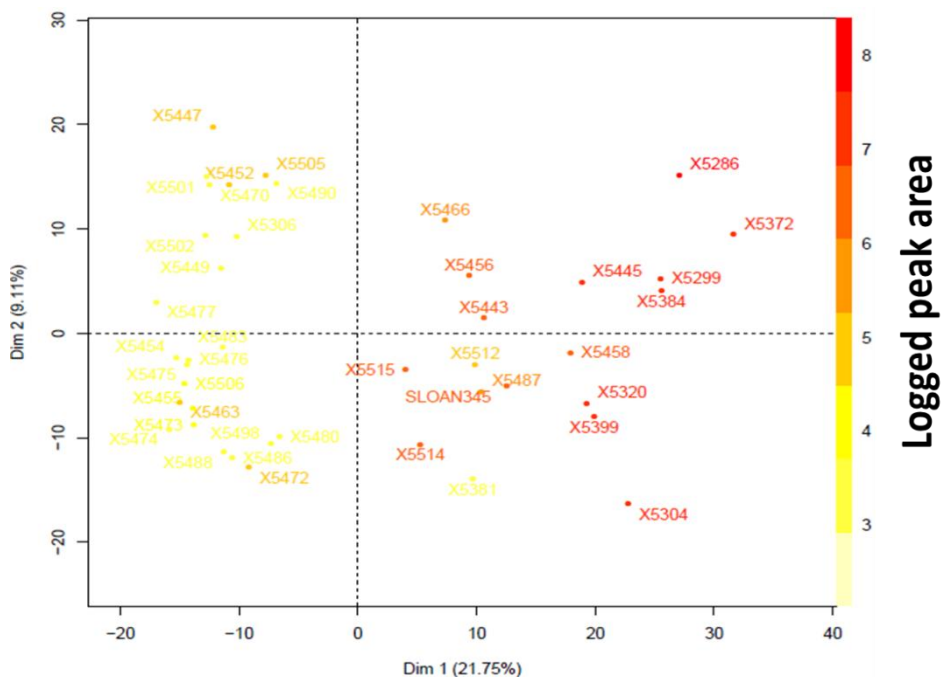


Figure 28- PCA of group 2 metabolomics data generated in negative ionization mode. Samples are coloured by the peak area of altenuisol. Darker red areas indicate larger peak areas detected

Table 10- Summary of significant metabolites detected in both negative and positive ionization mode, and evaluated by the Wilcoxon test for significance

	1A	1B	2A	2B
2,5-dimethyl-7-hydroxychromone	++	+		
ACTG toxins/TCAs	++	++		
Altechromone B	++	+		
Alternarian acid	++	+		
Altenusin	++	+	++	
Altenuisol (altertenuol)	++	+	++	
3-hydroxyalternariol 5-O-methyl ether (I)	++	+		
3-hydroxyalternariol 5-O-methyl ether (II)	++	+		
Dehydroaltenusin (DHA)	++	+	+	
Altenuic acid II	++	+		
Tricycloalternarene A (TCA A)	+	++		
Unknown 219				++
Infectopyrone				++
SO ₃ of <i>m/z</i> 219 unknown				++
Abscisic acid				++
3-methoxy-3-epiradicinol				++
Phomapyrone (A, F, E/G)				++
Alternariol (AOH)	++	++	++	
Alternariol monomethyl ether (AME)	++	++	++	
Talaroflavone	++	++	++	
Alternarienoic acid	++	++	++	
AME-SO ₃	++	++	++	
Brassicicene F	++	++	++	
DHA-SO ₃	++	++	++	
Altersetin	++	++	++	
Tenuazonic acid	++	++		
Tentoxin	++	++		

2.5 Conclusions and future work

The distribution of metabolites produced by 148 pathogenic Canadian species of *Alternaria* was examined using non-targeted high resolution mass spectrometry (HRMS), (Table 10). Through statistical analysis of the global metabolome, there is a better consensus of the specific Canadian chemotypes that are present, and their associated secondary metabolites as a risk assessment for their production in Canadian crops.

The non-targeted metabolomics approach was capable of differentiating *A. infectoria* and *A. alternata* (subgroups 2B and 2A respectively) from the four subgroup chemotypes detected based on the presence or absence of numerous metabolites. Subgroups 1A and 1B share similar metabolites, with many being upregulated approximately 50 fold in subgroup 1A. The accompanying species level differentiation information based on the RGP2 primer is reported as supplementary, however no species-level definitions could be reported based solely on the metabolite differences between strains.^[32] The differences may assist mycologists in future species-level or section assignments. Metabolomics data appears to be able to solely differentiate between different sections of *Alternaria*. However, metabolomics data from closely related species within sections should be combined with sporulation group information, or with molecular methods, such as DNA fragment separation by pulsed field gel electrophoresis (PFGE).^[88]

Chapter 3- Semi-targeted detection of new mycotoxins and secondary metabolites in Canadian agricultural commodities

Identification of six new *Alternaria* sulfoconjugated metabolites by high-resolution neutral loss filtering

Kelman, M.J., Renaud, J.B., Seifert, K.A., Mack, J., Sivagnanam, K., Yeung, K., Sumarah, M.W. Identification of six new *Alternaria* sulfoconjugated metabolites by high resolution neutral loss filtering. *Rapid Commun Mass Sp.* **2015**, 29(19), 1805, DOI: 10.1002/rcm.7286

Detection of total AAL-toxins and enniatins using product ion filtering

Renaud, J.B., Kelman, M.J., Qi, T., Seifert, K.A., Sumarah, M.W. Product ion filtering with rapid polarity switching for the detection of all fumonisins and AAL-toxins. *Rapid Commun Mass Sp.* **2015**, 29(22), 2131, DOI: 10.1002/rcm.7374

3.1 Chapter 3 objectives

The objective of chapter 3 was to validate post data-acquisition semi-targeted screening methods using neutral loss filtering, and product ion filtering. Both semi-targeted methods were evaluated for use in tandem with targeted mass spectrometry to describe new, emerging and modified mycotoxins in agricultural commodities.

Identification of six new *Alternaria* sulfoconjugated metabolites by high-resolution neutral loss filtering

3.2- Introduction

Alternaria is a cosmopolitan genus of fungi, and the genus has been reported as a plant pathogen for several important pre and post-harvest agricultural commodities, including: wheat, cereal grains, tomatoes, olives, fruits, and seeds.^[106-108] More than 70 phytotoxic secondary metabolites from *Alternaria* spp. have been described to date, some of which have also been described as mycotoxins.^[113,114] In addition to contributing to nonspecific interactions with plants, some secondary metabolites of *Alternaria* have also been reported as having host-specific interactions; such interactions control pathogenicity or virulence factors in certain host plants.^[115,116] One strain of *A. arborescens* isolated from tomatoes in California was reported to produce AAL-toxins; these are structurally similar to fumonisins, which are within the polyketide class of mycotoxins responsible for disruption of sphingolipid metabolism.^[117] The most common *Alternaria* metabolites found in food, alternariol (AOH) and alternariol monomethyl ether (AME), were first isolated and characterized by Raistrick et al. in 1953.^[118] Although not acutely toxic, AOH and AME have been reported to be *in vitro* mutagens.^[119,120] *Alternaria* spp. have also been reported to produce altenuene (ALT) which is genotoxic *in vitro*, and teratogenic in rats.^[36] Some *Alternaria* mycotoxins have been shown to be stable under typical food processing conditions.^[114] These mycotoxins have been detected in carrots, berries, onions, tomatoes, as well as in their processed food products including vegetable and fruit juices, and baked bread.^[32,121-124] At present, there are no regulations for *Alternaria* toxins in food. The European Food Safety Authority (EFSA) provided an opinion on a number of *Alternaria* metabolites. The

Threshold of Toxic Concern (TTC) methodology is often used to assess the potential hazards and provide a risk assessment for compounds with unknown toxicity based on the known chemical structures.^[125] Based on the TTC data for *Alternaria* secondary metabolites, the EFSA has suggested a tolerable daily intake of 2.5 ng/kg body weight per day and has recommended further exposure assessments.^[126] Targeted LC-MS methods have been developed to screen agricultural commodities and their processed products for secondary metabolites produced by *Alternaria*.^[34,36,119,121,122] However, secondary metabolites and mycotoxins may also occur in conjugated forms, where the metabolite is modified by the fungus (or the host plant) and is conjugated to another molecule such as glucose, acetyl groups, or even to macromolecules.^[25] As such, any conjugated metabolites would be missed using a targeted LC-MS screening method; this demonstrates the need for additional semi-targeted screening tools for mycotoxin analysis. It has been speculated that conjugated *Alternaria* secondary metabolites, along with their parent forms could occur in affected foods.^[119] Sulfoconjugated forms of AOH and AME have been previously reported from *Alternaria*.^[129] Alternariol 5-O-sulfate (AOH-SO₃) was screened against L5178Y mouse lymphoma cells *in vitro* for cytotoxic activity. It demonstrated lower bioactivity than the free AOH, but higher bioactivity compared to free AME.^[129] These compounds could be critical when determining safe levels for human and animal consumption due to the fact that many conjugated mycotoxins such as deoxynivalenol (DON) glucoside are not detected by traditional analytical methods.^[25,119,126]

Upon collisional activation, many sulfated ions display a distinctive neutral mass loss of SO₃. Neutral loss scanning (NLS) on a triple quadrupole mass spectrometer can monitor this transition for the semi-targeted detection of sulfoconjugated metabolites.^[130–132] High resolution instruments such as the Orbitrap Q-Exactive are not able to perform true NLS, however, post-acquisition data processing techniques such as neutral loss filtering (NLF) of MS² datasets allows for detection of a specific neutral loss, in this case SO₃. Increased resolution and mass measurement accuracy have been shown to greatly lower the amount of interference ions and thus increase the selectivity of NLF.^[133] A rapid LC, data dependent MS² method with NLF was implemented to screen 148 Canadian strains of *Alternaria* spp. for production of sulfoconjugated metabolites in a variety of different fermentation media.

3.2- Experimental

3.2.1 Fungal material and identification

As previously described for the global metabolomics screening (2.2.1), 148 Canadian strains of *Alternaria* spp. were isolated from plant material or were obtained from the Canadian Collection of Fungal Cultures (CCFC) in Ottawa, Ontario. The majority of these strains were isolated from grain, with additional strains isolated from tomato, apple, grape, and various perennial shrubs. Individual strains were identified within the genus *Alternaria* based on molecular ITS sequencing using ITS1 and ITS4 primers (Life Technologies), and by comparison to the NCBI BLAST database. Morphological identifications were performed at Agriculture and Agri-Food Canada (AAFC) in Ottawa, Ontario by Dr. Keith Seifert and Mr. Jonathan Mack. Strains were transferred onto potato dextrose agar (PDA) plates (Sigma Aldrich) as 3-point inoculations and incubated at 25°C in the darkness for 7 days, or until the colonies reached approximately 4 cm in diameter. Additional information about the strains is provided in Appendix A2.

3.2.2 Plug extraction and fermentation in liquid media, on Cheerios and rice

Initial metabolomic screening of the 148 *Alternaria* spp. strains was performed as previously described (2.2.2) by removing six agar plugs from each three-point inoculum using a 6 mm cork borer and extracting the plugs with ethyl acetate containing 1% formic acid (Sigma, St. Louis, MO) prior to LC-MS screening.^[91,95]

Based on initial metabolomic screening, seven strains were selected for three week fermentations in potato dextrose broth (PDB), (Sigma Aldrich), which included three strains isolated from wheat, two from apples, one from tomatoes, and one from grapes. The fungal mycelium (cells) from the fermentations was filtered (Whatman #4) from the liquid media, lyophilized, extracted with ethyl acetate and analyzed by LC-HRMS and MS² analysis (3.2.3). The filtrate from the same PDB fermentations were similarly subsequently extracted with ethyl acetate and analyzed by LC-MS, (3.2.3).^[134]

The same seven strains were also inoculated onto Cheerios and rice to ensure the metabolites observed were not artefacts of the artificial media, in addition to assessing their potential occurrence in grains. 50 g sterile cooked long grain white rice was inoculated with a 3x3 cm portion of macerated fungal material in 25 mL sterilized distilled water and extracted with chloroform and 1:1 methanol:water after three weeks of fermentation.^[129] 80 mL portions of

moistened Cheerios, supplemented with 0.3% sucrose and 0.005% chloramphenicol, were similarly inoculated and extracted as above after four week fermentations.^[135] Extracts from rice and Cheerios were dried, reconstituted in methanol and filtered with 0.45 μ m PTFE syringe filters (Pall Acrodisc) prior to LC-MS analysis.

3.2.3 LC-HRMS and MS² analysis

HRMS and HRMS² data were obtained using a Thermo Q-Exactive Quadrupole Orbitrap Mass Spectrometer, coupled to an Agilent 1290 high-performance liquid chromatography (HPLC) system using a C18 Zorbax Eclipse Plus RRHD column (2.1 x 50 mm, 1.8 μ m; Agilent) held at 35 °C. 2 μ L sample injections were used at a flow rate of 0.3 mL/min. The mobile phase was comprised of water with 0.1% formic acid (A), and acetonitrile with 0.1% formic acid (B) (Optima grade, Fisher Scientific, Lawn, NJ). Mobile phase A was held at 100% for 30 seconds, before increasing to 100% B over three and a half minutes. B was kept at 100% for 1 and a half minutes, before returning to 100% A in 30 seconds. Negative HESI conditions used were as follows: capillary voltage, 3.7 kV; capillary temperature, 400°C; sheath gas, 17.00 units; auxiliary gas, 8.00 units; probe heater temperature, 450 °C; S-Lens RF level, 45.00. The data dependent MS² (ddMS²) used the following settings for full MS: scan range, 75 – 800 m/z ; resolution, 70 000; AGC, 3e6; max IT, 250 ms. The top five ions based on intensity from the MS were mass selected using a 1.2 m/z isolation window, and selected ions were excluded from further MS² scans for 10 s. Selected ions were monitored using the following conditions: resolution, 17 500; AGC target, 1e5; max IT, 60 ms; NCE, 27; threshold intensity, 1.2e5. Samples were also analyzed by LC-MS as described above at a resolution of 140 000 using a max IT of 500 ms. Neutral loss plots were visualized using MZmine 2.13.1 using acquired HRMS and HRMS² data.^[136] Pseudo MS³ scans were performed in negative ionization mode by applying in-source CID of 35 eV and 5 units of sweep gas, and a mass selection for the free metabolite under a 1.2 m/z isolation window, (Figure 29).^[64]

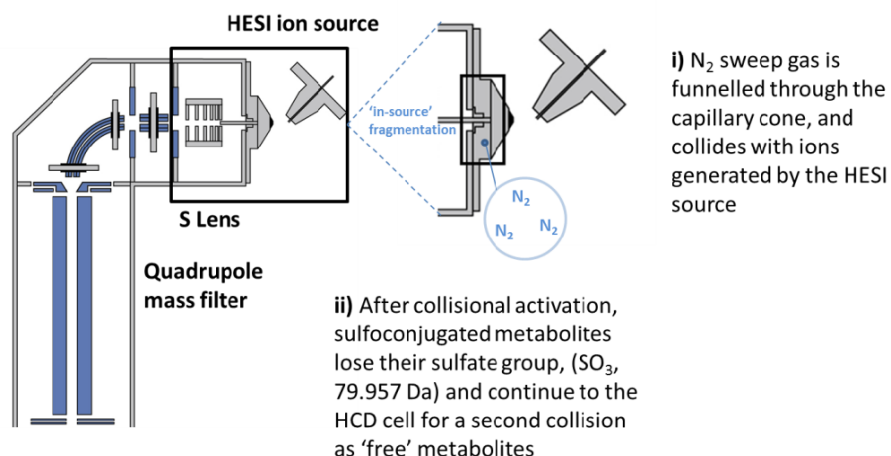


Figure 29- 'In source' generated fragment ions for pseudo MS³ of sulfoconjugated metabolites[64]

3.3 Results and Discussion

As part of an ongoing study of emerging mycotoxins in Canadian agricultural commodities, cultures of *Alternaria* spp. were examined to assess the potential for secondary metabolite production by Canadian strains, and the subsequent crop contamination by these metabolites. 148 strains of *Alternaria* spp. were screened for secondary metabolite production using a rapid LC-MS method in both positive and negative mode. Initial inspection of the MS² data in negative ion mode revealed that a number of metabolites displayed a distinct neutral mass loss of 79.957 Da, which is indicative of the presence of a SO₃. As several sulfoconjugated secondary metabolites of *Alternaria* had been previously reported^[129], post data-acquisition NLF was used to assess the extent of sulfoconjugation in *Alternaria* extracts. NLF was visualized through a neutral loss plot, which was constructed (Figure 30) in MZmine 2.13.1 using complete datasets of individual samples.

Neutral loss plots aid in the quick inspection of mass spectrometry data through the observation of precursor metabolite ions losing characteristic neutral masses. Figure 30 demonstrates the extensive sulfation present in the *Alternaria* extract. The Q-Exactive's high mass accuracy of less than 2 ppm results in a decrease in interfering signals surrounding the actual metabolite peak; this is particularly important if the metabolites are in low abundance. Combined with resolutions measured above 100 000, the Q-Exactive is able to fully resolve the ¹³Cx2 isotope

peak from the ^{34}S isotope peak in the fine isotope pattern of the full MS data. This leads to the confirmation of the elemental formulae of the metabolites; differentiation between other closely related masses using lower resolution instruments, such as a triple quadrupole, would not be possible.

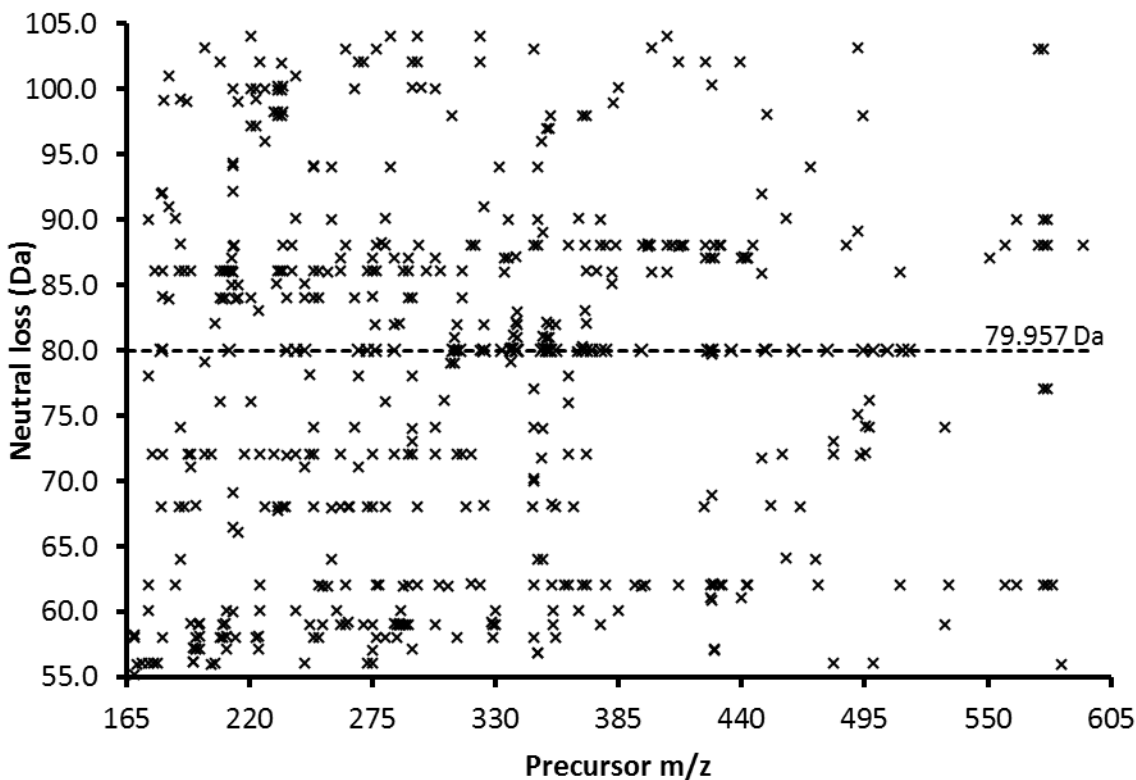


Figure 30- Constructed neutral loss plot of an *Alternaria* sp. extract, showing the precursor metabolite m/z and the observed neutral mass loss (Da). The neutral mass loss of SO_3 (79.957 Da) is highlighted with a dashed line, with each 'x' corresponding to a sulfoconjugated parent metabolite along the x-axis.

Sulfoconjugated metabolites identified on the neutral loss plot had accurate neutral mass losses of SO_3 to within 1 mDa (\pm). In addition to the accurate mass loss of SO_3 (79.957 Da), the presence of the sulfate was further confirmed through the observation of the fine isotope pattern. Traditionally, the relative abundance of the isotopic peaks has been used to aid in the assignment of elemental formulae, which may be either monoisotopic or polyisotopic.^[137] Depending on the abundance of the isotopes, the contribution of their isotopes to mass spectra can be elucidated by inspection of the M (molecular ion), M+1 and M+2 isotope ions.

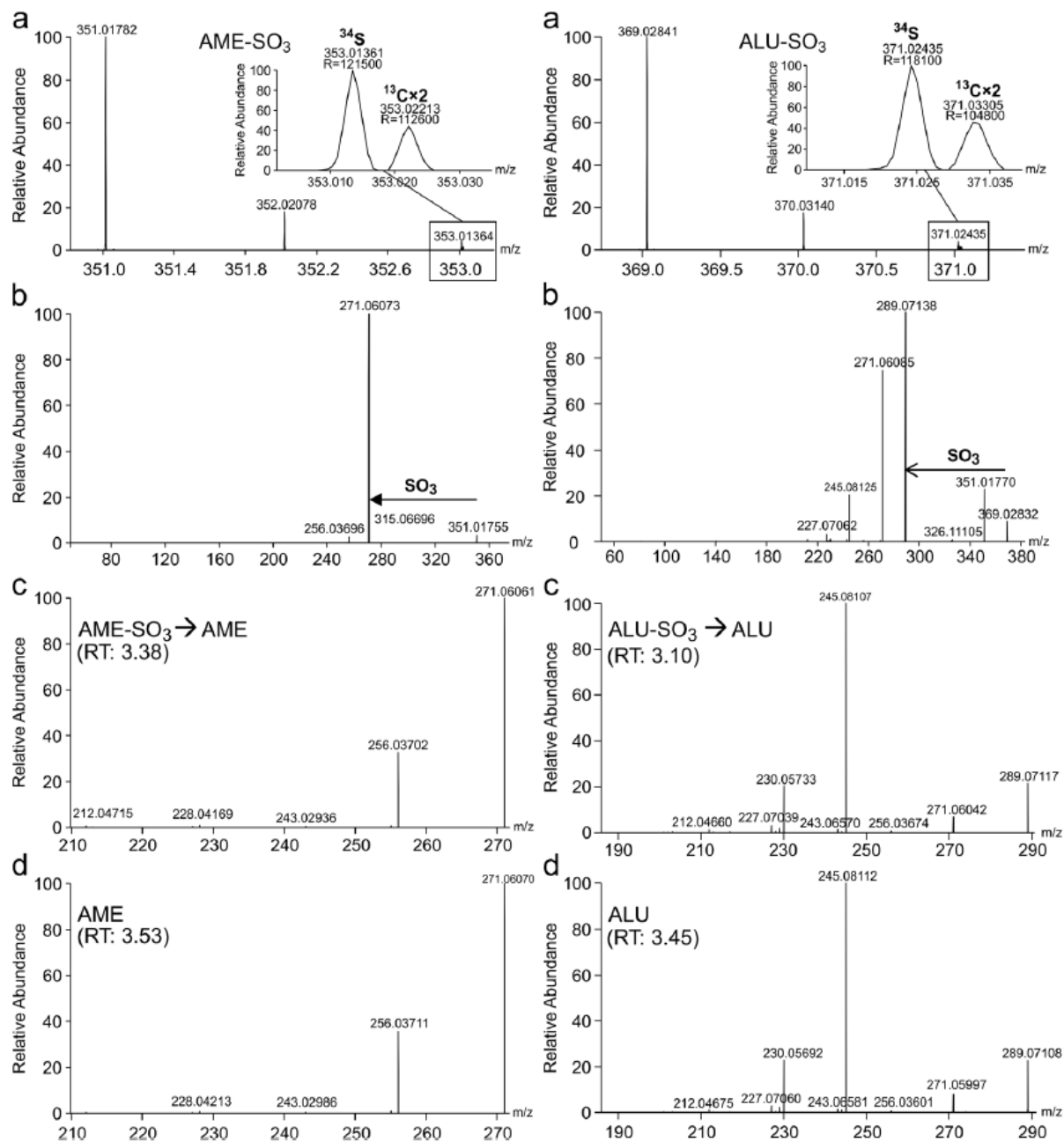


Figure 31- A) MS spectra including isotope pattern at high resolution showing the fully resolved ^{34}S peak as evidence for sulfoconjugation of the known metabolite AME and the new metabolite ALU-SO₃. B) MS² spectra for each metabolite confirming the neutral loss of SO₃ C) MS³ spectra for the sulfoconjugated version of each metabolite showing the fragment ions of the in source generated 'free' metabolite. D) MS² spectra for 'free' versions of both metabolites showing the same fragmentation patterns as the MS³ of the sulfoconjugated metabolites.

Higher resolution mass spectrometer instruments can resolve the individual isotopic peaks that are characteristic for the presence of certain polyisotopic elements. The Q-Exactive Orbitrap mass spectrometer has previously demonstrated its ability to resolve the ^{34}S isotope signal from the $^{13}\text{C}_x2$ isotope signal in the fine isotope pattern.^[138] Figure 31A shows the $^{13}\text{C}_x2$ isotopic peak at 2.00671 Da above the monoisotopic mass; it has been fully resolved from the ^{34}S isotopic peak, which has an abundance of 4.21%, at 1.99580 Da above the monoisotopic mass.

Initial plug screening detected several sulfoconjugated metabolites; two of which corresponded to previously reported sulfoconjugated *Alternaria* metabolites,^[129] while two corresponded to unreported sulfoconjugates of known ‘free’ *Alternaria* metabolites. To confirm the identity of the sulfoconjugated metabolites, the MS^2 spectra of the free (unsulfated) metabolites were compared to the pseudo MS^3 spectra of their related sulfoconjugated metabolites.

Figure 31C shows the same fragment ions and relative intensities observed in the pseudo MS^3 for sulfoconjugated AME and ALU, as observed in the MS^2 spectra from the free metabolites, (Figure 31D). Different metabolites can yield the same fragments, however the highly comparable relative intensities of the fragment ions observed in the MS^2 spectra suggest dissociation pathways that are energetically similar. Therefore, the sulfoconjugated metabolites are likely structurally equivalent. The presence of the sulfate group is also supported by the shift in retention time observed due to the reverse phase separation; the more polar sulfate group causes the conjugated compounds to elute earlier than the free metabolites.

The rapid LC- MS^2 screening of 148 *Alternaria* spp. strains grown on agar plates showed that 108 produced sulfoconjugated metabolites, including 47 of 79 wheat strains. The four most commonly detected sulfoconjugates were the two previously reported sulfoconjugates of alternariol (AOH- SO_3) and alternariol monomethyl ether (AME- SO_3), as well as two new sulfoconjugates of altenusin (ALU- SO_3) and dehydroaltenusin (DHA- SO_3), (Figure 32). Andersen (2015) reported similar findings for the free metabolites of AOH, AME and DHA from small-spored *Alternaria* spp..^[34]

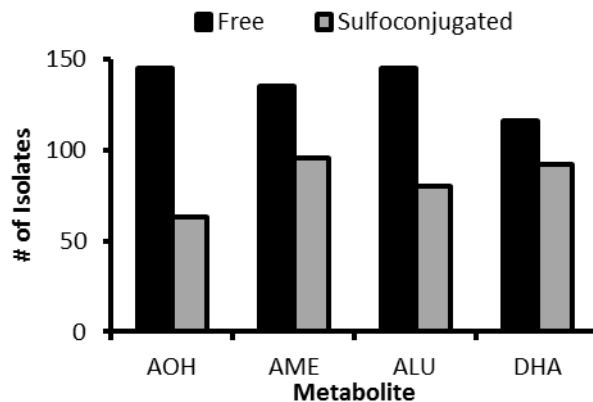


Figure 32- Production of the four predominant free and sulfoconjugated metabolites (AOH, AME, ALU and DHA) by the 148 Canadian *Alternaria* sp. isolates from the plug screening method

The top seven producers of sulfoconjugated metabolites, as determined from the initial plug screening analysis, were selected with additional fermentations in liquid culture media, rice and Cheerios. Rice and Cheerios were selected due to the natural occurrence of *Alternaria* on grains^[32,34], and to ensure that the production of sulfoconjugates was not an artefact of their production on artificial media.

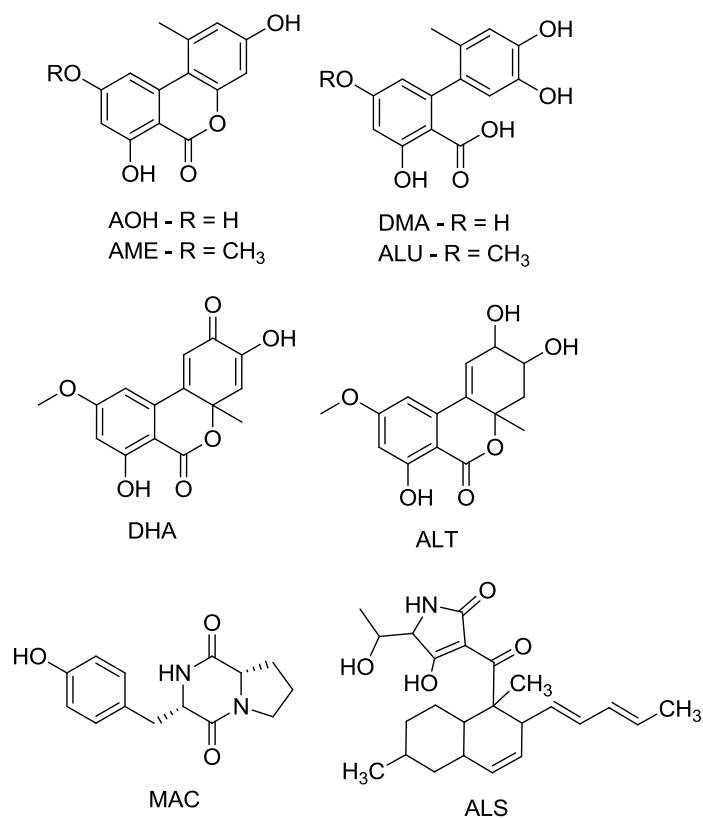


Figure 33- Chemical structures of the known free *Alternaria* metabolites: Alternariol (AOH), Alternariol monomethyl ether (AME), Alternuene (ALT), Dehydroaltenuis (DHA), Altenuis (ALU), Desmethylaltenuis (DMA), Altersetin (ALS) and Maculosin (MAC).

Table 11- Accurate mass precursors of the conjugated *Alternaria* spp. metabolites, found by NLF of SO₃ observed in ddMS2 spectra generated in negative mode

Metabolite	Free		Sulfated	
	RT (min)	m/z (error)	RT (min)	m/z (error)
Alternariol (AOH)	3.07	257.04554 (1.66 ppm)	2.76	337.00236 (0.74 ppm)
Alternariol monomethyl ether (AME)	3.53	271.06119 (1.17 ppm)	3.32	351.01801 (1.31 ppm)
Alternuene (ALT)	2.93	291.08741 (1.07 ppm)	2.78	371.04423 (1.90 ppm)
Dehydroaltenuis (DHA)	3.30	287.05611 (1.33 ppm)	3.38	367.01293 (1.54 ppm)
Altenuis (ALU)	3.23	289.07176 (1.83 ppm)	3.11	369.02858 (1.45 ppm)
Desmethylaltenuis (DMA)	2.75	275.05611 (1.86 ppm)	2.58	355.01293 (1.01 ppm)
Altersetin (ALS)	4.54	398.23368 (0.96 ppm)	4.41	478.19050 (1.36 ppm)
Maculosin (MAC)	2.44	259.10826 (0.63 ppm)	2.22	339.06563 (1.68 ppm)

Applying NLF analysis to the HRMS² data from the liquid culture extracts led to the detection of 38 sulfoconjugated metabolites. Two were the previously reported metabolites, AOH-SO₃ and AME-SO₃, six were determined to be the sulfoconjugated versions of known free *Alternaria* metabolites, (Figure 33, Table 11), and 30 were unknown sulfoconjugated metabolites, (Supplementary Table S1). All eight sulfoconjugated metabolites (six new, two known) were detected in extracts from three week fermentations of liquid media. Fermentations of rice and Cheerios afforded both known sulfoconjugates of AOH and AME, in addition to the new sulfoconjugates of ALT, DHA, ALU and DMA. These *Alternaria* strains, which were previously isolated from grains and fruit, have demonstrated their ability to produce sulfoconjugates on rice and Cheerios, which suggests that these metabolites may be present alongside their free metabolites in contaminated agricultural grains and foodstuff.

3.4 Conclusions and Future Work

NLF of HRMS² data sets is a powerful tool for the rapid detection of sulfoconjugated metabolites in cultures of *Alternaria*. Mass accuracy below 2 ppm drastically decreased interfering signals that would otherwise result in the false identification of sulfated metabolites by traditional analysis methods. Similar strategies employing neutral loss filtering could be applied to the detection of other important conjugated mycotoxins, including glycosides. Methods that are capable of detecting regulated mycotoxins in conjugated forms must be developed and applied because of the potential for conjugated metabolites to either retain biological activity or be reduced to the ‘free’ metabolite after consumption. This knowledge is imperative to regulators so that safe levels of the toxic metabolite can be set and monitored in both processed and unprocessed food products.

This work has been published in *Rapid Commun. Mass Sp.*, however future work will focus on the relative quantification of the sulfoconjugated metabolites. The presence of the sulfate group increases the ionization efficiency in the mass spectrometer, therefore masking the actual concentration of these sulfoconjugates relative to their free metabolites. However, by using a sulfatase enzyme, we can cleave off the sulfate ester group from the free metabolite. Using authentic standards of the free *Alternaria* metabolites, we can then compare the relative intensities both before and after enzymatic digestion to the intensities from the free standards to

obtain a relative concentration. The relative quantification method is particularly important due to the lack of available commercial standards for the new sulfoconjugates.

Semi-targeted detection of total AAL-toxins and enniatins using product ion filtering

3.5 Introduction

3.5.1 *Alternaria arborescens* and AAL-toxins

Some of the phytotoxins produced by *Alternaria* are also mycotoxins, as a number of *Alternaria* secondary metabolites have demonstrated some cytotoxic or genotoxic effects *in vitro*. One of the species, *A. arborescens*, which was first isolated from a tomato in California, USA, was demonstrated to produce host-specific AAL-toxins.^[117,139] AAL-toxins are structurally related to fumonisins, which share a characteristic tricarballylic ester moiety which resembles cellular sphingolipids (Figure 34).^[23] Both AAL-toxins and fumonisins elicit similar genotoxic effects within their host plants, resulting in the inhibition of cell proliferation, and rapid cell apoptosis.^[139] Similar to fumonisins, AAL-toxins have also demonstrated genotoxicity in cultured animal hepatoma and kidney cells *in vitro*.^[119,140] It has been demonstrated that both fumonisins and AAL-toxins disrupt membrane and sphingolipid metabolism through disruption of the ceramide synthase enzyme, resulting in cell death in the liver, kidneys and nervous system.^[141,142] While there is evidence to support fumonisin toxicoses in animals and humans, there is a lack of current toxicological *in situ* information available for AAL-toxins.^[143–148]

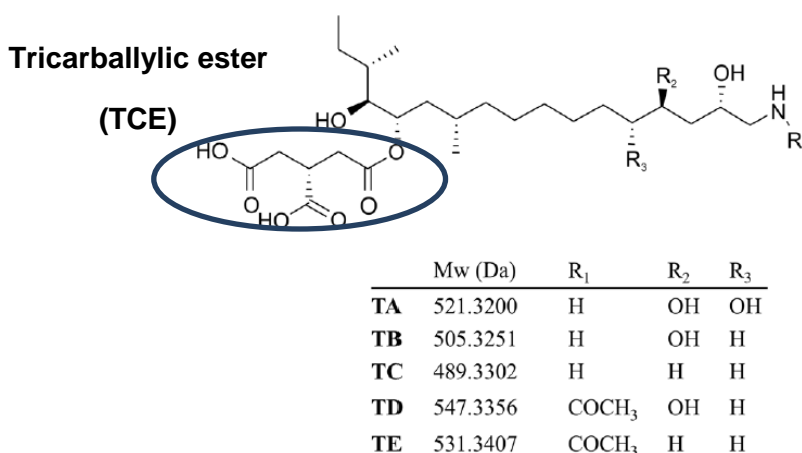


Figure 34- Commonly detected AAL toxins of current agricultural importance, with highlighted TCE functional group

AAL-toxin screening traditionally involves either Enzyme-Linked Immunosorbent Assay (ELISA) toxicity testing, or a targeted search for TA, TB, TC, TD, and TE AAL-toxins in positive ESI mode, though the molecules possess functional groups for both positive and negative ionization.^[149,150] Collisional activation in positive mode ESI yields information regarding the backbone of the AAL-toxin, such as the number and relative location of hydroxyl groups. Upon collisional activation in negative ionization mode, all AAL-toxins produce the major common product anion $C_6H_5O_5^-$ (m/z 157.0142) from the TCE group. Utilizing the common anion of the TCE group by product ion filtering in negative mode allows for the detection of total AAL-toxins in a sample, while positive ESI characterizes the detected molecules. A semi-targeted ddMS² method was made which included rapid polarity switching between detection in negative mode, and characterization in positive mode, followed by manual inspection of the TCE peak post data acquisition.

3.5.2 *Fusarium* and enniatins

Fusarium species are common plant pathogens of cereal grains and corn. In cereals, such as wheat, barley, and oats, *Fusarium* infection results in a disease known as Fusarium Head Blight (FHB), which is also termed Gibberella ear rot if present in corn. The most common species in Canada responsible for pathogenicity are *F. avenaceum*, *F. graminearum*, and *F. culmorum*, which thrive in cool climates, and are also potent producers of mycotoxins. *Fusarium* infection and subsequent mycotoxin contamination currently pose the greatest threats to Canadian crop contamination, specifically in maize and wheat.

Enniatins exist as a class of cyclohexadepsipeptides, which are alternating residues of D-2-hydroxyisovaleric acid, and differing amino acid side chains (Figure 35), which together, act as ionophores in biological membranes.^[151] In plants, enniatins are produced as non-specific virulence factors during the infection process to overcome the cell wall barriers of the host.^[152] In addition to their phytotoxicity, enniatins are also emerging mycotoxins, primarily produced by some members of *Fusarium*, including *F. avenaceum*, and the weakly pathogenic species *F. acuminatum* and *F. subglutinans*. The most common enniatins are A, A1, B and B1, and are frequently studied and detected in cereal grains, corn, ensiled feedstock for cattle, and even in processed commodities for human consumption, such as flours, cereals, bread, and beer.^[153–157] Enniatins have demonstrated cytotoxicity *in vitro* to human carcinoma-line Hep G2 and

fibroblast lung cells, and A, A1, B, and B1 have also demonstrated synergistic cytotoxicities towards both ovarian and intestinal cells when combined.^[158–160] The EFSA has also provided an opinion on the risk of human toxicity of enniatins, and suggests that while there appears to be associated genotoxicity in animals, the risk for acute toxicity is not of concern to humans, though they mention that *in vivo* toxicity data are missing for a chronic exposure assessment.^[161] There are currently 29 enniatins described with various modifications to the depsipeptide skeleton and functional groups, resulting in differences in toxicity. Many different species of *Fusarium* are capable of producing diverse mixtures with varying concentrations of enniatins, both *in vitro* and *in situ*. Many different modifications of the amino acid residues suggest that additional enniatins may also exist.^[162]

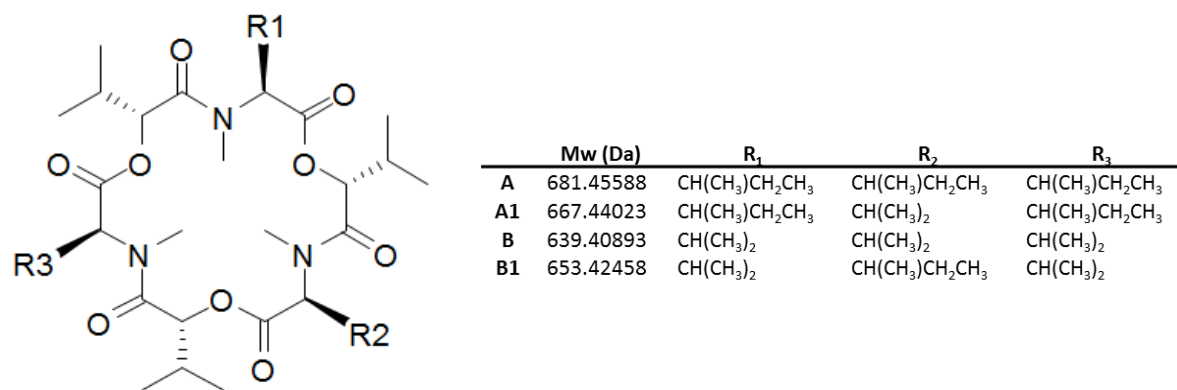


Figure 35- Cyclohexadepsipeptide skeleton, and commonly detected enniatins in agricultural products

Typically, enniatins are detected by LC-MS/MS or targeted screening methods for the common A, A1, B and B1 molecules, with their toxicity reported as a total sum of all enniatins present.^[27] These methods may present challenges when screening for new or additional enniatins produced by different species of *Fusarium*. On collisional activation in positive ionization mode, enniatins produce shared product ions due to the cleavage of the depsipeptide skeleton. The common product ion observed for enniatins is m/z 196.13321 ($C_{11}H_{17}NO_2$)⁺, which is the result of ring cleavage at the oxygens between the hydroxyisovaleric acid and isoleucine, where the R group is an isopropyl (Figure 36). Another common product ion, which is especially common to A class sec-butyl and iso-butyl-containing enniatins, is the m/z 210.14886 product ion, ($C_{12}H_{19}NO_2$)⁺.

To overcome the detection challenges for the large variety of enniatins, the developed product ion filtering experiment was modified to detect and characterize total and potentially new enniatins using the product ions m/z 196.13321 and 210.14886.^[163]

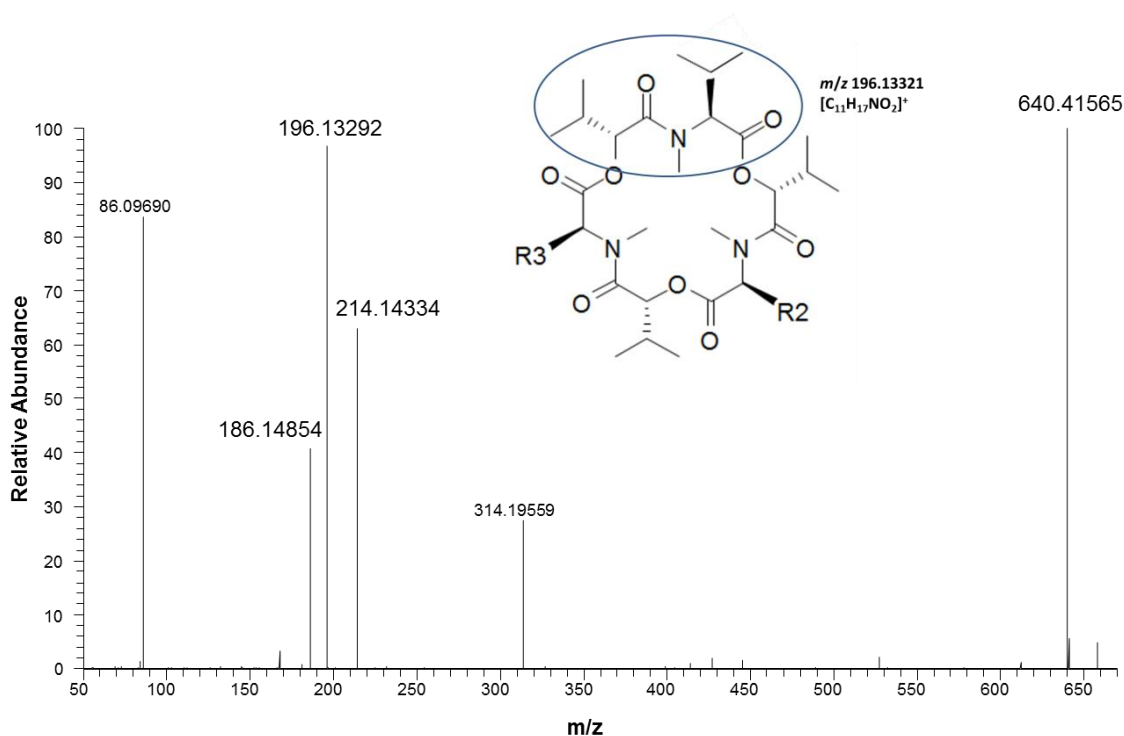


Figure 36- MS² spectrum of enniatin B in positive ionization mode, showing the common 196.13321 product ion

Collisional activation of the depsipeptide ring at sufficient collision energy (approximately 30 NCE) results in intense fragment ions, which are indicative of the particular functional groups present for enniatin characterization. However, the parent ion is lost, so the molecular formula cannot be easily discerned. Consequently, lower collision energies (10 NCE) preserve the parent ion, but there is little fragmentation for the proper characterization. To overcome this, the method was modified to include a stepped collision energy setting of 30 and 10 NCE to investigate total enniatins in individual cultures, and in processed flour products.

3.6 Experimental

3.6.1 Fungal material

The *Alternaria arborescens* type strain (CBS 102605), which was first isolated in California, USA, was acquired from CBS (Centraal Bureau Voor Schimmelcultures), import permit No. P-2014-03314. Strains of *Fusarium avenaceum*, *F. acuminatum*, *F. subglutinans* were provided by Prof. David Miller from Carleton University, in Ottawa, Ontario. Morphological identifications on the *Fusarium* cultures were performed by Dr. Keith A. Seifert at Agriculture and Agri-Food Canada in Ottawa, Ontario. Strains known to produce AAL-toxins or enniatins were selected for growth on agricultural sources that they naturally contaminate. Strains were prepared as 3-point inoculations on PDA, and were incubated for 7 days at 25°C. Additional *Fusarium* strain information is provided in Appendix A2 Table 3S.

3.6.2 *Alternaria arborescens* fermentation in tomatoes and extraction

Cherry tomatoes were purchased locally from a market in London, Ontario. Tomatoes were first washed with reverse osmosis water, and then rinsed with sterilized distilled water. Tomatoes were blot dry on sterile paper towels, and then irradiated with biocidal UV light at 254 nm in a biosafety cabinet (Purifier Logic biological safety cabinet) for 10 minutes on each side. Surface sterilized tomatoes were placed inside 2L Erlenmeyer flasks containing filter paper, (Whatman P4, 125 mm) and capped with foam plugs. Fungal inoculum was prepared by macerating a 3 x 3 cm portion of the prepared PDA plate in 25 mL sterile water with a Polytron blender, before adding the inoculant solution to the flask. Inoculated tomatoes were fermented for 3 weeks at 25°C. Fermented tomatoes were then blended using a laboratory blender, and 6 g aliquots were placed in 50 mL Falcon tubes. The tomato aliquots were extracted with 15 mL extraction solvent (79/20/1 acetonitrile/water/acetic acid) by sonication for 1 hour at 30°C. After the liquid was allowed to settle, 1 mL of the extracted solution was filtered into an amber glass HPLC vial using a 0.45 µm PTFE syringe filter, (ChromeSpec). Uninoculated tomatoes were also analyzed to ensure there were no AAL-toxins.

3.6.3 General conditions, ddMS² and rapid polarity switching- AAL-toxins from *Alternaria arborescens*

HRMS and HRMS² data were obtained using a Thermo Q-Exactive Quadrupole Orbitrap Mass Spectrometer, coupled to an Agilent 1290 HPLC. A Zorbax Eclipse Plus RRHD C18 column (2.1 x 50 mm, 1.8 µm; Agilent) was maintained at 35 °C. The mobile phase was comprised of

water with 0.1% formic acid (A), and acetonitrile with 0.1% formic acid (B) (Optima grade, Fisher Scientific, Lawn, NJ). Mobile phase B was held at 0% for 30 seconds, before increasing to 100% over three minutes. B was held at 100% for 1 minute, before returning to 0% B in 30 seconds. 2 μ L injections were used at a flow rate of 0.3 mL/min. The following conditions were used for HESI: capillary voltage, 3.7 kV in negative mode, 3.9 kV in positive mode; capillary temperature, 400°C; sheath gas, 17.00 units; auxiliary gas, 8.00 units; probe heater temperature, 450 °C; S-Lens RF level, 45.00. The full MS was first acquired in negative ion mode using following settings: scan range, 450 – 850 m/z ; resolution, 17 500; AGC, 5e5; max IT, 60 ms. The 5 most intense peaks in the data-dependent MS² (ddMS²) spectra were sequentially mass selected under a 1.0 m/z isolation window and analyzed at a resolution of 17 500; AGC target, 1e5; max IT, 60 ms; NCE, 25; threshold intensity, 4.2e4; first fixed mass 75 m/z . Selected ions were excluded from further MS² scans for 6 s. A second full MS scan was acquired in positive mode, followed by ddMS² of the top 5 peaks at 17 500 resolution. Each MS² dataset was first mined for the tricarballylic product ion (m/z 157.0143 \pm 2 ppm) in negative mode. Any tricarballylic ion peaks detected in the negative MS² filters prompted both full MS and MS² searches in positive ion mode for the protonated or ammoniated adducts. Compounds and their transitions were compared to authentic standards when available, as well as by comparison to literature values.

3.6.4 *Fusarium* spp. fermentation and extraction in liquid media and corn

Fusarium cultures were first inoculated into 200 mL enniatin liquid media as per Visconti et al, 1992, (Figure 37) and fermented for seven days in roux bottles.^[164] Cells were filtered (Whatman No. 1), and the filtrate was extracted first with ethyl acetate, and then with hexane. Ethyl acetate and hexane extracts were evaporated to dryness, and reconstituted in 1 mL methanol before syringe filtration with 0.45 μ m PTFE filters (ChromeSpec). Samples were analyzed on the LC-MS as described in 3.6.6.

Ensiled maize used for the *Fusarium* cultures was obtained from a local feed mill in Ontario, Canada. 20 g of maize was left to imbibe overnight with 80 mL water in a 500 mL Erlenmeyer flask. Prior to autoclaving, the water was decanted and then autoclaved on a solid cycle. Inocula were prepared by excising 3 x 3 cm agar sections from *Fusarium* strains grown on Potato Dextrose Agar (Sigma Aldrich), and grinding them in 25 mL sterile water. 10 mL of the prepared inoculant solution was added to each flask, and the corn was allowed to ferment in the dark at

25°C. After 1 week, the fungal mycelial mat containing the corn was first broken apart with a spatula. Extraction solvent (79/20/1 acetonitrile/water/acetic acid) was prepared as per Varga and Sulyok, 2013. 80 mL extraction solvent was added to each flask, followed by shaking on a rotary shaker for 1.5 hours. Corn and mycelia were filtered (Whatman No. 1) into round bottom flasks, and filtrates were dried by rotary evaporation. Extracts were reconstituted in extraction solvent into 7 mL scintillation vials, and dried under a stream of nitrogen. Prior to LC-MS analysis, the vials were reconstituted in 500 µL extraction solvent, before being diluted 1:1 with 20/79/1 acetonitrile/water/acetic acid and filtered into an amber glass HPLC vial using a 0.45 µm PTFE syringe filter, (ChromeSpec). Uninoculated corn samples were also analyzed similarly (3.6.6) to monitor for naturally-contaminated enniatins.



Figure 37- Fusarium isolates inoculated into liquid enniatin media (left) and maize (right)

3.6.5 Extraction of naturally-contaminated flour for enniatin analysis

All-purpose unbleached, whole wheat, oat, barley, dark rye and gluten flour samples were purchased from a commercial source in London, Ontario. 5.0 g ± 0.1 g samples were prepared and extracted as per Sulyok et al., 2006 with the addition of an initial vortexing step, followed by sonication for 15 minutes.^[165] Extracts were diluted 1:1 with 20/79/1 acetonitrile/water/acetic acid, filtered with a 0.45 µm PFTE syringe filter into HPLC vials, and analyzed by LC/MS².

3.6.6 HRMS and MS² analysis of total enniatins

HRMS and HRMS² data were obtained using a Q-Exactive Quadrupole Orbitrap mass spectrometer (Thermo Fisher Scientific), coupled to an Agilent 1290 high-performance liquid chromatography (HPLC) system. A Zorbax Eclipse Plus RRHD C8 column (2.1 × 50 mm, 1.8 µm; Agilent) was maintained at 35 °C. The mobile phase was comprised of water with 0.1% formic acid (A), and acetonitrile with 0.1% formic acid (B) (Optima grade, Fisher Scientific,

Lawn, NJ, USA). Mobile phase B was held at 70% for 1 min, before increasing to 100% over 2.5 min. Mobile phase B was held at 100% for 1.5 min, before returning to 0% B in 1 min. Injections of 2 μ L were used with a flow rate of 0.3 mL/min. The following conditions were used for positive HESI: capillary voltage, 3.9 kV; capillary temperature, 400 $^{\circ}$ C; sheath gas, 17.00 units; auxiliary gas, 8.00 units; probe heater temperature, 450 $^{\circ}$ C; S-Lens RF level, 45.00. The full MS for the data-dependent MS² (ddMS²) used the following settings: scan range, 75–800 m/z ; resolution, 70,000; AGC, 3e6; max IT, 250 ms. The five highest intensity ions from the MS scan were sequentially mass selected under a 1.2 m/z isolation window and analyzed at a resolution of 17,500; AGC target, 1e5; max IT, 60 ms; stepped NCE 10, 35; threshold intensity, 1.2e5. Selected ions were excluded from further MS² scans for 10 s. MS² datasets were inspected for the 196 and 210 product ions for enniatins (\pm 1 mDa) post-acquisition using Xcalibur 2.0. Unknown enniatins and cyclodepsipeptides were searched on Antibase 2013.

3.7 Results and Discussion

3.7.1 Total AAL toxins in artificially inoculated tomatoes

The application of the product ion filter of the TCE anion (m/z 157.0142) made for rapid analysis of all precursor masses containing the product anion, (Figure 38). The product ion filter plot is represented as a series of vertical lines corresponding to both the retention time and intensity of the detected product anion in MS² scans.

In total, 5 known AAL toxins and acetylated derivatives were detected using the product ion filtering of the m/z 157.0142 product anion in negative ionization mode, (Table 12). All AAL-toxins detected by the product TCE anion were further characterized by positive mode MS² scans and retention time comparison using rapid polarity switching.

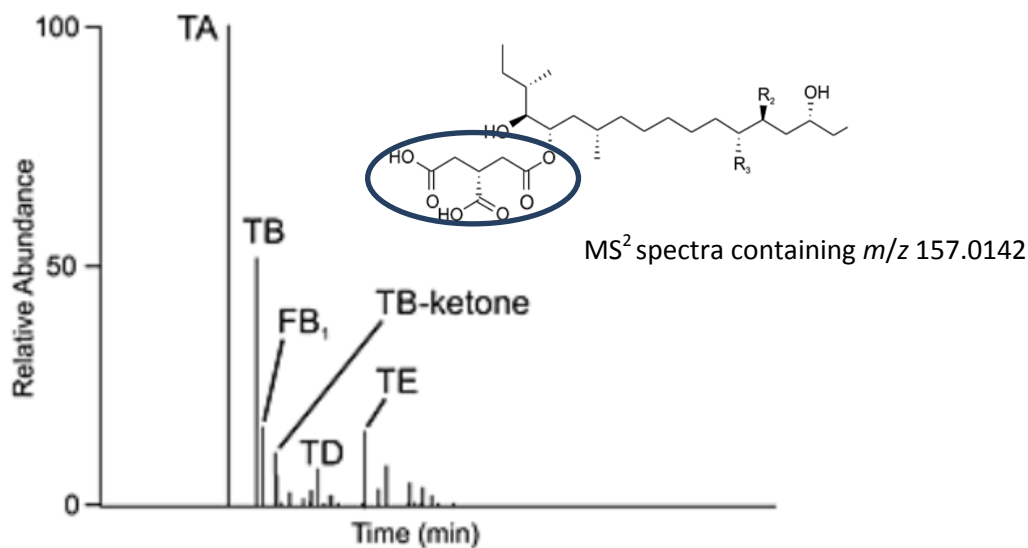


Figure 38- Product ion filter plot in negative ionization mode from artificially-infected tomatoes. The plot shows all MS² spectra which contain the TCE fragment, and the retention time that they were detected

Table 12- Total AAL toxins and molecules detected by the TCE product anion in tomato artificially inoculated with *A. arborescens*

	RT (min)	Precursor m/z [M-H]	Product anion [M-H]	Precursor m/z [M+H]	Product cation [M+H]
TA	2.60	520.3143	157.0143	522.3289	257.2260
Acetyl-TA	2.81	562.3259	157.0142	564.3405	257.2266
Acetyl-TA ketone	2.90	560.3126	157.0143	562.3271	255.2118
TB	2.72	504.3196	157.0143	506.3342	259.2406
TB-ketone	2.78	502.3042	157.0143	504.3187	257.2268
TD	2.97	546.3307	157.0143	548.3452	259.2423
TD-ketone	3.08	544.3147	157.0143	546.3292	257.2265
TE	3.28	530.3355	157.0142	532.3492	261.2578
TE-ketone	3.40	528.3194	157.0144	530.3330	259.2425
FB ₁	2.72	720.3842	157.0143		
Unknown1	2.60	480.2600	157.0142		
Unknown2	2.94	488.3384	157.0143		
Unknown3	3.80	514.3344	157.0143		

Upon collisional activation in positive mode, the polyol backbone of AAL toxins results in initial losses of water, followed by the loss of the TCE ester group, (Figure 39). On inspection, several molecules also detected by product ion filtering displayed precursor masses 2.0157 Da smaller ($-H_2$) than the common AAL-toxins in both negative and positive ionization mode, suggesting the addition of a double bond.

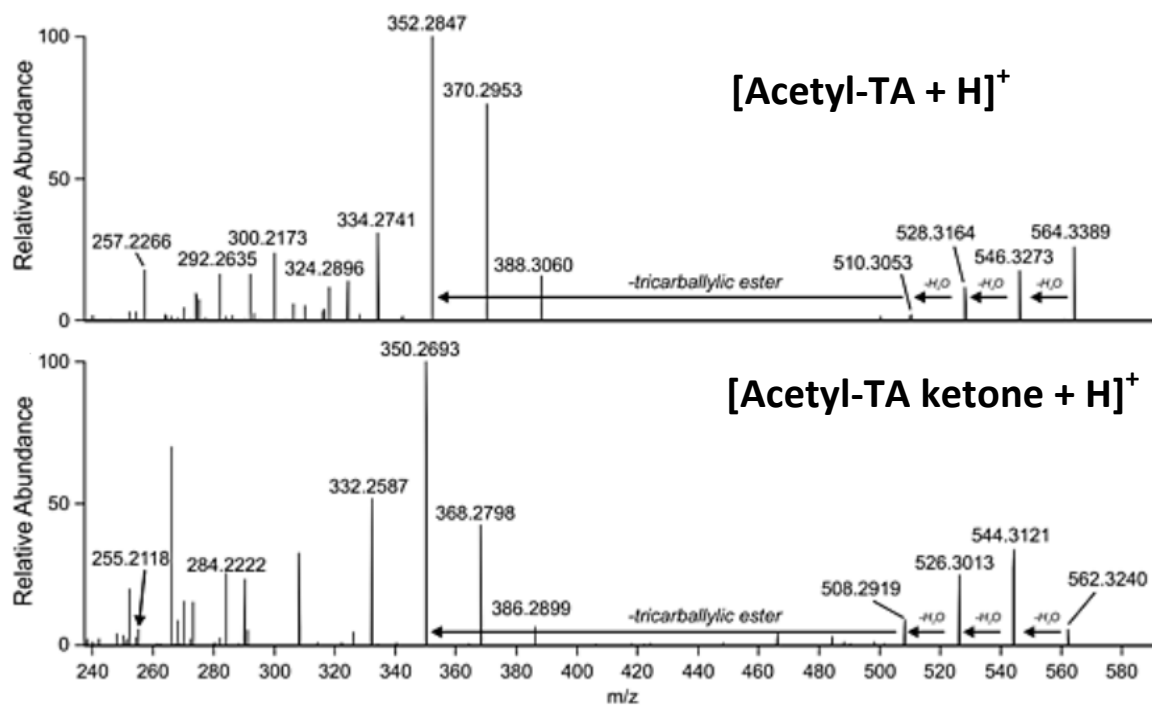


Figure 39- Characterization of AAL toxins by MS² spectra of acetyl-TA and the new acetyl-TA ketone AAL toxins in positive ionization mode [158]

There is precedence for ketone-containing fumonisins in the literature, such as fumonisin AK₁, (FAK₁) which is produced by *Fusarium avenaceum* during the biosynthesis of fumonisin by the enzymatic replacement of the carboxylic acid on the TCE at C-15 with a ketone.^[166,167] As FB₁ was detected, it can be assumed that the enzyme functionality that would produce these keto-derivatives may be shared between *F. avenaceum* and *A. arborescens*. Thus, the compounds were suspected to be ketone derivatives of TA, acetyl-TA, TB, TD, and TE, which have not yet been reported. 3 unknown TCE-containing molecules were also detected from the artificially

contaminated tomatoes, in addition to fumonisin B₁ (FB₁), which also contains the characteristic TCE product anion.

3.7.2 Method validation for total enniatin analysis in artificially inoculated liquid media and corn

The suitability of the 196 and 210 product ions for total enniatin analysis was first evaluated using extracts from *Fusarium* cultures inoculated into enniatin liquid media, (Figure 40A) and maize (Figure 40B). The liquid artificial media was conducive to the production of a wide variety of enniatins, while the maize was indicative of whether the detected enniatins could be produced on agricultural sources. The product ion filter plots (Figure 40A, B) suggest that the 196 fragment is commonly detected in the wide variety of enniatins produced. B-series enniatins, which predominantly contain isopropyl R groups had more intense 196 fragments. A-series enniatins, in addition to containing the 196 product ion, also contain secbutyl or isobutyl R groups, which the 210 product ion is more selective for.

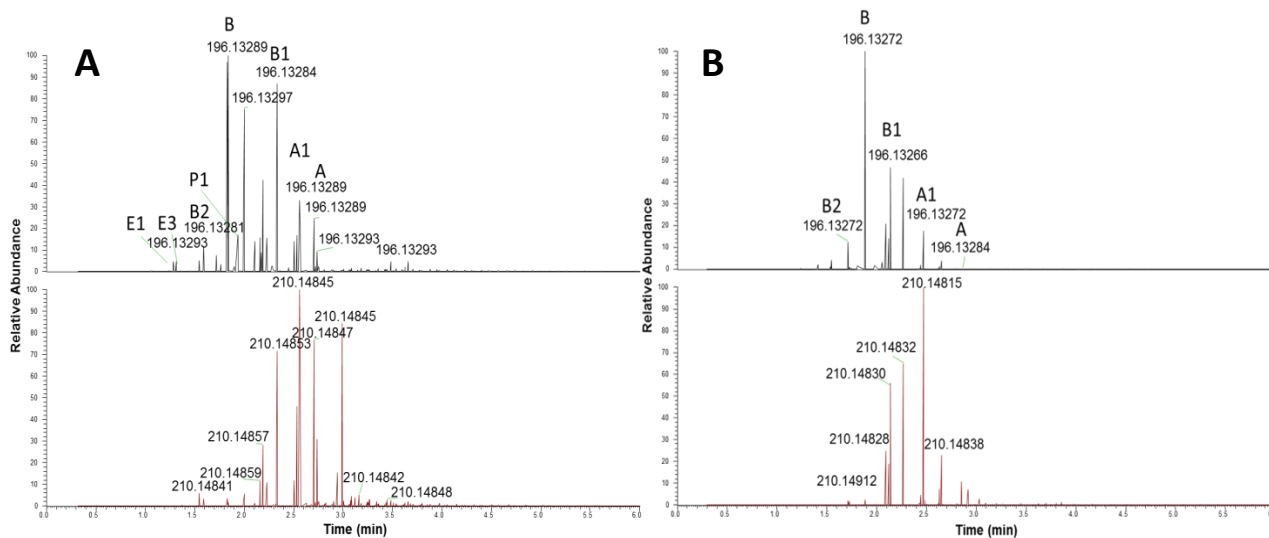


Figure 40- Product ion filter plots showing MS² spectra containing the 196 and 210 fragments. A) Extract from *F. avenaceum* inoculated into liquid artificial enniatin media B) Extract from *F. avenaceum* inoculated into maize

Table 13- Total enniatins detected in artificially inoculated liquid enniatin media and maize using product ion filtering in positive ionization mode

Enniatin	<i>F. avenaceum</i>										<i>F. acuminatum</i>		<i>F. subglutinas</i>	
	KAS1907		KAS1914		KAS2925		KAS2926		KAS2927		KAS1912		KAS2903	
	Media	Maize	Media	Maize	Media	Maize	Media	Maize	Media	Maize	Media	Maize	Media	Maize
B	+	+	+	+	+	+	+	+	+	+	+	+	+	+
B1	+	+	+	+	+	+	+	+	+	+	+	+	+	+
B2			+		+		+		+		+			
A	+		+		+		+		+		+		+	
A1	+	+	+	+	+	+	+	+	+	+	+	+	+	+
P1					+				+		+			
P2					+				+					
E1					+				+		+			
E3			+		+		+		+		+			
M1/M2					+				+		+			
N					+									
O1/2/3					+		+		+		+			
C ₃₀ H ₅₁ N ₃ O ₉	+		+	+	+		+		+	+	+	+	+	+
C ₃₂ H ₅₃ N ₃ O ₉			+		+		+		+	+	+			
C ₃₃ H ₅₅ N ₃ O ₉	+		+		+		+		+		+		+	
C ₃₄ H ₅₇ N ₃ O ₉	+		+		+		+		+		+		+	
C ₃₅ H ₅₉ N ₃ O ₉	+				+		+		+		+		+	
C ₃₇ H ₆₅ N ₃ O ₉			+		+						+			
C ₄₃ H ₇₄ N ₄ O ₁₂					+		+		+		+			
C ₄₄ H ₇₆ N ₄ O ₁₂					+				+	+				
C ₄₅ H ₇₈ N ₄ O ₁₂					+						+			
C ₄₆ H ₈₀ N ₄ O ₁₂					+						+	+		
C ₄₇ H ₈₂ N ₄ O ₁₂					+				+	+				

The artificial liquid media was more conducive to enniatin and cyclodepsipeptide production than inoculated maize extracts, (Table 13). Product ion filtering using the 196 and 210 product

ions detected 23 total enniatins, enniatin-like cyclodepsipeptides and unknown cyclooctadepsipeptide metabolites from artificially inoculated liquid media, including 6 unknown enniatins (Supplementary Figure 3S) and 2 unknown cyclooctadepsipeptides (Table 13, Supplementary Figure 4S).

Several of the unknown enniatins detected in liquid media and maize contained fragments that were 2.015 Da smaller ($-H_2$) than the known enniatin class fragmentation, (Figure 41) suggesting the addition of a double bond on the molecule.

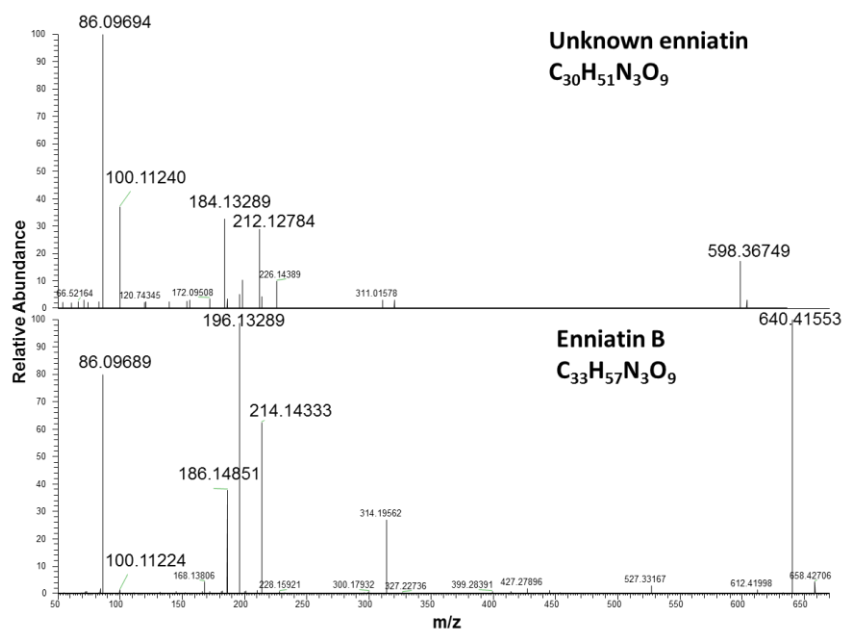


Figure 41- MS² spectra of the unknown enniatin (top) and enniatin B (bottom) in positive ionization mode

Isolates from *F. avenaceum* and *F. acuminatum* produced the largest variety of enniatins, which included series less commonly detected in agricultural products such as E, M, N, O and P. In contrast, the commonly detected enniatins in maize were B, B1 and A1, in addition to several of the unknown enniatins and unknown cyclooctadepsipeptide (C_xH_yN₄O₁₂) metabolites. The presence of unknown enniatins and cyclooctadepsipeptides in maize suggests a potential risk for their contamination in agricultural products.

The cyclooctadepsipeptides produced by several species of fungi, ($C_xH_yN_4O_{12}$), were commonly detected in *F. avenaceum* and *F. acuminatum* extracts, but were absent in *F. subglutinans* extracts. This is especially important as *F. avenaceum* is the most frequently isolated enniatin-producing fungal species from maize affected by pathogenic Fusarium Head Blight (FHB) in Canada.^[126] These cyclooctadepsipeptides have not yet been reported to be produced by *Fusarium*, though it seems likely that they share a similar biosynthesis with enniatins and bassianolides.^[168] Thus, the product ions selected were not only selective for the commonly detected enniatins (A and B series), but were also selective for the other enniatin series and related cyclodepsipeptide compounds.

3.7.3 Product ion filtering for the detection of total enniatins in naturally-contaminated flour

It was demonstrated that there was a risk for the production of new enniatins and cyclooctadepsipeptides in agricultural commodities. Therefore, commercial flour samples were similarly screened using the validated product ion filtering method to assess the occurrence of total cyclodepsipeptides in naturally contaminated agricultural products (Figure 42).

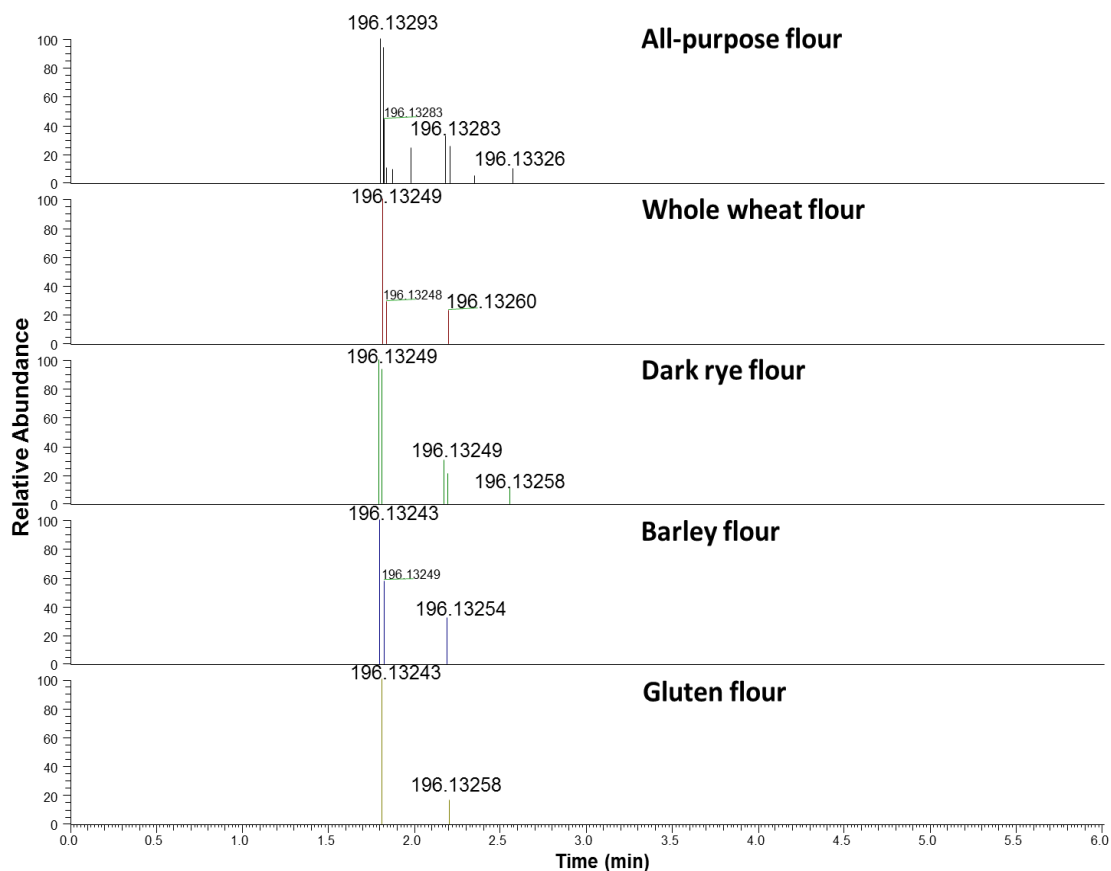


Figure 42- Product ion filter plots in positive ionization mode showing MS² spectra containing the 196 product ion. Extracts were obtained from commercial flour samples

The data are similar to the artificially inoculated maize samples (Figure 40B), which shows the presence of only enniatins B, B1 and A1. However, unlike the artificially contaminated maize samples, the unknown enniatins and cyclooctadepsipeptides were not detected. Both the A and B series enniatins are commonly detected due to their relative abundance over the other series of enniatins produced by *Fusarium*. This is supported by previous studies where the A and B series enniatins were detected in naturally contaminated wheat and processed flour samples.^[169–171] Vaclavikova (2013) reported that the concentration of enniatins A, A1, B and B1 decreased during both flour processing and baking during beer and bread production.^[170] During flour production, much of the milling waste goes directly to animal feed, which introduces a slight exposure risk during feed consumption. However, the risk for contamination by the new enniatins and cyclooctadepsipeptides in processed flour is likely to be negligible, especially after further baking or flour processing by chemical bleaching agents.

3.8 Conclusions and Future Work

Post data-acquisition product ion filtering of HRMS² data sets was demonstrated to be an effective method for the detection and characterization of total AAL-toxins and total enniatins and cyclodepsipeptides in agricultural commodities. Despite the potential matrix effects of the tomato and maize substrates, the high mass accuracy (± 2 ppm) and resolution of the Orbitrap contributed to the observed sensitivities of the detected analytes, thus allowing for the discovery of new AAL-toxins and enniatins. It was also demonstrated that these new AAL-toxins and cyclodepsipeptides could be produced in agricultural products, demonstrating the risk for their contamination, and the need to understand their occurrence.

Due to the lack of both toxicological data and readily available commercial standards, total detection and characterization of AAL-toxins and cyclodepsipeptides by product ion filtering may be an important regulatory tool for LC-MS screening of agricultural commodities. In addition to known compounds, potentially unknown mycotoxins can be detected through product ion filtering of MS² scans, which would be missed using traditional targeted LC-MS methods. Similar mycotoxin discovery methods have been applied to fumonisins, ergot alkaloids and *Stachybotrys* toxins, though it remains unknown if the method has been employed for regulatory screening purposes.

Product ion filtering of AAL-toxins was published along with new fumonisins in *Rapid Communications in Mass Spectrometry*.^[163] Compound isolation is on-going for the characterization of the enniatin and cyclooctadepsipeptide unknowns by Nuclear Magnetic Resonance (NMR). The product ion filtering for total enniatins in agricultural products will be submitted to *Toxins* for a special issue on LC-MS/MS methods for mycotoxin analysis. Despite not being detected in flour, the new cyclooctadepsipeptide metabolites and enniatins were detected in silage (Chapter 4) for animal feed; those results will be published in the *Toxins* article, in addition to the silage manuscript (in progress).

Chapter 4- Combining data independent acquisition-digital archiving mass spectrometry (DIA-DA) with next-generation sequencing to profile fungal contaminated silage

4.1 Chapter 4 objectives

The research objective of this chapter was to create a comprehensive analysis of both the microbial community profile, and the secondary metabolites detected in toxicosis-linked contaminated Canadian silage.

4.2 Introduction

Farmers have become increasingly dependent on silage as a daily feed source for their livestock. However, due to the ubiquitous nature of fungi such as *Penicillium*, silages are susceptible to spoilage and mycotoxin contamination. Silage spoilage is not only a large profit loss for farmers, but feed contamination by mycotoxins can cause genetic abnormalities and mycotoxicosis after consumption, with many mycotoxins also possibly persisting in the animal byproducts, such as the milk and meat.^[41,172] Such contamination occurs both in the field prior to the crop being harvested, during the transportation of the foraged material, and after traditional ensiling with lactic acid-producing bacteria to promote storage capabilities.

While many mycotoxigenic fungi produce distinct secondary metabolites, some fungal genera share similar biosynthetic pathways, and therefore share similar metabolites. For instance, citrinin is a common fungal secondary metabolite shared between several species of *Penicillium*, *Aspergillus*, and *Monascus*, all of which can be present in contaminated silage. While many genera of fungi produce their own distinct metabolites, which implies their presence (satratoxins, enniatins), evaluating the risk of specific pathogenic and mycotoxin-producing species based solely on the metabolites observed is difficult. Predominant fungal species and seasonal dynamics from contaminated silage have been well characterized.^[17,173-176] Similarly, the *in vitro* cytotoxicity of extracts from isolated fungal cultures has been evaluated as an initial toxicity risk assessment in contaminated maize silage.^[38] However, there is still a discrepancy between the

production of mycotoxins on artificially (*in vitro*) and naturally contaminated (*in situ*) sources.^[177] Similarly, due to differing growth conditions between the field, post-harvest and ensiling environments, different fungi may be preferentially producing differing mycotoxins at different times. Additionally, not all mycotoxigenic species are culturable; many preharvest fungi are outcompeted and replaced by postharvest storage fungi.^[174] This introduces a disparity between the mycotoxins and secondary metabolites actually detected in the silage, and the species that in fact produced them, which is imperative for generating risk assessments to assist farmers. Molecular methods are required in tandem to fill in the gaps between the secondary metabolites and the fungi present in order to evaluate the principal source of toxin production; such information is vital for farmers to implement farming practices aimed at targeted mycotoxin prevention. Denaturing gradient gel electrophoresis (DGGE), which is a qualitative PCR-based approach, has been used to profile total microbial dynamics in artificially inoculated silage.^[178] However, DGGE is a time consuming method to obtain the genus and species level identifications of individual excised bands, so it is typically used for monitoring the dynamics of predominant fungal and bacterial species. The trend for evaluating microbial diversity has diverged towards next-generation sequencing (NGS), which uses unique barcoded primers to obtain microbial profiles from the total DNA present. NGS is capable of potentially detecting thousands of species which are otherwise difficult to isolate, and has already been used to describe the bacterial biodiversity in silage used for biogas production.^[179]

Numerous multi-mycotoxin monitoring studies of animal feed have previously reported that the majority ($\geq 75\%$) of the samples tested contained more than one mycotoxin, which even at trace levels, could be toxic to livestock when consumed.^[180] Thus, there are concerns regarding synergistic toxicities from both known and potentially unknown mycotoxins and secondary metabolites co-occurring in agricultural products. Masked and conjugated mycotoxins, which commonly evade traditional targeted screening methods, are also detected in food products.^[26,111,163] Due to advances in instrumentation, new and conjugated mycotoxin derivatives are being described more frequently, but typically require additional method development and validation prior to analysis on foodstuffs. In addition, incorporating any newly described mycotoxins into a method to screen older samples requires that the sample be re-run and re-analyzed. As traditional targeted or data-dependent MS² (ddMS²) LC-MS screening techniques rely solely on the detection of known regulated mycotoxins with available

commercial standards, there is little emphasis on the emerging or conjugated mycotoxins which tend to lack toxicological data for regulatory purposes. Malachova et al., (2014) built on successful screening methods developed from Sulyok and others, (2006) to detect 295 bacterial and fungal secondary metabolites, which was later validated in food products.^[165,181] As strict regulatory guidelines for mycotoxin allowances in food and feed change, the number of mycotoxins that will need to be screened in a single run will invariably increase.

Though commonplace in proteomics, liquid chromatography data independent acquisition MS (LC-DIA) has only recently been validated in *Fusarium graminearum* infected maize for mycotoxin analysis.^[182,183] The non-targeted small molecule analysis method developed by Renaud and Sumarah, (2016) combines the sensitivity from the introduction of small mass windows, (11, 15, and 20 Da) with the selectivity of a high resolution ion trap mass spectrometer.^[183] Selective analysis over the three mass ranges allowed for digital archiving (DA) of all ionisable compounds within the samples for successful retrospective analysis of the newly reported 15-acetyl-DON-3-O- β -D-glucoside without sample re-analysis.^[184]

Beyond the predominant species and mycotoxins detected in spoiled silage, there is limited information available regarding the fate and toxicities of co-occurring mycotoxins from contaminated silage after being fed to livestock; especially in meat and milk.^[41] Similarly, little is known about the cool climate total fungal and bacterial microbiota in Canadian silage samples that can influence the toxins actually detected in silage; such information could provide a risk assessment of the potential mycotoxins that may be produced by the fungi present in cooler climates as conditions become more favourable for their production. By combining next-generation sequencing (NGS) with liquid chromatography-MS DIA-DA, unique metabolomic and microbial profiles can be compiled from contaminated silage samples from 26 Canadian farms. As mycotoxigenic fungi and emerging secondary metabolites become of regulatory importance, both the digitally archived LC-MS silage samples and the NGS data can be mined for retrospective analysis.

4.3- Experimental

4.3.1 Silage material

Silage material, which included maize, barley and haylage silage blends, was collected by Dr. Danica Baines, (Agriculture and Agri-Food Canada, Lethbridge, Alberta). Visibly mouldy silage (hot spots) were selected from 26 Canadian production sites in Alberta, Saskatchewan and Ontario where dairy goats and beef cattle were experiencing variable signs of toxicoses.^[185–187] Site 24 had to be removed from data processing due to a lack of material available for paired metabolite extraction.

4.3.2 Fungal isolations and identification

Raw silage material was plated on Potato Dextrose Agar (PDA, Sigma-Aldrich), PDA supplemented with 50 mg/L chloramphenicol (Sigma-Aldrich) and Czapek Yeast Autolysate Agar (Czapek-dox broth and 5 g/L yeast extract, Sigma-Aldrich).^[188] Growing colonies were isolated as single spore isolates onto PDA using the dissecting microscope (Nikon SMZ745T) for 3-point inoculations. Representative isolated species were deposited within the Canadian Collection of Fungal Cultures, (Ottawa, ON, Canada). The DNA of each isolated species was extracted using the MoBio PowerLyzer UltraClean Microbial DNA Isolation Kit (MoBio Laboratories, Solana Beach, CA, USA) using a bead-based homogenization, (Bio101 Savant FastPrep FP120 cell disrupter). Isolated DNA was used in PCR using ITS1/4, β tub2a/2b, and An/Aw primers (Invitrogen, Supplementary Table 4S) using an Eppendorf Mastercycler Nexus Gradient Thermal Cycler.^[81,189,190] PCR mixtures were performed in a total volume of 25 μ L, and consisted of 2 μ L genomic DNA, (15 ng/ μ L), 20 μ L Platinum Blue SuperMix (Invitrogen, Carlsbad, CA, USA), and 0.6 μ M of each forward and reverse primer (4.2.2.1).

4.3.2.1 PCR Conditions

ITS1/4 and β tub2a/2b Primers

Both the ITS and β -tubulin regions were amplified using an initial denaturation step of 94 °C for three minutes, followed by 35 cycles of 94 °C for 30 s, 55 °C for 30 s, and 72 °C for 30 s with a final elongation step at 72 °C for five minutes.

An/Aw Primers

The *A. niger* (An) and *A. welwitschiae* (Aw) specific primers were used to confirm the identity of any *A. niger* isolates from the β -tubulin sequences, and have been previously optimized by Qi, 2016.^[191] AnF/R primers were amplified using an initial denaturation step of 95 °C for five minutes, followed by 35 cycles of 95 °C for 30 s, 62.3 °C for 30 s, and 72 °C for 30 s with a final elongation step at 72 °C for five minutes. AwF/R primers were amplified using an initial denaturation step of 95 °C for five minutes, with 35 cycles of 95 °C for 30 s, 61.1 °C for 30 s, 72 °C for 30 s, with a final elongation step of 72 °C for five minutes.

4.3.2.2 Sequencing analysis

PCR products were cleaned using ExoSAP-IT (Affymetrix, Santa Clara, CA, USA), and sequenced in forward and reverse directions at the Robarts Research Institution, (Western University, London, ON, Canada) using 4 μ L PCR product with 2 μ L of each forward and reverse primer (2 μ M stock solutions). Forward and reverse sequences were aligned using SeqMan Pro software (Lasergene 10 Core Suite, DNASTAR) and trimmed to exclude terminal nucleotides. Aligned sequences were searched using NCBI GenBank using the nucleotide BLAST (Basic Local Alignment Search Tool) interface for fungal organisms. Sequences were confirmed by matching sequences from type material using a query coverage cut-off and an identification confidence of $\geq 95\%$. Sequences were further confirmed by comparison to generated phylogeny from the generated distance blast tree results using the fast minimum evolution method.

4.3.3 Next-generation sequencing of total silage DNA

Silage samples were lyophilized and ground into a powder using mortar and pestles under liquid nitrogen; both the mortar and pestles were soaked in 25% bleach and wiped clean with 70% ethanol prior to use to limit DNA carryover. DNA was extracted from approximately 3 g ground material using the MoBio PowerMax Soil DNA Isolation Kit (10 g, MoBio Laboratories, Solana Beach, CA, USA). Prior to PCR, the DNA was cleaned using DNA Clean and Concentrator (Zymo Research Corporation, Irvine, CA, USA). PCR analysis was performed in 25 μ L final volume, using 1.0 – 4.0 μ L purified DNA, 12.5 μ L AccuStart PCR Toughmix (Quanta Biosciences, Beverly, MA, USA), and 1.25 μ L of each forward and reverse primer, (Supplementary, Table 5S).

4.3.3.1 PCR Conditions

All PCR conditions were previously developed and validated by Asemaninejad et al., 2016 using LSU200A-F, LSU476A-R ascomycete-specific primers, and 16S rRNA-based bacterial primers (V4) in Dr. Greg Thorn's research laboratory, (Western University, Department of Biology, London, ON, Canada).^[83]

Ascomycete-specific primers (LSU200A-F, LSU476A-R) and 16S rRNA-based bacterial primers (V4)

For amplification, an initial denaturation step of 94 °C for two minutes was applied, followed by 29 cycles of 94 °C for 30 s, 55 °C for 30 s (first cycle only, 62 °C for 30 s for the remainder), and an elongation temperature of 72 °C for 18 s.

4.3.3.2 Sequencing analysis

PCR products were sent to the London Regional Genomics Centre (Robarts Research Institute, lrgc.ca, London, ON, Canada) and quantified using a Qubit 2.0 Fluorimeter using double-stranded DNA-specific fluorescent probes (dsDNA HS assay kit, Life Technologies) for normalization, prior to being processed for paired-end MiSeq Illumina sequencing (2 x 300 bp cycles, version 3 reagents). Raw FASTQ was analyzed using an established processing pipeline from Dr. Greg Gloor, (Western University, Department of Biochemistry, London, ON,

Canada).^[192] The PANDAseq assembler (Paired-end assembler for DNA sequences) was used to overlap reads, using a minimum overlap of 30 nucleotides, and any ambiguous or mismatched reads were removed. FASTQ output from the pipeline was grouped into identical sequence units (ISUs) by identity. Chimeras were removed using UCHIME, and sequences were grouped as operational taxonomic units (OTUs) at 97% similarity to a centroided representative sequence within each OTU using UCLUST within USEARCH v7.0.1090.^[193,194] OTUs with less than 1% abundance of the total reads per sample were removed from the dataset. MOTHUR v.1.35.1 was used for taxonomic assignment for each OTU group using assignment using the UNITE database (for ascomycetes) and SILVA (for bacteria) with a 95% similarity cut-off at the highest confidence taxonomic rank.^[195,196] Non-specific OTUs corresponding to basidiomycete sequence matches were removed. Taxonomy assignments were verified using NCBI BLAST searching (Ascomycetes) and the Ribosomal Database Project (RDP, rdp.cme.msu.edu) using SeqMatch (bacteria).^[197] Weighted UniFrac distances between samples, representing beta diversity used for dendrogram production, was calculated using QIIME.^[198] Barplots were produced using sample proportions in R (r-project.org), and were clustered by beta diversity similarity according to the calculated weighted UniFrac distances.

4.3.4 Plug extraction of isolated fungal cultures

3-point inoculations of isolated fungal cultures were incubated at 25 °C on PDA for seven days. Screening of the isolated strains was performed by removing six agar plugs from each three-point inoculum using a 6 mm cork borer and extracting the plugs with ethyl acetate containing 1% formic acid (Sigma, St. Louis, MO) prior to LC-MS screening by ddMS² and DIA.^[91,199]

4.3.5 Metabolite extraction of silage

Lyophilized ground silage samples (0.5 ± 0.02 g) were extracted as Sulyok et al., 2006 using 2 mL 79/20/1 ACN/H₂O/HAc.^[165] Samples were vortexed for 30 seconds prior to placement on a rotary shaker for 90 minutes. Following centrifugation, the supernatant was diluted 1:1 with 20/79/1 ACN/H₂O/HAc and filtered through 0.45 µm PTFE syringe filters into amber vials for LC-DIA analysis. 5 µL of the diluted sample was injected on column for LC-DIA analysis.

4.3.6 LC-HRMS, ddMS² analysis for isolated cultures

HRMS and HRMS² data were obtained using a Thermo Q-Exactive Quadrupole Orbitrap Mass Spectrometer, coupled to an Agilent 1290 HPLC. A Zorbax Eclipse Plus RRHD C18 column (2.1 x 50 mm, 1.8 μ m; Agilent) was maintained at 35 °C. The mobile phase was comprised of water with 0.1% formic acid (A), and acetonitrile with 0.1% formic acid (B) (Optima grade, Fisher Scientific, Lawn, NJ). Mobile phase B was held at 0% for 30 seconds, before increasing to 100% over three and a half minutes. B was held at 100% for 1 and a half minutes, before returning to 0% B in 30 seconds. 2 μ L injections were used at a flow rate of 0.3 mL/min. The following conditions were used for negative HESI: capillary voltage, 3.7 kV; capillary temperature, 400°C; sheath gas, 17.00 units; auxiliary gas, 8.00 units; probe heater temperature, 450 °C; S-Lens RF level, 45.00. The full MS for the data dependent MS² (ddMS²) used the following settings: scan range, 75 – 800 m/z ; resolution, 70 000; AGC, 3e6; max IT, 250 ms. The five highest intensity ions from the MS were sequentially mass selected under a 1.2 m/z isolation window and analyzed at a resolution of 17 500; AGC target, 1e5; max IT, 60 ms; NCE, 35; threshold intensity, 1.2e5. Selected ions were excluded from further MS² scans for 10 s. The most intense peaks from the mass spectra were analyzed using Thermo Xcalibur Qual Browser software. Unknown metabolites were searched in AntiBase 2013 and SciFinder. In addition to ddMS², all plug extracts were similarly run using the DIA method, (4.2.7). All metabolite information from the plug extracts, including precursor mass, five fragments and retention time, were recorded in the digital archive database.

4.3.7 LC-HRMS DIA analysis for isolated cultures and contaminated silage

Mass spectra were acquired using a Thermo Q-Exactive Orbitrap mass spectrometer coupled to an Agilent 1290 HPLC using a Zorbax Eclipse Plus RRHD C18 column (2.1 x 50 mm, 1.8 μ m, Agilent). The following LC-MS conditions are as reported by Renaud and Sumarah, 2016.^[183] Two μ L of sample were injected on column, which was maintained at 35 °C. A flow rate of 0.3 mL/min was used for analyte separation, using LC-MS grade (Thermo Scientific, Fairlawn, NJ) water with 0.1% formic acid (mobile phase A) and acetonitrile with 0.1% formic acid (mobile

phase B) as mobile phases. Mobile phase A was held at 100% for 30 seconds, before decreasing to 0% over three minutes. A was held at 0% (100% B) for 2 minutes, before returning to 100% mobile phase A over 30 seconds. Heated electrospray ionization (HESI) had the following conditions for full MS analysis: capillary temperature, 400 °C; sheath gas, 17 units; auxiliary gas, 8 units; probe heater temperature, 450 °C; S-Lens radiofrequency (RF) level, 45%; capillary voltage 3.9 kV; resolution, 35,000. DIA analysis used the following settings: normalized collision energy (NCE), 35; automatic gain control (AGC), 2e5, injection time (IT), 64 ms; resolution, 17,500. Three independent six minute LC runs were conducted for three mass ranges: low mass (LM, 130-350), medium mass (MM, 350-650) and high mass (HM, 650-1050). LC-DIA-DA settings (Table 14) were optimized based on the mass distribution of 86 fungal secondary metabolite standards (Supplementary, Table 6S) to include for 2 full MS and 20 MS² scans across each mass range. All 86 fungal secondary metabolite standards were placed into the digital archive for silage sample analysis using Thermo Scientific Xcalibur software. Similarly, all DIA files have been recorded in the digital archive for retrospective analysis. Confidence levels for positive secondary metabolite identification was modified from SANCO/12495/2011 for pesticide analysis, which requires ≥ 2 product ions in addition to the HRMS precursor molecular ion, and retention time tolerance $\pm 2.5\%$ of the run time.^[56] Due to the matrix complexity, fungal secondary metabolites from contaminated silage were positively identified in samples processed at a higher confidence level to include six total features, which included the retention time, precursor molecular ion, and four associated fragments.

Table 14- Optimized LC-DIA conditions for 3 separate LC runs

Method	Mass range (m/z)	Mass window size (Da)	Cycle time (s)
LM	130-350	11	2.3
MM	350-650	15	2.3
HM	650-1050	20	2.3

4.4 Results and Discussion

4.4.1 Isolated fungal cultures

From the 26 Canadian sites, 26 unique species (Table 15, Supplementary Table 7S) were isolated from contaminated barley, haylage, silage and corn silage, including 11 species of *Penicillium*. The most commonly isolated species were *Penicillium roqueforti*, *P. paneum*, *P. aurantiogriseum*, *P. crustosum*, species belonging to the *Aspergillus* genus, and *Monascus ruber*. The large proportion of *Penicillium* species and their secondary metabolites has been previously observed for cool climate regions, while *Aspergilli* are more commonly isolated from warmer climate regions.^[183,200–203] Similar *Penicillium* species proportions (*P. roqueforti*, *P. paneum*, *P. crustosum*) have been reported from cool climate regions.^[201,204] In Quebec, the most commonly detected *Penicillium* species from contaminated silages associated with ruminant toxicosis was *P. paneum*.^[201] *Fusarium*, which is exclusively a cool climate pre-harvest pathogen, was isolated from individual ensiled maize kernels, but not from haylage or barley. Many of the genera detected, such as *Fusarium*, *Penicillium* and *Aspergillus*, produce potent mycotoxins that have been regulated and monitored by Health Canada and the Canadian Food Inspection Agency (CFIA) in food and feed (Supplementary, Table 8S).^[205] Many of the additional genera isolated have been reported to produce secondary metabolites which have associated regulatory guidance values in Canadian food and feed based on recommendations by the Food and Agriculture Organization of the United Nations (FAO).^[205]

Table 15- Fungal species isolated from contaminated silage. *Indicates that the fungus has been previously isolated from silage (Alonso, V.A et al., 2013). Bolded species were commonly isolated from the contaminated sites

Species isolated	Primer for DNA sequencing
<i>Aspergillus fumigatus</i> *	B-tubulin2a/b
<i>Aspergillus nidulans</i>	B-tubulin2a/b
<i>Aspergillus welwitschiae</i>	B-tubulin2a/b and <i>A. welwitschiae/A. niger</i> -specific primers
<i>Aspergillus glaucus</i>	ITS1/4
<i>Chaetomium globosum</i>	ITS1/4
<i>Cladosporium</i> sp.*	ITS1/4
<i>Fusarium</i> sp.*	ITS1/4
<i>Geotrichum</i> sp.*	ITS1/4
<i>Gliocladium roseum</i>	ITS1/4
<i>Ipex lacteus</i>	ITS1/4
<i>Leptosphaeria</i> sp.	ITS1/4
<i>Monascus ruber</i> *	ITS1/4
<i>Mucor circinelloides</i> *	ITS1/4
<i>Myceliophthora lutea</i>	ITS1/4
<i>Penicillium atrovenetum</i>	B-tubulin2a/b
<i>Penicillium aurantiogriseum</i>	B-tubulin2a/b
<i>Penicillium crustosum</i> *	B-tubulin2a/b
<i>Penicillium flavigenum</i>	B-tubulin2a/b
<i>Penicillium griseofulvum</i> *	B-tubulin2a/b
<i>Penicillium nordicum</i>	B-tubulin2a/b
<i>Penicillium paneum</i> *	B-tubulin2a/b
<i>Penicillium roqueforti</i> *	B-tubulin2a/b
<i>Penicillium rugulosum</i>	B-tubulin2a/b
<i>Penicillium simplicissimum</i>	B-tubulin2a/b
<i>Penicillium viridicatum</i>	B-tubulin2a/b
<i>Pseudallescheria boydii</i>	ITS1/4

4.4.2 Secondary metabolites from isolated cultures

Individual isolated cultures from the *Penicillium* and *Monascus* genera were assessed for their potential to produce mycotoxins and secondary metabolites under artificial conditions. 72 known (Table 16) and 53 unknown (Supplementary Table 9S) secondary metabolites and mycotoxins were detected from the plug extracts.

Several isolated *Penicillium* species produced regulated mycotoxins such as patulin, in addition to OTA, which was produced by *P. nordicum*. Both detected toxins are of current concern to Canadian agriculture for their inherent trace-level toxicity, as well as their predominant presence

in apple-based and wheat-based commodities respectively. Other unregulated *Penicillium* secondary metabolites with reported animal toxicoses are PR toxin and penitrem A, which were also detected from the isolated cultures.^[201,206]

4.4.3 Secondary metabolites from contaminated silage and retrospective analysis

Of the 125 mycotoxins and secondary metabolites produced on artificial media, only 48 of those same secondary metabolites were detected in the silage, (Table 16, Supplementary Table 9S). This is in agreement with previous studies that observed dramatic differences between metabolites reported in artificial media, and metabolites reported from naturally contaminated material.^[177,207] *Monascus ruber*, which was commonly isolated from contaminated silage, produced the largest variety of secondary metabolites *in situ*, which were subsequently detected in the silage sites. In addition to citrinin, numerous related *Penicillium* metabolites (Table 15), and six unknown secondary metabolites (Supplementary Table 9S), monacolin K (Lovastatin) was also detected in the silage. Lovastatin, which is a commercially manufactured cholesterol-lowering drug, has been frequently detected in silages in considerable quantities.^[208,209] The presence of Lovastatin in silages has been associated with the interference of ruminant gut mycoflora by inhibiting ergosterol synthesis of beneficial cellulolytic fungi, thus restricting fiber digestion.^[209]

PR toxin, which was detected in the silage and produced artificially by *P. roqueforti*, has been previously linked to the primary cause of ruminant toxicosis in Quebec from contaminated maize silages.^[201] Similarly, maize silage infected with *P. roqueforti* in which PR-toxin was the major secondary metabolite, was associated with loss of appetite, abortion, and gut inflammation in cattle.^[210-212] Penitrem A, which was also detected in both contaminated silage and plugs, has also been reported to cause acute acute toxicity in dogs.^[206]

Using the DIA fungal metabolite database, 42 secondary metabolites were detected in the 26 sites. The 42 secondary metabolites were predominantly associated with *Penicillium* spp. contamination, and includes andrastins, brevianamides, penitrem A, griseofulvin, cyclopiazonic acid, among others, (Table 16). Though *Penicillium* spp. are not strictly postharvest ensiling pathogens, their predominance does coincide with the large variety of *Penicillium* secondary metabolites detected.

Table 16- Mycotoxins and secondary metabolites detected in the plug isolates and extracted silage

Metabolite	Plugs	Silage	Metabolite	Plugs	Silage
15-acetyldeoxynivalenol (DIA)		X	Ergocorninine (DIA)		X
3/4/7-hydroxycoumarin	X ^a	X	Ergocryptinine (DIA)		X
12-Methoxycytromycin	X ^a		Fumonisin B1 (DIA)		X
Anacine	X ^{b,c}	X	Fumonisin B2 (DIA)		X
Andrastin A	X ^{a,d,e,f,g}	X	Fumonisin B3 (DIA)		X
Andrastin B	X ^{a,d,g,e}	X	Fusarenon X (DIA)		X
Andrastin C	X ^{a,d,e,f,g}	X	Fusarubin (DIA)		X
Andrastin D	X ^{a,d,g,e}	X	Gibberellin A	X ^g	X
Andrastin E/F	X ^{a,d,g,e}	X	Glandicoline B	X ^g	
Altenuene (DIA)		X	Griseofulvin (DIA)	X ^h	X
Altenuene-SO ₃ (Retrospective)		X	HT-2 toxin (DIA)		X
Alternariol (DIA)		X	5-hydroxyculmorin		X
Alternariol monomethyl ether		X	Kandavanolide	X ^e	X
Alternariol monomethyl ether-		X	Koninginin A (DIA)		X
Altenusin-SO ₃ (Retrospective)		X	Koninginin E (DIA)		X
Aspergione C (Retrospective)			Lovastatin (Monacolin K)	X ⁱ	X
Atranone B (DIA)		X	Macrosporin		X
Aurantiamine	X ^b	X	Maculosin		X
Aurantiomide A	X ^b		Marcfortine A	X ^a	X
Aurantiomide B	X ^b		Marcfortine B	X ^a	X
Aurantiomide C	X ^b		Marticin (DIA)		X
Beauvericin (DIA)		X	Meleagrins (DIA)	X ^{g,h}	X
Bostrycin (DIA)		X	Mellein (DIA)		X
Brevianamide K	X ^c	X	Methylenolactocin	X ^c	
Brevianamide V	X ^c		Monapurone A	X ⁱ	X
Bromogriseofulvin	X ^h		Monascin	X ⁱ	X
Chaetoviridin A (DIA)		X	Monascumic acid	X	X
Chaetoglobosin A		X	Monasfluore A	X ⁱ	X
Chaetoglobosin C		X	N6-Formyl roquefortine C	X ^{d,e,g}	
Chermesinone A	X ^e	X	Neosolaniol (DIA)		X
Citreopyrone E	X ⁱ	X	OTA	X ^c	
Citrinalin A/B	X ^h		OTB	X ^c	
Citrinin (DIA)	X ^{a,c,h,i}	X	OTB Me	X ^c	
Comazaphilone B?	X ⁱ	X	Patulin*	X ^{a,h}	(X)
Culmorin (DIA)		X	Penicitrinol H	X ⁱ	
Curvularin	X ^a		Penitrem A (DIA)	X ^{d,g}	X
Cyclo(Δ-Ala-L-Val)	X ⁱ	X	Phacidin (DIA)		X
Cyclo(L-Phe-L-Pro)	X ⁱ	X	PR Toxin	X ^e	X
Cyclo(L-Pro-L-Leu)	X ^a	X	Pyrenocine C	X ^j	
Cyclopeptide	X ^d	X	Pyrenopherol		X
Cyclopiamine A/B	X ^h	X	Restrictinol (Retrospective)		X
Cyclopiamine A/B- related	X ^h	X	Roquefortine C (DIA)	X ^{a,d,e,g,h}	X
α-cyclopiazonic acid (DIA)		X	Roquefortine F	X ^{e,g}	

Dechlorogriseofulvin	X ^h	X	Rubropunctatin	X ^l	
Dehydrocurvularin	X ^a		Satratoxin G (DIA)		X
Dehydroaltenusin-SO ₃		X	Satratoxin H (DIA)		X
Deoxynivalenol		X	Sclerotigenin	X ^c	
3/15-deoxynivalenol glucoside		X	Simplicissin	X ^f	
Descarestrictin E	X ^j		Sterigmatocystin (DIA)		X
Descarestrictin I	X ⁱ		3,7,15-		X
Dihydrocitrinin	X ⁱ		T-2 Toxin (DIA)		X
Dihydrocurvularin	X ^a		Terrestric acid	X ^{b,d}	X
Enniatin A1 (DIA)		X	Viridicatin (DIA)	X ^d	X
Enniatin B (DIA)		X	Walleminone (DIA)		X
Enniatin B1 (DIA)		X	Wortmannilactone F	X ^{e,f}	
Epoformin	X ^b	X	Xanthomegnin	X ^j	
Eremofortin A	X ^c	X	Zearalenone (DIA)		X
Eremofortin B	X ^c	X	15-acetyl-DON-3-O-		
Eremofortin C	X ^c		15-acetyl-DON-3-sulfate		
Eremofortin D	X ^c	X			

Legend: ^a*Penicillium paneum*, ^b*P. aurantiogriseum*, ^c*P. nordicum*, ^d*P. crustosum*, ^e*P. roqueforti*, ^f*P. simplicissimum*, ^g*P. flavigenum*, ^h*P. griseofulvum*, ⁱ*Monascus sp.*, ^j*P. viridicatum*

Though OTA was produced in artificial plug extracts from *P. nordicum*, it was not detected in contaminated silage. OTA contamination by *P. nordicum* commonly occurs during the postharvest storage of wheat or cereal commodities; however it was not detected under ensiling conditions. However, there is still potential for OTA to be detected in ensiled material after its postharvest production, as it is stable in stored grain.^[213] It is unknown whether *P. nordicum* could continue producing OTA as conditions become more favourable for its growth during further silage spoiling.

There were numerous mycotoxins and secondary metabolites detected, which are associated with preharvest pathogens and other contaminant fungi which could not be isolated, such as *Fusarium* spp., *Alternaria* spp., *Stachybotrys* spp., *Trichoderma* spp., and *Claviceps* spp.. Enniatins were detected in high abundances in both silage and maize silage, in addition to the regulated mycotoxins deoxynivalenol (DON, vomitoxin) and HT-2 toxin which implies the presence of *Fusarium* as a preharvest pathogen in cereal or maize crops. Likewise, the ergot alkaloids ergocorninine and ergocryptinine produced by *Claviceps* spp. were detected in a single site

comprised of barley silage. Ergot alkaloids are concentrated in sclerotia that grow on cereal crops, and are removed during the milling and cleaning of the grain destined for human consumption.^[214] However, much of the spent grain from the milling process is destined for livestock feed, and thus would concentrate the ergot sclerotia and alkaloids in the feed. Exposure to ergot alkaloids by ruminants, which can accumulate in tissues, has been associated with constriction of blood vessels resulting in the inability of the animal to modulate its body temperature, and a decrease in prolactin release in dairy cattle.^[215]

In contrast, N6-formyl roquefortine C, which was detected in the plug extracts, and was previously reported in maize silage artificially inoculated with *P. roqueforti*, was not detected in naturally contaminated maize silage.

The effectiveness and sensitivity of the DIA method is demonstrated in the retrospective analysis of trace molecules. Using retrospective analysis, seven additional secondary metabolites with published high resolution mass spectra were confirmed, including several sulfoconjugated secondary metabolites produced by *Alternaria*. Despite their poor ionization efficiencies in positive ionization mode, numerous features were detected using previously analyzed spectra that allowed for their characterization in positive ionization mode. The implementation of a negative mode DIA could render the poor ionization efficiencies for both *Alternaria* secondary metabolites, and the regulated *Penicillium* mycotoxin patulin.

4.4.4 Next-generation sequencing of fungi for the community profiling of contaminated silage

Some of the secondary metabolites detected in silage implied the presence of several fungal genera, but were not isolated, such as *Fusarium*, *Alternaria*, *Stachybotrys*, *Trichoderma* and *Claviceps*. It becomes important to be able to confirm the fungi producing the secondary metabolites in order to control for their occurrence during preharvest or postharvest conditions. Assigning potential taxonomy to detected secondary metabolites becomes difficult, as numerous genera can share biosynthetic gene clusters, which produce shared classes of mycotoxins. For instance, both *Fusarium* and *Stachybotrys* produce different mycotoxins, (non-macrocylic and macrocylic respectively) within the trichothecene class, and are isolated in different substrates and conditions.^[216] Similarly, koniginins, which are predominantly produced by *Trichoderma*,

can also be produced by certain species of *Penicillium*.^[217] Thus, next-generation sequencing was used to obtain fungal profiles of the contaminated sites to both confirm the presence of suspected mycotoxigenic fungi, and to examine their relative species proportions which can be linked to their detected secondary metabolites.

NGS was used to estimate the biodiversity of fungi in contaminated silage, which includes minor fungal populations, and preharvest mycotoxigenic fungi which cannot easily be isolated under standard conditions. The most common fungal species associated with silage spoiling between all sites were *Penicillium* sp., *Monascus ruber* and *Aspergillus* sp., which coincides with the predominant fungi that were isolated. However, the majority of fungal species detected by NGS were of preharvest origin, such as several species of *Fusarium*, *Verticillium*, and *Alternaria* (Figure 43).

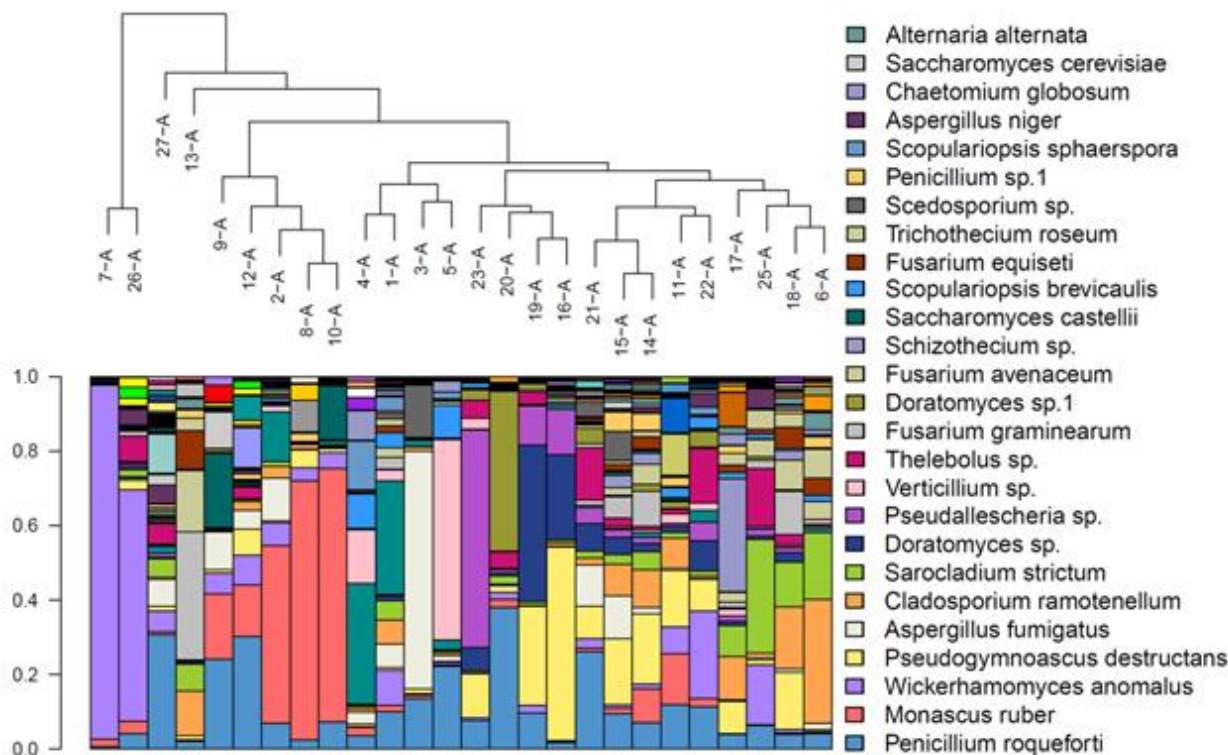


Figure 43- Barplot of Ascomycetes by proportion in contaminated silage, showing the most abundant 26 fungal species. The commonly detected species between sites are listed in highest abundance to lowest abundance from bottom to top

Several species of *Fusarium* were detected, including *F. equiseti*, and *F. graminearum*, which can produce the secondary metabolites DON and zearalenone. Interestingly, *F. avenaceum*, which can produce enniatins, was not as predominant as *F. graminearum* and *F. equiseti* (Supplementary Table 10S), despite the high concentration of enniatins detected in the silage.

A caveat of the general fungal primer design, which was based on the D1 variable of the nuclear large ribosomal subunit region, lies in the differentiation between species of *Penicillium*. While 11 species of *Penicillium* were independently isolated from the contaminated silage, the non-specificity of the D1-based primer only distinguished three DNA sequences, (OTUs) at the cut-off level. Thus, the different species were likely grouped together as different reads within the three OTUs.

In contrast, *Trichoderma*, *Stachybotrys* and *Claviceps* were not detected by NGS, despite the presence of their characteristic secondary metabolites. Presently, conclusions cannot be confidently drawn regarding their presence or absence, as the sensitivity of the general fungal

barcoded D1 primers may not be particular to the genera. However, it cannot be ruled out that different fungal genera are producing these shared mycotoxins and secondary metabolites.

4.4.5 Next-generation sequencing of bacteria for the community profiling of contaminated silage

Several species of lactic acid-producing bacteria (LAB) are common silage additives due to their deterrence of spoilage microorganisms. However, Li and others (2011) have previously demonstrated that the addition of LAB is not always indicative of a better quality of silage, as some strains are easily outcompeted by the more predominant bacterial species present.^[218] Previous profiling of predominant bacterial species has been accomplished using DGGE to evaluate the complexity of potentially changing communities in spoiled silage.^[178]

121 bacterial species were detected in all 26 contaminated sites by NGS. *Yersinia*, and *Clostridium* have all been previously reported as common anaerobic bacterial genera associated with spoiled silage. The most predominant beneficial LAB detected in the 26 contaminated silage sites were *Lactobacillus kefir* and *L. plantarum* (Figure 44). Despite the predominance of both LAB species in sites 21, 25 & 13, all three sites contained diverse fungal populations, (Figure 43) including the mycotoxigenic acid-tolerant genera *Penicillium* and *Monascus* and their related secondary metabolites. Thus, the presence of LAB does little to deter acid-tolerant fungal genera, and thus prevent the occurrence of their secondary metabolites in silage.

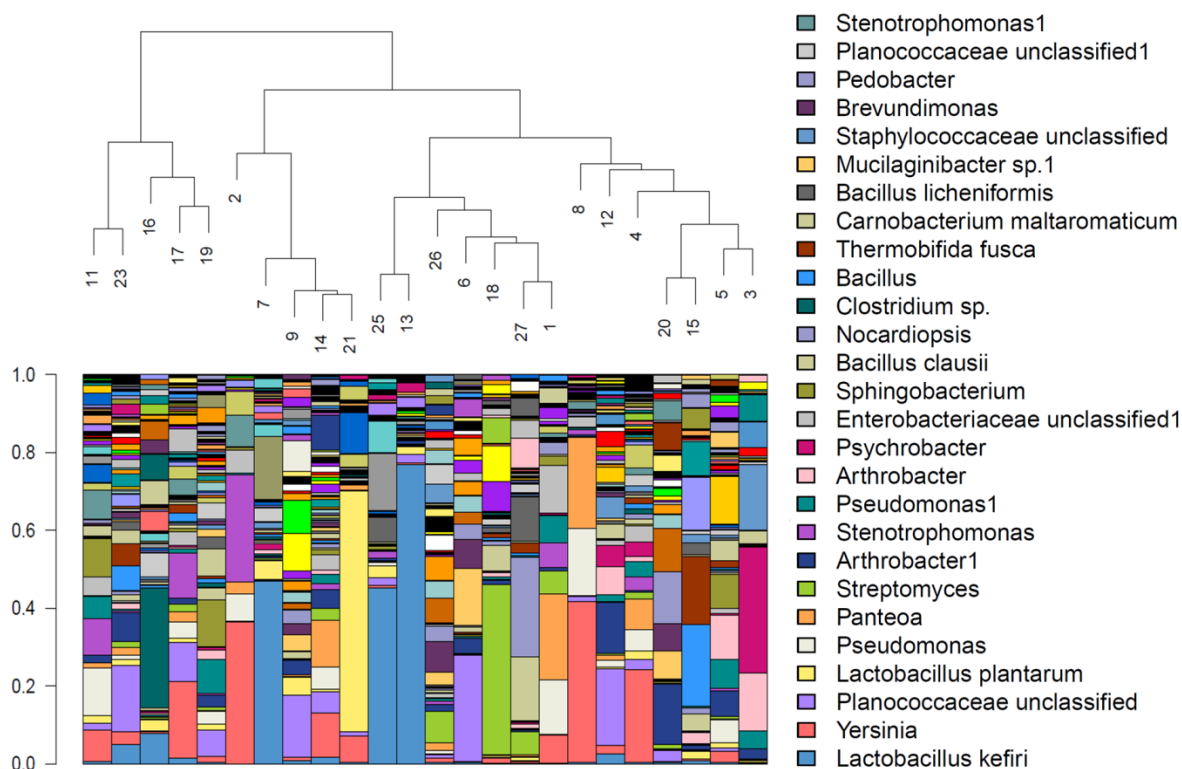


Figure 44- Barplot of bacteria by proportion in contaminated silage, showing the most abundant 27 bacterial species. The commonly detected species between sites are listed in highest abundance to lowest abundance from bottom to top

4.5 Conclusions and Future Work

Despite the complexity of the contaminated silage matrix, DIA-DA was an effective method for the analysis of mycotoxins and secondary metabolites. The DIA method also demonstrated a high sensitivity and selectivity for analytes that allowed for retrospective analysis at trace levels.

The most abundant fungal species (*Penicillium*, *Monascus*) were screened by the plug extract method, but the additional fungal isolates need to be screened and added to the silage processing method.

While the DIA method was previously demonstrated to be quantifiable, efforts are on-going to develop appropriate matrix-matched calibration curves for mycotoxins and secondary metabolites currently of regulatory concern. Similarly, methods are being developed for on-going performance verifications by the addition of several internal standards over the three mass

ranges, (LM/MM/HM). In addition, several mycotoxins and secondary metabolites have poor ionization efficiencies in positive mode, thus work is currently underway towards the development and validation of DIA in negative ionization mode.

Total microbial community profiling of contaminated silage by NGS had not been previously undertaken, and may prove to be useful in the determination of the total fungi and bacteria present in cool climates, and how it influences secondary metabolite production. Future projects will likely focus on the cooler climate mycotoxigenic *Penicillium* species, thus new primer design will include barcoded regions specific to the β -tubulin region for *Penicillium* differentiation. Similarly, the combination of NGS with metabolomics data could be used for determination of mycotoxins in the ruminant diet, and the fate of those same secondary metabolites and mycotoxins in the animal by-products for human consumption. Possible positive and negative correlations between the bacterial and fungal proportions are currently being investigated, though further inoculation experiments will be required to confirm the direction of correlation.

Chapter 5- Conclusions

5.1 Conclusions

Alternaria is a common saprophyte and plant pathogen of a number of agriculturally-relevant crops, and is known to produce a number of secondary metabolites of toxicological concern.^[32,114,119,124] The high degree of similarity of their genomes makes it difficult to differentiate between species.^[30,31] Additionally, their distribution and associated secondary metabolites in Canadian agricultural commodities was relatively unknown. Thus, an untargeted metabolomics method with statistical validation was completed in Chapter 2 using HRMS for 148 Canadian strains of *Alternaria* to determine: 1) their distribution in Canada and Canadian agriculture, and 2) their risk of secondary metabolite contamination in agricultural commodities. It was demonstrated that there were four predominant chemotypes in Canada, corresponding to their presence or absence of certain secondary metabolites, such as infectopyrone and an additional unknown novel biomarker (*A. infectoria*), tenauzonic acid and altenuisol. The general secondary metabolome was evaluated, and a risk assessment was provided for secondary metabolite contamination in agriculturally-relevant food crops, including wheat, tomato and grape. However, there does not seem to be a general consensus on the identification of many *Alternaria* species, thus it is presently unclear if the specific chemotypes are species-level definitions, or if the metabolite variations are related to the superfluous chromosome in *A. alternata*.

New and emerging mycotoxins are constantly being described due to the technological advances towards instrumentation and method development, which results in trace level detection of target analytes.^[165,181] Targeted LC-MS methods are commonly used to detect regulated mycotoxins, as well as secondary metabolites with guidance values.^[180] However, mycotoxins may exist as conjugated or modified derivatives, which would evade traditional screening methods.^[25,26,184] Therefore, post-data acquisition semi-targeted screening methods, such as neutral loss filtering and product ion filtering were investigated. The investigation in Chapter 3 focussed on: 1) the detection of new sulfoconjugated derivatives, 2) the detection of total AAL toxins, enniatins and cyclodepsipeptides, and 3) their potential addition to established targeted screening methods in artificial and agricultural commodities. Using semi-targeted HRMS and ddMS² methods, new

secondary metabolites were described, which were also demonstrated present in agricultural commodities.^[111,163] As the semi-targeted methods are post-data acquisition, the processing can be accomplished on high resolution instruments on the same samples without compromising scan time.

Silage, which is LAB-ensiled forage material, is fed year-round to cattle, with some ruminants eating kilograms per day.^[37] However, silage can become contaminated with mycotoxin-producing fungal genera, such as *Penicillium* and *Aspergillus*.^[201,202] However, there are currently no comprehensive analyses of the Canadian cool climate silage microbiome as it relates to secondary metabolites and mycotoxins detected. Similarly, even in silages linked to animal toxicoses, it remains unclear on the specific toxins involved in animal toxicity, or whether there are synergistic effects enhancing toxicity from mycotoxin co-contamination. To the same effect, there are no methods of re-evaluating newly discovered mycotoxins in older samples without sample re-analysis and re-processing. Thus, fungal contaminated silages linked to dairy animal toxicoses were extracted and evaluated in Chapter 4 to: 1) assess the predominant Canadian fungal species after ensiling, 2) determine the total fungal and bacterial communities using NGS, 3) assess the major fungal secondary metabolites produced artificially by isolated cultures and their risk of contamination in silage and 4) assess the total fungal secondary metabolites detected in a complex matrix using DIA with digital archiving and retrospective analysis. The predominant mycotoxin-producing fungi in contaminated Canadian silage were the cold and acid-tolerant genera of *Penicillium* and *Monascus*, and their presence and associated secondary metabolites were not deterred by beneficial LAB. It was also demonstrated that there is a large discrepancy between the secondary metabolites produced artificially, and those detected in the silage. NGS provided fungal and bacterial profiles which were supported by the predominant secondary metabolites detected and isolated fungi. The DIA method with digital archiving was validated to be sensitive enough for trace analysis of mycotoxins in a complex matrix. However, the true power of the DIA method was demonstrated by the retrospective analysis of digitally archived samples, for which analytes could be confidently assigned without the need for sample re-analysis and re-processing. This is especially important for generating risk assessments in Canadian agriculture, and for the continued monitoring of mycotoxins and secondary metabolites of toxicological concern.

References

- [1] M. Blackwell. The fungi: 1,2,3...5.1 million species? *Am. J. Bot.* **2011**, 98, 426.
- [2] R. P. Jaques, W. R. Jarvis, Chapter 2- Crop losses and their causes, in *Diseases and Pests of Vegetable Crops in Canada*. The Canadian Phytopathological Society And Entomological Society Of Canada, **1994**.
- [3] Statistics Canada. Global Trade Atlas. can be found under <http://www.statcan.gc.ca/tables-tableaux/sum-som/101/cst01/gdps04a-eng.htm>, **2016**.
- [4] Agriculture and Agri-Food Canada. Agriculture and Agri-Food Canada Scientists Looking to Nature to Control the Disease that Caused the Irish Potato Famine. can be found under <http://www.agr.gc.ca/eng/news/science-of-agricultural-innovation/agriculture-and-agri-food-canada-scientists-looking-to-nature-to-control-the-disease-that-caused-the-irish-potato-famine/?id=1433168638577>, **2015**.
- [5] Statistics Canada. Canada's population estimates, fourth quarter 2015. can be found under <http://www.statcan.gc.ca/daily-quotidien/160316/dq160316c-eng.htm?HPA>, **2016**.
- [6] FAO, Global agriculture towards 2050, in *How to Feed the World 2050 High-Level Expert Forum*. Rome, **2016**.
- [7] N. A. Hassanain, M. A. Hassanain, W. M. Ahmed, R. M. Shaapan, A. M. Barakat, H. A. El-Fadaly. Public Health Importance of Foodborne Pathogens. *World Journal of Medical Sciences* **2013**, 9, 208.
- [8] J. W. Bennett, M. Klich. Mycotoxins. *Clin. Microbiol. Rev.* **2003**, 16, 497.
- [9] B. Kendrick, The Fifth Kingdom- Third Edition, in *The Fifth Kingdom*. Focus Publishing, R. Pullins Company, Newburyport, MA, USA, **2000**.
- [10] L. Coates, G. Johnson, Postharvest diseases of fruits and vegetables, in *Plant Pathogens and Plant Disease*. Australasian Plant Pathology Society, **1997**, pp. 533–547.
- [11] A. M. Calvo, R. A. Wilson, J. W. Bok, N. P. Keller. Relationship between secondary metabolism and fungal development. *Microbiol Mol Biol Rev* **2002**, 66, 447.
- [12] Mycology - Growth and Development - Hyphal Growth. can be found under http://bugs.bio.usyd.edu.au/learning/resources/Mycology/Growth_Dev/hyphalGrowth.shtml, **n.d.**
- [13] J. C. Frisvad, B. Andersen, U. Thrane. The use of secondary metabolite profiling in chemotaxonomy of filamentous fungi. *Mycol. Res.* **2008**, 112, 231.
- [14] J. C. Frisvad, C. Rank, K. F. Nielsen, T. O. Larsen. Metabolomics of *Aspergillus fumigatus*. **n.d.**, 47, 53.
- [15] J. M. Frank, Special metabolites in relation to conditions of growth., in *Chemical Fungal Taxonomy*. Marcel Dekker, New York, **n.d.**, pp. 321–344.
- [16] N. A. J. C. Furtado, S. Said, I. Y. Ito, J. K. Bastos. The antimicrobial activity of *Aspergillus fumigatus* is enhanced by a pool of bacteria. *Microbiol. Res.* **2002**, 157, 207.
- [17] F. Cheli, A. Campagnoli, V. Dell'Orto. Fungal populations and mycotoxins in silages: From occurrence to analysis. *Animal Feed Sci. Technol.* **2013**, 183, 1.
- [18] A. Casadevall, L.-A. Pirofski. Host-Pathogen Interactions: The Attributes of Virulence. *J. Infect. Dis.* **2001**, 184, 337.
- [19] G. S. Saharan, N. Mehta, P. D. Meena. *Alternaria Diseases of Crucifers: Biology, Ecology and Disease Management*. Springer Science And Business Media, Singapore, **2016**.
- [20] J. Bennett. Inhibition of chloroplast development by tentoxin. *Phytochemistry* **1976**, 152, 263.

- [21] S. Nishimura, K. Kohmoto. Host-specific toxins and chemical structures from *Alternaria* species. *Annu. Rev. Phytopathol.* **1983**, *21*, 87.
- [22] D. G. Gilchrist, R. G. Grogan. Production and Nature of a Host-Specific Toxin from *Alternaria alternata* f.sp *lycopersici*. *Phytopathology* **1975**, *66*, 165.
- [23] H. Stockmann-Juvala, K. Savolainen. A review of the toxic effects and mechanisms of action of fumonisin B1. *Hum. Exp. Toxicol.* **2008**, *27*, 799.
- [24] Health Canada. Summary of Comments Received on Health Canada's Proposed Maximum Limits for Ochratoxin A in Certain Foods- August 2008 to June 2009. can be found under <http://www.hc-sc.gc.ca/fn-an/securit/chem-chim/toxin-natur/summary-resume-eng.php>, **2013**.
- [25] F. Berthiller, R. Schuhmacher, G. Adam, R. Krska. Formation, determination and significance of masked and other conjugated mycotoxins. *Anal Bioanal Chem* **2009**, *395*, 1243.
- [26] F. Berthiller, C. Dall'Asta, R. Schuhmacher, M. Lemmens, G. Adam, R. Krska. Masked mycotoxins: determination of a deoxynivalenol glucoside in artificially and naturally contaminated wheat by liquid chromatography-tandem mass spectrometry. *J. Agric. Food Chem* **2005**, *53*, 3421.
- [27] E. Streit, C. Schwab, M. Sulyok, K. Naehrer, R. Krska, G. Schatzmayr. Multi-Mycotoxin Screening Reveals the Occurrence of 139 Different Secondary Metabolites in Feed and Feed Ingredients. *Toxins* **2013**, *5*, 504.
- [28] R. Russell. How will climate change affect mycotoxins in food? *Food. Res. Int.* **2010**, *43*, 1902.
- [29] D. P. Lawrence, P. B. Gannibal, T. L. Peever, B. M. Pryor. The sections of *Alternaria*: formalizing species-group concepts. *Mycologia* **2013**, *105*, 530.
- [30] J. H. C. Woudenberg, J. Z. Groenewald, M. Binder, P. W. Crous. *Alternaria* redefined. *Stud. Mycol.* **2013**, *75*, 171.
- [31] J. H. C. Woudenberg, M. F. Seidl, J. Z. Groenewald, M. de Vries, J. B. Stielow, B. P. H. J. Thomma, P. W. Crous. *Alternaria* section *Alternaria*: Species, formae speciales or pathotypes? *Stud. Mycol.* **2015**, *82*, 1.
- [32] P. M. Scott, W. Zhao, S. Feng, B. P.-Y. Lau. *Alternaria* toxins alternariol and alternariol monomethyl ether in grain foods in Canada. *Mycotoxin Res.* **2012**, *28*, 261.
- [33] Canola Council of Canada. *Alternaria* black spot. can be found under <http://www.canolacouncil.org/canola-encyclopedia/diseases/alternaria-black-spot/>, **n.d.**
- [34] B. Andersen, K. F. Nielsen, V. Fernandez Pinto, A. Patriarca. Characterization of *Alternaria* strains from Argentinean blueberry, tomato, walnut and wheat. *Int J Food Microbiol* **2015**, *196*, 1.
- [35] A. M. Rychlik. Potential health hazards due to the occurrence of the mycotoxin tenuazonic acid in infant food. *Eur. Food. Res. Technol.* **2013**, *236*, 491.
- [36] EFSA Panel on Contaminants in the Food Chain (CONTAM). Scientific Opinion on the risks for animal and public health related to the presence of *Alternaria* toxins in feed and food. *EFSA J.* **2011**, *9(10):2407 [97 pp.]*, 2407.
- [37] R. J. Wilkins, Silage: a global perspective, in *Grasslands. Developments, Opportunities, Perspectives*. Science Publisher Inc., New Hampshire, **n.d.**, pp. 111–1132.
- [38] P. H. Rasmussen, T. O. Larsen, T. T. Bladt, M. L. Binderup. In vitro cytotoxicity of fungi spoiling maize silage. *Food and Chem. Toxicol.* **2011**, *49*, 31.

- [39] V. A. Alonso, C. M. Pereyra, L. A. M. Keller, A. M. Dalcero, C. A. R. Rosa, S. M. Chiacchiera, L. R. Cavaglieri. Fungi and mycotoxins in silage: an overview. *Appl. Microbiol.* **2013**, *115*, 637.
- [40] B. Flannigan, R. A. Samson, J. D. Miller, Mycological investigations of indoor environments., in *Microorganisms in Home and Indoor Work Environments: Diversity, Health Impacts, Investigation and Control*. Taylor And Francis, New York, **n.d.**, pp. 231–246.
- [41] J. Fink-Gremmels. Mycotoxins in cattle feeds and carry-over to dairy milk: A review. *Food. Addit. Contam.* **2008**, *25*, 172.
- [42] M. O'brien, D. Egan, P. O'kiely, P. D. Forristal, F. M. Doohan, H. T. Fuller. Morphological and molecular characterization of *P. roqueforti* and *P. paneum* isolated from baled grass silage. *Mycol. Res.* **2008**, *112*, 921.
- [43] M. O. Tapia, M. D. Stem, R. L. Koski, A. Bach, M. J. Murphy. Effects of patulin on rumen microbial fermentation in continuous culture fermenters. *Animal Feed Sci. Technol.* **2002**, *97*, 239.
- [44] R. Bentley. Mycophenolic acid: a one hundred year odyssey from antibiotic to immunosuppressant. *Chem. Microbiol. Rev.* **2000**, 497.
- [45] J. Wang, C. L. Lee, T. M. Pan. Modified mutation method for screening low citrinin-producing strains of *Monascus purpureus* on rice culture. *J. Agric. Food Chem* **2004**, *52*, 6977.
- [46] B. Kopp, H. J. Rehm. Antimicrobial action of roquefortine. *Eur. J. Appl. Microbiol. Biotechnol.* **1979**, *6*, 379.
- [47] R.-D. Wei, P. E. Still, E. B. Smalley, H. K. Schnoes, F. M. Strong. Isolation and Partial Characterization of a Mycotoxin from *Penicillium roqueforti*. *Appl. Microbiol.* **1973**, *25*, 111.
- [48] B. P. Bowen, T. R. Northern. Dealing with the unknown: metabolomics and metabolite atlases. *J. Am. Soc. Mass Spec.* **2010**, *21*, 1471.
- [49] W. B. Dunn, D. I. Ellis. Metabolomics: current analytical platforms and methodologies. *Trends Anal. Chem.* **2005**, *24*, 285.
- [50] J. P. A. Gummer, C. Krill, L. Du Fall, D. C. W. Ormonde, R. D. Trengove, R. P. Oliver, P. S. Solomon, Metabolomics protocols for filamentous fungi, in *Fungal Plant Pathogens*. Humana Press, **2011**, pp. 237–254.
- [51] J. Jansson, B. Willing, M. Lucio, A. Fekete, J. Dicksved, J. Halfvarson, C. Tysk, P. Schmitt-Kopplin. Metabolomics reveals metabolic biomarkers of Crohn's Disease. *PLoS ONE* **2009**, *4*.
- [52] Y. Iijima, Y. Nakamura, Y. Ogata, K. Tanaka, N. Sakurai, K. Suda, T. Suzuki, H. Suzuki, K. Okazaki, M. Kitayama, S. Kanaya, K. Aoki, D. Shibata. Metabolite annotations based on the integration of mass spectral information. *Plant J.* **2008**, *54*, 949.
- [53] A. G. Brenton, A. R. Godfrey. Accurate mass measurement: terminology and treatment of data. *J. Am. Soc. Mass Spec.* **2010**, *21*, 1821.
- [54] T. Kind, O. Fiehn. Seven golden rules for heuristic filtering of molecular formulas obtained by accurate mass spectroscopy. *BMC Bioinformatics* **2007**, *8*, 105.
- [55] L. Sleno. The use of mass defect in modern mass spectrometry. *J. Mass Spectrom.* **2012**, *47*, 226.
- [56] European Commission. Method Validation & Quality Control Procedures for Pesticide Residues Analysis in Food and Feed. **2016**.

- [57] M. Ringner. What is principal component analysis? *Nature Biotechnol.* **2008**, 26, 303.
- [58] H. Abdi, L. Williams. Principal component analysis. *Wiley Interdisciplinary Reviews: Computational Statistics* **2010**, 2, 433.
- [59] R. Van den Berg, H. Hoefsloot, J. Westerhuis, A. Smilde, M. Van der Werf. Centering, scaling, and transformations: improving the biological information content of metabolomics data. *BMC Genomics* **2006**, 8, 142.
- [60] F. Wilcoxon. Individual comparisons by ranking methods. *Biometrics* **1945**, 1, 80.
- [61] Y. Benjamini, Y. Hochberg. Controlling the false discovery rate: a practical and powerful approach to multiple testing. *J. R. Stat. Soc. Series B Stat. Methodol.* **1995**, 57, 289.
- [62] Waters. How Does High Performance Liquid Chromatography Work? can be found under http://www.waters.com/waters/en_CA/How-Does-High-Performance-Liquid-Chromatography-Work%3F/nav.htm?cid=10049055&locale=en_CA, **n.d.**
- [63] International Bureau of Standards and Measurements. The International System of Units (SI), 8th edition. **2006**.
- [64] Thermo Fisher :: Orbitrap :: Q Exactive. can be found under <http://planetorbitrap.com/q-exactive#tab:schematic>, **n.d.**
- [65] D. Zhan, J. B. Fenn. Gas phase hydration of electrospray ions from small peptides. *Int. J. Mass Spectrom.* **2002**, 219, 1.
- [66] M. Dole, L. L. Mack, R. L. Hines, R. C. Mobley, L. D. Ferguson, M. B. Alice. Molecule beams of macroions. *J. Chem. Phys.* **1968**, 49, 2240.
- [67] M. Yamashita, J. B. Fenn. Electrospray ion source. Another variation on the free-jet theme. *J. Phys. Chem.* **1984**, 88, 4451.
- [68] C. S. Ho, C. W. K. Lam, M. H. . Chan, R. C. K. Cheung, L. K. Law, L. C. W. Lit, K. F. Ng, M. W. M. Suen, H. L. Tai. Electrospray ionisation mass spectrometry: principles and clinical applications. *Clin. Biochem. Rev.* **2003**, 24, 3.
- [69] A. P. Bruins. Mechanistic aspects of electrospray ionization. *J. Chromatogr. A.* **1998**, 794, 345.
- [70] M. Wilm. Principles of Electrospray Ionization. *Mol. Cell Proteomics* **2011**, 10.
- [71] J. Iribarne, B. Thompson. On the evaporation of small ions from charged droplets. *J. Chem. Phys.* **1976**, 64, 2287.
- [72] P. E. Miller, B. M. Denton. The quadrupole mass filter: basic operating concepts. *J. Chem. Ed.* **1986**, 63.
- [73] J. V. Olsen, L. M. F. de Godoy, G. Q. Li, B. Macek, P. Mortensen, R. Pesch, A. Makarov, O. Lange, S. Horning, M. Mahn. Parts per million mass accuracy on an orbitrap mass spectrometer via lock mass injection into a C-trap. *Mol. Cell Proteomics* **2005**, 4, 2010.
- [74] K. H. Kingdon. A method for the neutralization of electron space charge by positive ionization at very low gas pressures. *Phys. Rev.* **1923**, 21, 408.
- [75] R. D. Knight. Storage of ions from laser-produced plasmas. *Appl. Phys. Lett.* **1981**, 38, 221.
- [76] A. Makarov. Mass spectrometer. 5,886,346,7.
- [77] A. Makarov. Electrostatic axially harmonic orbital trapping: a high-performance technique of mass analysis. *Anal. Chem.* **2000**, 72, 1156.
- [78] S. Eliuk, A. Makarov. Evolution of Orbitrap Mass Spectrometry Instrumentation. *Annu. Rev. Anal. Chem.* **2015**, 8, 61.
- [79] G. S. Sidhu. Mycotoxin genetics and gene clusters. *Eur. J. Plant Pathol.* **2002**, 108, 705.

- [80] C. L. Schoch, K. A. Seifert, S. Huhndorf, V. Robert, J. L. Spouge, C. A. Levesque, W. Chen. Fungal barcoding consortium. Nuclear ribosomal internal transcribed spacer (ITS) region as a universal DNA barcode marker for Fungi. *Proc. Natl. Acad. Sci. USA* **2012**, *109*, 6241.
- [81] N. L. Glass, G. C. Donaldson. Development of primer sets designed for use with PCR to amplify conserved genes from filamentous ascomycetes. *Appl Environ Microb.* **1995**, *61*, 1323.
- [82] Illumina. An Introduction to Next-Generation Sequencing Technology. **2016**.
- [83] A. Asemaninejad, N. Weerasuriya, G. Gloor, Z. Lindo, G. Thorn. New Primers for Discovering Fungal Diversity using Nuclear Large Ribosomal DNA. *PLoS ONE* **2016**, *11*(7).
- [84] B. Andersen, E. Kroger, R. . Roberts. Chemical and morphological segregation of *Alternaria alternata*, *A. gaisen* and *A. longipes*. *Mycol. Res.* **2001**, *105*, 291.
- [85] G. de Hoog, R. Horre. Molecular taxonomy of the *Alternaria* and *Ulocladium* species from humans and their identification in the routine laboratory. *Mycoses* **2002**, *45*, 259.
- [86] A. Arya, A. Perello, *Alternaria infectoria* complex associated with Black Point and Leaf Blight Symptoms in Argentina, in *Management of Fungal Plant Pathogens*. CABI, **2010**, p. 234.
- [87] A. Armitage, D. Barbara, R. Harrison, C. Lane, S. Sreenivasaprasad, J. Woodhall, J. Clarkson. Discrete lineages within *Alternaria alternata* species group: Identification using new highly variable loci and support from morphological characters. *Fungal Biology* **2015**, DOI 10.1016/j.funbio.2015.06.012.
- [88] E. G. Simmons. *Alternaria: An Identification Manual*. **2007**.
- [89] J. Pitt, A. Hocking, Identification media and methods, in *Fungi and Food Spoilage*. Springer Science And Business Media, **2012**, p. 47.
- [90] K. B. Christensen, J. W. Van Klink, R. T. Weavers, T. O. Larsen, B. Andersen, R. K. Phipps. Novel chemotaxonomic markers of the *Alternaria infectoria* species-group. *J. Agric. Food Chem* **2005**, *53*, 9431.
- [91] B. Andersen, A. Dongo, B. M. Pryor. Secondary metabolite profiling of *Alternaria dauci*, *A. porri*, *A. solani*, and *A. tomatophila*. *Mycol. Res.* **2008**, *112*, 241.
- [92] P. Ntasiou, C. Myresiotis, S. Konstantinou, E. Papadopoulou-Mourkidou, G. S. Karaoglanidis. Identification, characterization and mycotoxigenic ability of *Alternaria* spp. causing core rot of apple fruit in Greece. *Int. J. Food Microbiol.* **2015**, *197*, 22.
- [93] S. Brun, H. Madrid, B. Gerrits van den Ende, B. Andersen, C. Marinach-Patrice, D. Mazier, G. . de Hoog. Multilocus phylogeny and MALDI-TOF analysis of the plant pathogenic species *Alternaria dauci* and relatives. *Fungal Biol.* **2013**, *117*, 32.
- [94] R. Hatta, K. Ito, Y. Hosaki, T. Tanaka, A. I. Tanaka, M. Yamamoto, K. Akimitsu, T. Tsuge. A conditionally dispensable chromosome controls host-specificity pathogenicity in the fungal plant pathogen *Alternaria alternata*. *Genetics* **2002**, *161*, 59.
- [95] J. C. Frisvad, J. Smedsgaard, R. A. Samson, T. O. Larsen, U. Thrane. Fumonisin B2 Production by *Aspergillus niger*. *J. Agric. Food Chem.* **2007**, *55*, 9727.
- [96] H. Benton, E. Want, T. M. . Ebbels. Correction of mass calibration gaps in liquid chromatography-mass spectrometry metabolomics data. *Bioinformatics* **2010**, *26*, 2488.
- [97] C. Smith, E. Want, G. O'Maille, R. Abagyan, G. Siuzdak. XCMS: Processing mass spectrometry data for metabolite profiling using nonlinear peak alignment, matching and identification. *Anal Chem* **2006**, *78*, 779.

- [98] R. Tautenhahn, C. Boettcher, S. Neumann. Highly sensitive feature detection for high resolution LC/MS. *BMC Bioinformatics* **2008**, *9*, 504.
- [99] A. McMillan, S. Rulisa, M. W. Sumarah, J. M. Macklaim, J. B. Renaud, J. Bisanz, G. Gloor, G. A. Reid. A multi-platform metabolomics approach identifies highly specific biomarkers of bacterial diversity in the vagina of pregnant and non-pregnant women. *Sci. Reports* **n.d.**, *5*.
- [100] J. B. MacQueen, Some methods for classification and analysis of multivariate observations, in *Proceedings of 5th Berkley Symposium on Mathematical Statistics and Probability*. University Of California Press, Berkeley, **1967**, pp. 281–297.
- [101] A. McMillan, J. B. Renaud, G. B. Gloor, G. Reid, M. W. Sumarah. Post-acquisition filtering of salt cluster artefacts for LC-MS based human metabolomic studies. *J. Chemoinform.* **2016**, *8*.
- [102] A. Bottalico, A. Logrieco, Toxicogenic *Alternaria* species of economic importance, in *Mycotoxins in Agriculture and Food Safety*. Mercel Dekker, New York, **1998**, pp. 65–108.
- [103] B. Andersen, E. Kroger, R. . Roberts. Chemical and morphological segregation of *Alternaria arborescens*, *A. infectoria* and *A. tenuissima*. *Mycol. Res.* **2002**, *106*, 170.
- [104] V. Hellwig, T. Grothe, A. Mayer-Bartschmid, R. Endermann, F. U. Geschke, T. Henkel, M. Stadler. Altersetin, a new antibiotic from cultures of endophytic *Alternaria* spp. Taxonomy, fermentation, isolation, structure elucidation and biological activities. *J. Antibiot. (Tokyo)* **2002**, *55*, 881.
- [105] B. Liebermann, R. Ellinger, W. Gunther, W. Ihn, H. Gallander. Tricycloalternarenes produced by *Alternaria alternata* related to ACTG-toxins. *Phytochemistry* **1997**, *46*, 297.
- [106] B. Andersen, U. Thrane. Differentiation of *Alternaria infectoria* and *Alternaria alternata* based on morphology, metabolite profiles, and cultural characteristics. *Can J Microbiol* **1996**, *42*, 685.
- [107] M. Lorenzini, G. Zapparoli. Characterization and pathogenicity of *Alternaria* spp. strains associated with grape bunch rot during post-harvest withering. *Int. J. Food Microbiol.* **2014**, *186*, 1.
- [108] H. Akamatsu, M. Taga, M. Kodama, R. Johnson, H. Otani, K. Kohmoto. Molecular karyotypes for *Alternaria* plant pathogens to produce host-specific toxins. *Current Genetics* **1999**, *35*, 647.
- [109] A. Perello, M. Moreno, M. Sisterna. *Alternaria infectoria* species-group associated with black point of wheat in Argentina. *Plant Pathol.* **2008**, *57*, 379.
- [110] A. Perello, M. Sisterna. Formation of *Lewia infectoria*, the teleomorph of *Alternaria infectoria*, on wheat in Argentina. *Australas. Plant Path.* **2008**, *37*, 589.
- [111] M. J. Kelman, J. B. Renaud, K. A. Seifert, J. Mack, K. Sivagnanam, K. K.-C. Yeung, M. W. Sumarah. Identification of six new *Alternaria* sulfoconjugated metabolites by high-resolution neutral loss filtering. *Rapid Commun. Mass Spectrom.* **2015**, *29*.
- [112] R. M. Clear, S. K. Patrick, D. Gaba, D. Abramson, D. M. Smith. Prevalence of fungi and fusariotoxins on hard red spring and amber durum wheat seed from western Canada, 2000 to 2002. *Can. J. Plant Pathol.* **2005**, *27*, 528.
- [113] S. Marin, A. J. Ramos, G. Cano-Sancho, V. Sanchis. Mycotoxins: Occurrence, toxicology, and exposure assessment. *Food Chem. Toxicol.* **2013**, *60*, 218.
- [114] C. Dall'Asta, M. Cirlini, C. Falavigna. Mycotoxins from *Alternaria*: Toxicological Implications. *Adv. Mol. Toxicol.* **2014**, *8*, 107.

- [115] S. Takaoka, M. Kurata, Y. Harimoto, R. Hatta, M. Yamamoto, K. Akimitsu, T. Tsuge. Complex regulation of secondary metabolism controlling pathogenicity in the phytopathogenic fungus *Alternaria alternata*. *New Phytol* **2014**, *202*, 1297.
- [116] T. Tsuge, Y. Harimoto, K. Akimitsu, K. Ohtani, M. Kodama, Y. Akagi, M. Egusa, M. Yamamoto, H. Otani. Host-selective toxins produced by the plant pathogenic fungus *Alternaria alternata*. *FEMS Microbiol Rev* **2013**, *37*, 44.
- [117] A. T. Bottini, J. R. Bowen, D. G. Gilchrist. Phytotoxins. II. Characterization of a phytotoxic fraction from *alternaria alternata* f. sp. *lycopersici*. *Tetrahedron Lett* **1981**, *22*, 2723.
- [118] H. Raistrick, C. E. Stickings, R. Thomas. Studies in the biochemistry of Micro-organisms. 90. Alternariol and alternariol monomethyl ether, metabolic products of *Alternaria tenuis*. *Biochem.J.* **1953**, *55*, 421.
- [119] V. Ostry. *Alternaria* mycotoxins: an overview of chemical characterization, producers, toxicity, analysis and occurrence in foodstuffs. *World Mycotoxin J.* **2008**, *1*, 175.
- [120] P. M. Scott, 17 - Other mycotoxins, in *Mycotoxins in Food*, (Eds: N. Magan, M. Olsen). Woodhead Publishing, **2004**, pp. 406–440.
- [121] A. De Girolamo, M. Solfrizzo, C. Vitti, A. Visconti. Occurrence of 6-Methoxymellein in Fresh and Processed Carrots and Relevant Effect of Storage and Processing. *J Agric Food Chem* **2004**, *52*, 6478.
- [122] M. Solfrizzo, C. Vitti, A. De Girolamo, A. Visconti, A. Logrieco, P. Fanizzi. Radicinols and Radicinin Phytotoxins Produced by *Alternaria radicina* on Carrots. *J Agric Food Chem* **2004**, *52*, 3655.
- [123] E. Van de Perre, N. Deschuyffeleer, L. Jaxens, F. Vekeman, W. Van der Hauwaert, S. Asam, M. Rychlik, F. Devlieghere, B. De Meulenaer. Screening of moulds and mycotoxins in tomatoes, bell peppers, onions, soft red fruits and derived tomato products. *Food Control* **2014**, *37*, 165.
- [124] B. P.-Y. Lau, P. M. Scott, D. A. Lewis, S. R. Kanhere, C. Cl  roux, V. A. Roscoe. Liquid chromatography–mass spectrometry and liquid chromatography–tandem mass spectrometry of the *Alternaria* mycotoxins alternariol and alternariol monomethyl ether in fruit juices and beverages. *J. Chromatogr. A* **2003**, *998*, 119.
- [125] R. Kroes, J. Kleiner, A. Renwick. The Threshold of Toxicological Concern Concept in Risk Assessment. *Toxicol Sci* **2005**, *86*, 226.
- [126] J. D. Miller, S. N. Richardson. Mycotoxins in Canada: A Perspective for 2013. **2013**.
- [127] M. Zachariasova, T. Cajka, M. Godula, A. Malachova, Z. Veprikova, J. Hajslova. Analysis of multiple mycotoxins in beer employing (ultra)-high-resolution mass spectrometry. *Rapid Commun Mass Spectrom* **2010**, *24*, 3357.
- [128] V. Roscoe, G. A. Lombaert, V. Huzel, G. Neumann, J. Melietio, D. Kitchen, S. Kotello, T. Krakalovich, R. Trelka, P. M. Scott. Mycotoxins in breakfast cereals from the Canadian retail market: A 3-year study. *Food Addit Contam A* **2008**, *25*, 347.
- [129] A. H. Aly, R. Edrada-Ebel, I. D. Indriani, V. Wray, W. E. G. M  ller, F. Totzke, U. Zirrgiebel, C. Sch  chtele, M. H. G. Kubbutat, W. H. Lin, P. Proksch, R. Ebel. Cytotoxic Metabolites from the Fungal Endophyte *Alternaria* sp. and Their Subsequent Detection in Its Host Plant *Polygonum senegalense*. *J. Nat. Prod.* **2008**, *71*, 972.
- [130] R. M. Pope, C. S. Raska, S. C. Thorp, J. Liu. Analysis of heparan sulfate oligosaccharides by nano-electrospray ionization mass spectrometry. *Glycobiology* **2001**, *11*, 505.

- [131] D. Q. Liu, Y. Xia, R. Bakhtiar. Use of a liquid chromatography/ion trap mass spectrometry/triple quadrupole mass spectrometry system for metabolite identification. *Rapid Commun Mass Spectrom* **2002**, *16*, 1330.
- [132] A. Lafaye, C. Junot, B. Ramounet-Le Gall, P. Fritsch, E. Ezan, J. Tabet. Profiling of sulfoconjugates in urine by using precursor ion and neutral loss scans in tandem mass spectrometry. Application to the investigation of heavy metal toxicity in rats. *J Mass Spectrom* **2004**, *39*, 655.
- [133] Q. Ruan, S. Peterman, M. A. Szewc, L. Ma, D. Cui, W. G. Humphreys, M. Zhu. An integrated method for metabolite detection and identification using a linear ion trap/Orbitrap mass spectrometer and multiple data processing techniques: application to indinavir metabolite detection. *J Mass Spectrom* **2008**, *43*, 251.
- [134] S. N. Richardson, A. K. Walker, T. K. Nsiama, J. McFarlane, M. W. Sumarah, A. Ibrahim, J. D. Miller. Griseofulvin-producing *Xylaria* endophytes of *Pinus strobus* and *Vaccinium angustifolium*: evidence for a conifer-understorey species endophyte ecology. *Fungal Ecol.* **2014**, *11*, 107.
- [135] B. Wang, J. You, J. B. King, S. Cai, E. Park, D. R. Powell, R. H. Cichewicz. Polyketide Glycosides from *Bionectria ochroleuca* Inhibit *Candida albicans* Biofilm Formation. *J. Nat. Prod.* **2014**, *77*, 2273.
- [136] T. Pluskal, S. Castillo, A. Villar-Briones, M. Orešič. MZmine 2: Modular framework for processing, visualizing, and analyzing mass spectrometry-based molecular profile data. *BMC Bioinforma.* **11395** **2010**, *2.0*.
- [137] S. Ojanpera, A. Pelander, M. Pelzing, I. Krebs, E. Vuori, I. Ojanpera. Isotopic pattern and accurate mass determination in urine drug screening by liquid chromatography/time-of-flight mass spectrometry. *Rapid Commun Mass Spectrom* **2006**, *20*, 1161.
- [138] A. Kaufmann. Strategy for the elucidation of elemental compositions of trace analytes based on a mass resolution of 100 000 full width at half maximum. *Rapid Commun Mass Spectrom* **2010**, *24*, 2035.
- [139] E. D. Caldas, A. D. Jones, B. Ward, C. K. Winter, D. G. Gilchrist. Structural characterization of three new AAL toxins produced by *Alternaria alternata* f.sp. *lycopersici*. *J. Agric. Food Chem* **1994**, *42*, 327.
- [140] C. J. Mirocha, D. G. Gilchrist, W. T. Shier, H. K. Abbas, Y. Wen, R. F. Vesonder. AAL toxins, fumonisins (biology and chemistry) and host-specificity concepts. *Mycopathologica* **1992**, *117*, 47.
- [141] A. H. Merrill, G. van Echten, E. Wang, K. Sandhoff. Fumonisin B1 inhibits sphingosine (sphinganine) N-acyltransferase and de novo sphingolipid biosynthesis in cultured neurons in situ. *J. Biol. Chem.* **1993**, *268*, 27299.
- [142] K. Desai, M. C. Sullards, J. Allegood, E. Wang, E. M. Schmelz, M. Hartl, H. U. Humpf, D. C. Liotta, Q. Peng, A. H. Merrill. Fumonisin and fumonisin analogs as inhibitors of ceramide synthase and inducers of apoptosis. *Biochim. Biophys. Acta.* **2002**, *1585*, 188.
- [143] W. M. Haschek, L. A. Gumprecht, G. Smith, M. E. Tumbleson, P. D. Constable. Fumonisin toxicosis in swine: an overview of porcine pulmonary edema and current perspectives. *Environ. Health Perspect.* **2001**, *109* (Suppl. 2), 251.
- [144] D. R. Ledoux, T. P. Brown, T. S. Weibking, G. E. Rottinghaus. Fumonisin toxicity in broiler chicks. *J. Vet. Diagn. Invest.* **1992**, *4*, 330.
- [145] G. J. Diaz, H. J. Boermans. Fumonisin toxicosis in domestic animals: a review. *Vet. Hum. Toxicol.* **1994**, *36*, 548.

- [146] P. K. Chelule, N. Gqaleni, M. F. Dutton, A. A. Chaturqoon. Exposure of rural and urban populations in KwaZulu Natal, South Africa, to fumonisin B(1) in maize. *Environ. Health Perspect.* **2001**, *109*, 253.
- [147] F. D. Groves, L. Zhang, Y. S. Chang, P. F. Ross, H. Casper, W. P. Norred, W. C. You, J. F. J. Fraumeni. Fusarium mycotoxins in corn and corn products in a high-risk area for gastric cancer in Shandong Province, China. *J. AOAC Int.* **1999**, *82*, 657.
- [148] J. M. Beardall, J. D. Miller, Diseases in humans with mycotoxins as possible causes, in *Mycotoxins in Grain: Compounds Other than Aflatoxin*. Eagan Press, St. Paul, Minnesota, USA, **1994**, pp. 487–539.
- [149] H. K. Abbas, R. T. Riley. The presence and phytotoxicity of fumonisins and AAL-toxin in *Alternaria alternata*. *Toxicon.* **1996**, *34*, 133.
- [150] E. D. Caldas, A. D. Jones, C. K. Winter, B. Ward, D. G. Gilchrist. Electrospray ionization mass spectrometry of sphinganine analog mycotoxins. *Anal. Chem.* **1995**, *67*, 196.
- [151] S. C. Gad, C. Reilly, K. Siino, F. A. Gavigan, G. Witz. Thirteen cationic ionophores: their acute toxicity, neurobehavioral and membrane effects. **1985**, *8*, 451.
- [152] M. Herrmann, R. Zocher, A. Haese. Effect of Disruption of the Enniatin Synthetase Gene on the Virulence of *Fusarium avenaceum*. *MPMI* **1996**, *9*, 226.
- [153] L. A. Blais, J. W. ApSimon, B. A. Blackwell, R. Greenhalgh, J. D. Miller. Isolation and characterization of enniatins from *Fusarium avenaceum* DAOM 196490. *Can. J. Chem.* **1992**, *70*, 1281.
- [154] A. Bottalico, G. Perrone. Toxigenic *Fusarium* species and mycotoxins associated with head blight in small-grain cereals in Europe. *Eur. J. Plant Pathol.* **2002**, *108*, 611.
- [155] J. Blesa, R. Marin, C. M. Lino, J. Manes. Evaluation of enniatins A, A1, B, B1 and beauvericin in Portuguese cereal-based foods. *Food Addit Contam A* **2012**, *29*.
- [156] L. Hu, P. Koehler, M. Rychlik. Effect of sourdough processing and baking on the content of enniatins and beauvericin in wheat and rye bread. *Eur. Food. Res. Technol.* **2014a**, *238*, 581.
- [157] L. Hu, M. Gastl, A. Linkmeyer, M. Hess, M. Rychlik. Fate of enniatins and beauvericin during the malting and brewing process determined by stable isotope dilution assays. *LWT Food Sci. Technol.* **2014b**, *56*, 469.
- [158] L. I. Ivanova, E. Skierve, G. S. Eriksen, S. Uhlig. Cytotoxicity of enniatins A, A1, B, B1, B2 and B3 from *Fusarium avenaceum*. *Toxicon.* **2006**, *47*, 866.
- [159] A. Prosperini, G. Font, M. J. Ruiz. Interaction of effects of *Fusarium* enniatins (A, A1, B and B1) combinations on in vitro cytotoxicity of Caco-2 cells. *Toxicol. In Vitro.* **2014**, *28*, 88.
- [160] H. Lu, M. Fernandez-Franzon, G. Font, M. J. Ruiz. Toxicity evaluation of individual and mixed enniatins using an in vitro method with CHO-K1 cells. *Toxicol. In Vitro.* **2013**, *27*, 672.
- [161] EFSA. Scientific Opinion on the risks to humans and animal health related to the presence of beauvericin and enniatins in food and feed. *EFSA J.* **2014**, *12*.
- [162] A. A. Sy-Cordero, C. J. Pearce, N. H. Oberlies. Revisiting the enniatins: a review of their isolation, biosynthesis, structure, determination and biological activities. *J. Antibiot. (Tokyo)* **2012**, *65*, 541.
- [163] J. B. Renaud, M. J. Kelman, T. F. Qi, K. A. Seifert, M. W. Sumarah. Product ion filtering with rapid polarity switching for the detection of all fumonisins and AAL-toxins. *Rapid Commun. Mass Spectrom.* **2015**, *29*, 2131.

- [164] A. Visconti, L. A. Blais, J. W. ApSimon, R. Greenhalgh, J. D. Miller. Production of enniatins by *Fusarium acuminatum* and *Fusarium compactum* in liquid culture: isolation and characterization of three new enniatins, B2, B3, and B4. *J. Agric. Food Chem* **1992**, *40*, 1076.
- [165] M. Sulyok, F. Berthiller, R. Krska, R. Schuhmacher. Development and validation of a liquid chromatography/tandem mass spectrometric method for the determination of 39 mycotoxins in wheat and maize. *Rapid Commun. Mass Spectrom.* **2006**, *20*, 2649.
- [166] S. M. Musser, R. M. Eppley, E. P. Mazzola, C. E. Hadden, J. P. Shockcor, R. C. Crouch, G. E. Martin. Identification of an N-acetyl keto derivative of fumonisin B1 in corn cultures of *Fusarium proliferatum*. *J. Nat. Prod.* **1995**, *58*, 1392.
- [167] R. A. Butchko, R. D. Plattner, R. H. Proctor. FUM13 encodes a short chain dehydrogenase/reductase required for C-3 carbonyl reduction during fumonisin biosynthesis in *Gibberella moniliformis*. *J. Agric. Food Chem* **2003**, *51*, 3000.
- [168] S. Sivanathan, J. Scherckenbeck. Cyclodepsipeptides: A rich source of biologically active compounds for drug research. *Molecules* **2014**, *19*, 12368.
- [169] A. Logrieco, R. Rizzo, R. Ferracane, A. Ritieni. Occurrence of Beauvericin and Enniatins in Wheat Affected by *Fusarium avenaceum* Head Blight. *Appl. Environ. Microbiol.* **2002**, *68*, 82.
- [170] M. Vaclavikova, A. Malachova, Z. Veprikova, M. Zachariasova, J. Hajslova. "Emerging" mycotoxins in cereal processing chains: changes of enniatins during beer and bread making. *Food Chem.* **2013**, *136*, 750.
- [171] A. Malachova, M. Dzuman, Z. Veprikova, M. Vaclavikova, M. Zachariasova, J. Hajslova. Deoxynivalenol, deoxynivalenol-3-glucoside and enniatins: the major mycotoxins found in cereal-based products on the Czech market. *J. Agric. Food Chem* **2011**, *59*, 12990.
- [172] J. W. Bennett, M. Klich. Mycotoxins. *Clin. Microbiol. Rev.* **2003**, *16*, 497.
- [173] J. Fink-Gremmels. Mycotoxins: their implications for human and animal health. *Vet. Q.* **1999**, *21*, 115.
- [174] K. A. Scudamore, C. T. Livesey. Occurrence and significance of mycotoxins in forage crops and silage: A review. *J. Sci. Food Agric.* **1998**, *77*, 1.
- [175] I. M. L. D. Storm, N. B. Kristensen, B. M. L. Raun, J. Smedsgaard, U. Thrane. Dynamics in the microbiology of maize silage during whole-season storage. *Appl. Microbiol.* **2010**, *109*, 1017.
- [176] I. M. L. D. Storm, J. L. Sorensen, R. R. Rasmussen, K. F. Nielsen, U. Thrane. Mycotoxins in silage. *Postharvest Rev.* **2008**, *4*, 1.
- [177] K. F. Nielsen, S. Gravesen, P. A. Nielsen, B. Andersen, U. Thrane, J. C. Frisvad. Production of mycotoxins on artificially and naturally infested building materials. *Mycopathologica* **1999**, *145*, 43.
- [178] Y. Li, N. Nishino. Effects of ensiling fermentation and aerobic deterioration on the bacterial community in Italian ryegrass, guinea grass, and whole-crop maize silages stored at high moisture content. *Asian-Australas. J. Anim. Sci.* **2013**, *26*, 1304.
- [179] R. Wirth, E. Kovacs, G. Maroti, Z. Bagi, G. Rakhely, K. L. Kovacs. Characterization of a biogas-producing microbial community by short-read next generation DNA sequencing. *Biotechnol. Biofuels* **2012**, *5*, 41.
- [180] E. Streit, C. Schwab, M. Sulyok, K. Naehrer, R. Krska, G. Schatzmayr. Multi-mycotoxin screening reveals the occurrence of 139 different secondary metabolites in feed and feed ingredients. *Toxins* **2013**, *5*, 504.

- [181] A. Malachova, M. Sulyok, E. Beltran, F. Berthiller, R. Krska. Optimization and validation of a quantitative liquid chromatography-tandem mass spectrometric method covering 295 bacterial and fungal metabolites including all regulated mycotoxins in four model food matrices. *J. Chromatogr. A* **2014**, 1362, 145.
- [182] A. Doerr. DIA mass spectrometry. *Nature Methods* **2015**, 12, 35.
- [183] J. B. Renaud, M. W. Sumarah. Data independent acquisition-digital archiving mass spectrometry: application to single kernel mycotoxin analysis of *Fusarium graminearum* infected maize. *Anal. Bioanal. Chem.* **2016**, 408, 3083.
- [184] C. Schmeitzl, B. Warth, P. Fruhmann, H. Michlmayr, A. Malachova, F. Berthiller, R. Schumacher, R. Krska. The metabolic fate of deoxynivalenol and its acetylated derivatives in a wheat suspension culture: identification and detection of DON-15-O-glucoside, 15-acetyl-DON-3-O-glucoside, and 15-acetyl-DON-3-sulfate. *Toxins* **2015**, 7, 3112.
- [185] D. Baines, S. Erb, K. Turkington, G. Kuldau, J. Juba, L. Masson, A. Mazza, R. Roberts. Mouldy feed, mycotoxins and Shiga-toxin-producing *Escherichia coli* colonization associated with Jejunal Hemorrhage Syndrome in beef cattle. *BMC Vet. Res.* **2011**, 7, 24.
- [186] D. Baines, S. Erb, K. Turkington, G. Kuldau, J. Juba, M. W. Sumarah, A. Mazza, L. Masson. Characterization of Haemorrhagic Enteritis in Dairy Goats and the Effectiveness of Probiotic and Prebiotic Application in Alleviating Morbidity and Production Losses. *Fungal Genom. Biol.* **2011**, 1.
- [187] D. Baines, M. W. Sumarah, G. Kuldau, J. Juba, A. Mazza, L. Masson. Aflatoxin, Fumonisin and Shiga Toxin-Producing *Escherichia coli* Infection in Calves and the Effectiveness of Celmanax/Dairyman's Choice Applications to Eliminate Morbidity and Mortality Losses. *Toxins* **2013**, 5, 1872.
- [188] R. A. Samson, J. . Pitt, Check list of common *Penicillium* species, in *Advances in Penicillium and Aspergillus Systematics*. Plenum Press, New York, **1985**, pp. 461–463.
- [189] T. J. White, T. Bruns, S. Lee, J. W. Taylor, Amplification and direct sequencing of fungal ribosomal RNA genes for phylogenetics, in *PCR Protocols: A Guide to Methods and Applications*. Academic Press Inc., San Diego, California, USA, **1990**.
- [190] J. D. Palumbo, T. L. O'Keeffe, Y. S. Ho, C. J. Santillan. Occurrence of ochratoxin A contamination and detection of ochratoxigenic *Aspergillus* species in retail samples of dried fruits and nuts. *J. Food Prot.* **2015**, 78, 836.
- [191] T. F. Qi, J. B. Renaud, T. McDowell, K. A. Seifert, K. K.-C. Yeung, M. W. Sumarah. Diversity of Mycotoxin-Producing Black *Aspergilli* in Canadian Vineyards. *J. Agric. Food Chem* **2016**, 64, 1583.
- [192] G. Gloor. Gloor Lab Sequencing Pipeline. can be found under https://github.com/ggloor/miseq_bin/tree/master, **n.d.**
- [193] R. C. Edgar, B. J. Haas, J. C. Clemente, C. Quince, R. Knight. UCHIME improves sensitivity and speed of chimera detection. *Bioinformatics* **2011**, 27, 2194.
- [194] R. C. Edgar. Search and clustering orders of magnitude faster than BLAST. *Bioinformatics* **2010**, 531, 2460.
- [195] U. Kõljalg, R. H. Nilsson, K. Abarenkov, L. Tedersoo, A. F. S. Taylor, M. Bahram, S. T. Bates, T. D. Bruns, J. Bengtsson-Palme, T. M. Callaghan, B. Douglas, T. Drenkhan, U. Eberhardt, M. Dueñas, et al. Towards a unified paradigm for sequence-based identification of Fungi. *Mol. Ecol.* **2013**.

- [196] C. Quast, E. Pruesse, P. Yilmaz, J. Gerken, T. Schweer, P. Yarza, J. Peplies, F. O. Glöckner. The SILVA ribosomal RNA gene database project: improved data processing and web-based tools. **2013**.
- [197] J. R. Cole, Q. Wang, J. A. Fish, B. Chai, D. M. McGarrell, Y. Sun, C. T. Brown, A. Porrass-Alfaro, C. R. Kuske, J. M. Tiedje. Ribosomal Database Project: data and tools for high throughput rRNA analysis. *Nucl. Acids Res.* **n.d.**, *42*, D633.
- [198] J. G. Caporaso, J. Kuczynski, J. Stombaugh, K. Bittinger, F. D. Bushman, E. K. Costello, et al. QIIME allows analysis of high-throughput community sequencing data. *Nat. Methods* **2010**, *7*, 335.
- [199] J. C. Frisvad, T. O. Larsen, R. de Vries, M. Meijer, J. Houbraken, F. J. Cananes, K. Ehrlich, R. A. Samson. Secondary metabolite profiling, growth profiles and other tools for species recognition and important *Aspergillus* mycotoxins. *Stud. Mycol.* **2007**, *59*, 31.
- [200] M. A. Mansfield, A. D. Jones, G. A. Kuldau. Contamination of fresh and ensiled maize by multiple *Penicillium* mycotoxins. *Phytopathology* **2008**, *98*, 330.
- [201] M. W. Sumarah, J. D. Miller, B. A. Blackwell. Isolations and metabolite production by *Penicillium roqueforti*, *P. paneum*, and *P. crustosum* isolated in Canada. *Mycopathologica* **2005**, *159*, 571.
- [202] C. M. Pereyra, V. A. Alonso, C. A. R. Rosa, S. M. Chiacchiera, A. M. Dalcero, R. R. Cavaglieri. Gliotoxin natural incidence and toxigenicity of *Aspergillus fumigatus* isolated from maize silage and ready dairy cattle feed. *World Mycotoxin J.* **2008**, *1*, 457.
- [203] M. L. Pereyra, S. M. Chiacchiera, C. A. Rosa, R. Sager, A. M. Dalcero, L. Cavaglieri. Comparative analysis of the mycobiota and mycotoxins contaminating corn trench silos and silo bags. *J. Sci. Food Agric.* **2011**, *91*, 1474.
- [204] K. F. Nielsen, M. W. Sumarah, J. C. Frisvad, J. D. Miller. Production of Metabolites from the *Penicillium roqueforti* Complex. *J. Agric. Food Chem* **2006**, *54*, 3756.
- [205] Canadian Food Inspection Agency (CFIA). RG-8 Regulatory Guidance: Contaminants in Feed. Section 1: Mycotoxins in Livestock Feed. **n.d.**
- [206] S. L. Walter. Acute penitrem A and roquefortine poisoning in a dog. *Can. J. Vet.* **2002**, *43*, 372.
- [207] I. Dosen, K. F. Nielsen, G. Clausen, B. Andersen. Potentially harmful secondary metabolites produced by indoor *Chaetomium* species on artificially and naturally contaminated building materials. *Indoor Air.* **2016**.
- [208] N. P. Keller, G. Turner, J. W. Bennett. Fungal secondary metabolism- from biochemistry to genomics. *Nature Rev. Microbiol.* **2005**, *3*, 937.
- [209] I. Schneweis, K. Meyer, S. Hormansdorfer, J. Bauer. Metabolites of *Monascus ruber* in silages. *J. Anim. Physiol. Anim. Nutr. (Berl)* **2001**, *85*, 38.
- [210] D. Vesely, D. Vesela, Adamkova. Occurrence of PR-toxin-producing *Penicillium roqueforti* in corn silage. *Vet. Med.* **1981**, *26*, 109.
- [211] W. Seglar, Case studies that implicate silage mycotoxins as the cause of dairy herd problems, in *Silage: Field to Feedbunk*. Northeast Regional Agricultural Engineering Service, Ithaca, New York, **1997**, pp. 242–254.
- [212] W. Seglar, C. Blake, D. Cinch, F. S. Chu, A. R. Gotlieb, M. Hinds, C. Thomas, E. Thomas, N. Tomes, L. Trenholm, D. Undersander, Comparison of Mycotoxin Levels Among Problem and Healthy Dairy Herds. Des Moines, IA, **1997**.
- [213] N. Magan, R. Hope, V. Cairns, D. Aldred. Post-harvest fungal ecology: Impact of fungal growth and mycotoxin accumulation in stored grain. *Eur. J. Plant Pathol.* **2003**, *109*, 723.

- [214] S. Coufal-Majewski, K. Stanford, T. McAllister, B. Blakley, J. McKinnon, A. V. Chaves, Y. Wang. Impacts of Cereal Ergot in Food Animal Production. *Front. Vet. Sci.* **2016**, *3*, 15.
- [215] M. T. Rhodes, J. A. Paterson, M. S. Kerley, H. E. Garner, M. H. Laughlin. Reduced blood flow to peripheral and core body temperatures in sheep and cattle induced by endophyte-infected tall fescue. *J. Anim. Sci.* **1991**, *69*, 2033.
- [216] B. Harrach, A. Bata, G. Sandor, A. Vanyi. Isolation of macrocyclic and non-macrocyclic trichothecenes (stachybotrys and fusarium toxins) from the environment of 200 III sport horses. *Myco. Res.* **1987**, *3*, 65.
- [217] D. R. McMullin, T. K. Nsiama, J. D. Miller. Secondary metabolites from *Penicillium corylophilum* isolated from damp buildings. *Mycologia* **2014**, *106*, 621.
- [218] Y. Li, N. Nishino. Bacterial and fungal communities of wilted Italian ryegrass silage inoculated with and without *Lactobacillus rhamnosus* or *Lactobacillus buchneri*. *Lett. Appl. Microbiol.* **2011**, *52*, 314.

Appendix A1- Chapter 2 Supplementary

Table S1- List of 148 *Alternaria* sp. with host, location of sample collection, tentative species assignment (2), and species assignment based on the RPB2 primer region. “*” indicated strains grown in liquid culture and on rice and Cheerios (3.1). Cultures with KAS numbers are in the laboratory culture collection of Keith A. Seifert, and the subject of ongoing taxonomic study for species identification.

Specimen Code	Host	Tentative species assignment	Species assignment based on RPB2 primer (Woudenberg)	City, Province
KAS5401	<i>Malus domestica</i>	<i>A. tenuissima</i>	<i>alternata</i>	Vineland, Ontario
KAS5400	<i>Malus domestica</i>	<i>A. tenuissima</i>	<i>A. arborescens</i> species complex	Vineland, Ontario
KAS5399*	<i>Malus domestica</i>	<i>A. alternata</i>	<i>A. arborescens</i> species complex	Vineland, Ontario
KAS5398	<i>Malus domestica</i>	<i>A. tenuissima</i>	<i>A. arborescens</i> species complex	Vineland, Ontario
KAS5392	<i>Eutrochium purpureum</i>	<i>A. infectoria</i>		Orleans, Ontario
KAS5387	<i>Lunaria annua</i>	No assignment	<i>A. arborescens</i> species complex	Orleans, Ontario
KAS5385	<i>Thalictrum</i> sp.	<i>A. tenuissima</i>	<i>alternata</i>	Orleans, Ontario
KAS5384	<i>Begonia</i> sp.	<i>A. alternata</i>		Orleans, Ontario
KAS5382	<i>Ipomea</i> sp.	<i>A. arborescens</i>		Orleans, Ontario
KAS5381	<i>Ipomea</i> sp.	<i>A. alternata</i>		Orleans, Ontario
KAS5380	<i>Astilbe</i> sp.	<i>A. arborescens</i>		Orleans, Ontario
KAS5379	Unknown	<i>A. arborescens</i>	<i>alternata</i>	Ottawa, Ontario
KAS5378	<i>Euchera americana</i>	<i>A. tenuissima</i>	<i>A. arborescens</i> species complex	Orleans, Ontario
KAS5377	<i>Thuja officinalis</i>	<i>A. tenuissima</i>		Nepean, Ontario
KAS5375	Unknown	<i>A. tenuissima</i>	<i>alternata</i>	Leitrim, Ontario
KAS5374	<i>Geranium</i> sp.	No assignment	<i>alternata</i>	Orleans, Ontario
KAS5373	<i>Silene vulgaris</i>	<i>A. arborescens</i>	<i>alternata</i>	Ottawa, Ontario
KAS5372	<i>Asclepias</i> sp.	<i>A. alternata</i>	<i>A. arborescens</i> species complex	Leitrim, Ontario
KAS5369	<i>Linaria vulgaris</i>	<i>A. tenuissima</i>	<i>alternata</i>	Orleans, Ontario
KAS5368	<i>Daucus carota</i>	<i>A. tenuissima</i>	<i>alternata</i>	Ottawa, Ontario
KAS5365	<i>Brassica</i> sp.	<i>A. arborescens</i>	<i>A. arborescens</i> species complex	Orleans, Ontario
KAS5364	<i>Pyrus</i> sp.	<i>A. infectoria</i>	<i>alternata</i>	Orleans, Ontario
KAS5339	<i>Dicentra canadensis</i>	No assignment	<i>alternata</i>	Orleans, Ontario
KAS5337	<i>Rhus typhina</i>	<i>A. tenuissima</i>	<i>alternata</i>	Orleans, Ontario
KAS5327	<i>Hibiscus rosa-sinensis</i>	<i>A. tenuissima</i>		Orleans, Ontario
KAS5325	<i>Scirpus</i> sp.	<i>A. arborescens</i>	<i>alternata</i>	Orleans, Ontario
KAS5324	<i>Delphinium</i> sp.	<i>A. arborescens</i>	<i>alternata</i>	Orleans, Ontario
KAS5322	<i>Acer</i> sp.	<i>A. arborescens</i>	<i>alternata</i>	Orleans, Ontario
KAS5321	<i>Lycopersicon esculentum</i>	<i>A. arborescens</i>		Orleans, Ontario
KAS5320	<i>Daucus carota</i>	<i>A. alternata</i>	<i>A. arborescens</i> species complex	Ottawa, Ontario
KAS5319	<i>Sphagnum</i> sp.	<i>A. arborescens</i>	<i>alternata</i>	Orleans, Ontario
KAS5313	<i>Lycopersicon esculentum</i>	<i>A. arborescens</i>	<i>alternata</i>	Ottawa, Ontario
KAS5312	<i>Pinus</i> sp.	<i>A. tenuissima</i>		Ottawa, Ontario
KAS5309	<i>Aesculus flava</i>	<i>A. arborescens</i>	<i>alternata</i>	Ottawa, Ontario
KAS5308*	<i>Malus baccata</i>	<i>A. tenuissima</i>		Ottawa, Ontario
KAS5307	<i>Ipomea baccata</i>	<i>A. arborescens</i>	<i>A. arborescens</i> species complex	Orleans, Ontario
KAS5306	<i>Ipomea baccata</i>	<i>A. infectoria</i>	<i>alternata</i>	Orleans, Ontario

KAS5305	<i>Juniperus virginiana</i>	<i>A. arborescens</i>	<i>alternata</i>	Ottawa, Ontario
KAS5304	<i>Weigela</i> sp.	<i>A. alternata</i>	<i>alternata</i>	Orleans, Ontario
KAS5303	<i>Sedum</i> sp.	<i>A. tenuissima</i>	<i>alternata</i>	Ottawa, Ontario
KAS5301	<i>Brassica</i> sp.	<i>A. arborescens</i>		Ottawa, Ontario
KAS5300	<i>Tamarix ramoissisima</i>	<i>A. arborescens</i>	<i>A. arborescens</i> species complex	Orleans, Ontario
KAS5299	<i>Lewisia longipetala</i>	<i>A. alternata</i>	<i>A. arborescens</i> species complex	Orleans, Ontario
KAS5298	<i>Alcea rosea</i>	<i>A. infectoria</i>	<i>A. arborescens</i> species complex	Orleans, Ontario
KAS5297	<i>Lewisia longipetala</i>	<i>A. arborescens</i>		Orleans, Ontario
KAS5296	<i>Salix</i> sp.	<i>A. tenuissima</i>	<i>alternata</i>	Ottawa, Ontario
KAS5295	<i>Hippeastrum</i> sp.	<i>A. arborescens</i>	<i>alternata</i>	Ottawa, Ontario
KAS5293	<i>Pilosella aurantiaca</i>	<i>A. arborescens</i>	<i>alternata</i>	Nepean, Ontario
KAS5287	<i>Hedera</i> sp.	<i>A. alternata</i>	<i>alternata</i>	Ottawa, Ontario
KAS5286	<i>Rosa</i> sp.	<i>A. alternata</i>	<i>A. arborescens</i> species complex	Orleans, Ontario
KAS5275	<i>Caragana</i> sp.	No assignment	<i>A. arborescens</i> species complex	Orleans, Ontario
KAS5274	<i>Papaver rhoeas</i>	<i>A. arborescens</i>	<i>alternata</i>	Orleans, Ontario
SLOAN361	House dust	<i>A. infectoria</i>	<i>infectoria</i>	Regina, Saskatchewan
SLOAN345	House dust	<i>A. alternata</i>		Regina, Saskatchewan
SLOAN220	House dust	<i>A. alternata</i>	<i>alternata</i>	Regina, Saskatchewan
SLOAN66	House dust	<i>A. alternata</i>	<i>alternata</i>	Regina, Saskatchewan
TOM2	<i>Solanum lycopersicum</i>	<i>A. tenuissima</i>	<i>alternata</i>	London, Ontario
TOMSTEM3a	<i>Solanum lycopersicum</i>	<i>A. arborescens</i>	<i>alternata</i>	London, Ontario
KAS5428*	<i>Solanum lycopersicum</i>	No assignment		London, Ontario
TOMSTEM3c	<i>Solanum lycopersicum</i>	<i>A. arborescens</i>	<i>alternata</i>	London, Ontario
TOMSTEM3d	<i>Solanum lycopersicum</i>	<i>A. tenuissima</i>	<i>alternata</i>	London, Ontario
BBJS14b	<i>Vaccinium</i> sp.	<i>A. tenuissima</i>		Vineland, Ontario
JSP4AR5*	<i>Vitis vinifera</i>	<i>A. arborescens</i>		Vineland, Ontario
NS1	<i>Vitis vinifera</i>	<i>A. arborescens</i>		Nova Scotia
NSFoch2	<i>Vitis vinifera</i>	<i>A. tenuissima</i>		Nova Scotia
MBBC37c	<i>Vaccinium angustifolium</i>	<i>A. alternata</i>	<i>alternata</i>	Mt. Thom, Nova Scotia
RJS1-2a	<i>Rubus</i> sp.	<i>A. arborescens</i>	<i>alternata</i>	Vineland, Ontario
RJS2-2c	<i>Rubus</i> sp.	<i>A. arborescens</i>	<i>A. arborescens</i> species complex	Vineland, Ontario
RJS1-4a	<i>Rubus</i> sp.	<i>A. arborescens</i>	<i>A. arborescens</i> species complex	Vineland, Ontario
KAS5521	<i>Hordeum vulgare</i> L. (Canada Eastern)	<i>A. arborescens</i>	<i>A. arborescens</i> species complex	P.E.I
KAS5520	<i>Secale cereale</i> (Canada Eastern)	<i>A. tenuissima</i>		Quebec
KAS5519	<i>Secale cereale</i> (Canada Eastern)	<i>A. tenuissima</i>	<i>alternata</i>	Quebec
KAS5518	<i>Secale cereale</i> (Canada Eastern)	<i>A. tenuissima</i>		Quebec
KAS5517	<i>Secale cereale</i> (Canada Eastern)	<i>A. arborescens</i>	<i>alternata</i>	Quebec
KAS5516	<i>Secale cereale</i> (Canada Eastern)	<i>A. arborescens</i>	<i>alternata</i>	Quebec
KAS5515	<i>Secale cereale</i> (Canada Eastern)	<i>A. alternata</i>	<i>alternata</i>	Quebec
KAS5514	<i>Secale cereale</i> (Canada Eastern)	<i>A. alternata</i>		Quebec
KAS5513	<i>Avena sativa</i> (Canada Western)	<i>A. arborescens</i>	<i>alternata</i>	Edmonton, Alberta
KAS5512	<i>Triticum</i> spp. (Amber Durum)	<i>A. alternata</i>	<i>alternata</i>	Beechy, Saskatchewan
KAS5511	<i>Triticum</i> spp. (Amber Durum)	<i>A. arborescens</i>		Beechy, Saskatchewan
KAS5510	<i>Triticum</i> spp. (Amber Durum)	<i>A. tenuissima</i>		Beechy, Saskatchewan
KAS5509	<i>Triticum</i> spp. (Amber Durum)	<i>A. tenuissima</i>	<i>alternata</i>	Beechy, Saskatchewan

KAS5508	<i>Triticum</i> spp. (Amber Durum)	<i>A. tenuissima</i>		Beechy, Saskatchewan
KAS5507	<i>Brassica napus</i> (Canada Western Canola)	<i>A. infectoria</i>		Western Canada
KAS5506	<i>Brassica napus</i> (Canada Western Canola)	<i>A. infectoria</i>	<i>infectoria</i>	Western Canada
KAS5505	<i>Brassica napus</i> (Canada Western Canola)	<i>A. infectoria</i>		Western Canada
KAS5504	<i>Triticum</i> spp. (Canadian Eastern Red Winter)	<i>A. arborescens</i>		Western Canada
KAS5503	<i>Triticum</i> spp. (Canadian Eastern Red Winter)	<i>A. arborescens</i>		Western Canada
KAS5502	<i>Triticum</i> spp. (Canadian Eastern Red Winter)	<i>A. infectoria</i>		Western Canada
KAS5501	<i>Triticum</i> spp. (Canadian Eastern Red Winter)	<i>A. infectoria</i>		Western Canada
KAS5500	<i>Triticum</i> spp. (Canadian Eastern Red Winter)	<i>A. arborescens</i>		Western Canada
KAS5499	<i>Brassica napus</i> (Canada Western Canola)	<i>A. arborescens</i>	<i>alternata</i>	Western Canada
KAS5498	<i>Brassica napus</i> (Canada Western Canola)	<i>A. infectoria</i>		Western Canada
KAS5497	<i>Brassica napus</i> (Canada Western Canola)	<i>A. tenuissima</i>	<i>alternata</i>	Western Canada
KAS5496	<i>Hordeum vulgare</i> L. (Canada Western)	<i>A. tenuissima</i>		Western Canada
KAS5495	<i>Hordeum vulgare</i> L. (Canada Western)	<i>A. tenuissima</i>		Western Canada
KAS5494*	<i>Hordeum vulgare</i> L. (Canada Western)	<i>A. arborescens</i>		Western Canada
KAS5493	<i>Hordeum vulgare</i> L. (Canada Western)	<i>A. tenuissima</i>	<i>alternata</i>	Western Canada
KAS5492	<i>Hordeum vulgare</i> L. (Canada Western)	<i>A. arborescens</i>	<i>alternata</i>	Western Canada
KAS5491	<i>Hordeum vulgare</i> L. (Canada Western)	<i>A. tenuissima</i>		Western Canada
KAS5490	<i>Hordeum vulgare</i> L. (Canada Western)	<i>A. infectoria</i>		Western Canada
KAS5489	<i>Hordeum vulgare</i> L. (Canada Western)	<i>A. tenuissima</i>	<i>alternata</i>	Western Canada
KAS5488	<i>Triticum</i> spp. (Canada Western Amber Durum)	<i>A. infectoria</i>	<i>infectoria</i>	Western Canada
KAS5487	<i>Triticum</i> spp. (Canada Western Amber Durum)	<i>A. alternata</i>		Western Canada
KAS5486	<i>Triticum</i> spp. (Canada Western Amber Durum)	<i>A. infectoria</i>	<i>infectoria</i>	Western Canada
KAS5485	<i>Triticum</i> spp. (Canada Western Amber Durum)	<i>A. arborescens</i>	<i>infectoria</i>	Western Canada
KAS5484	<i>Triticum</i> spp. (Canada Western Amber Durum)	<i>A. arborescens</i>		Western Canada
KAS5483	<i>Triticum</i> spp. (Canada Western Amber Durum)	<i>A. infectoria</i>		Western Canada
KAS5482	<i>Triticum</i> spp. (Canada Western Amber Durum)	<i>A. infectoria</i>		Western Canada
KAS5481	<i>Triticum</i> spp. (Canada Western Amber Durum)	<i>A. tenuissima</i>	<i>alternata</i>	Western Canada
KAS5480	<i>Triticum</i> spp. (Red)	<i>A. infectoria</i>		Western Canada
KAS5479	<i>Triticum</i> spp. (Red)	<i>A. tenuissima</i>		Western Canada
KAS5478	<i>Triticum</i> spp. (Red)	<i>A. tenuissima</i>		Western Canada
KAS5477	<i>Triticum</i> spp. (Red)	<i>A. infectoria</i>	<i>infectoria</i>	Western Canada
KAS5476	<i>Triticum</i> spp. (Canada Western Amber Durum)	<i>A. infectoria</i>		Western Canada
KAS5475	<i>Triticum</i> spp. (Canada Western Amber Durum)	<i>A. infectoria</i>		Western Canada
KAS5474	<i>Triticum</i> spp. (Canada Western Amber Durum)	<i>A. infectoria</i>	<i>infectoria</i>	Western Canada
KAS5473	<i>Triticum</i> spp. (Canada Western Red Winter)	<i>A. infectoria</i>		Western Canada
KAS5472	<i>Triticum</i> spp. (Canada Western Red Winter)	<i>A. infectoria</i>		Western Canada
KAS5471	<i>Triticum</i> spp. (Canada Western Red Winter)	<i>A. arborescens</i>		Western Canada
KAS5470	<i>Triticum</i> spp. (Canada Western Red Winter)	<i>A. infectoria</i>	<i>infectoria</i>	Western Canada
KAS5469	<i>Triticum</i> spp. (Canada Western Red Winter)	<i>A. infectoria</i>		Western Canada
KAS5468	<i>Triticum</i> spp. (Canada Western Red Winter)	<i>A. tenuissima</i>	<i>alternata</i>	Western Canada
KAS5467	<i>Triticum</i> spp. (Canada Western Red Winter)	<i>A. infectoria</i>		Western Canada
KAS5466	<i>Triticum</i> spp. (Canada Western Prairie Spring Red)	<i>A. alternata</i>		Western Canada
KAS5465	<i>Triticum</i> spp. (Canada Western Prairie Spring Red)	<i>A. arborescens</i>		Western Canada
KAS5464*	<i>Triticum</i> spp. (Canada Western Prairie Spring Red)	<i>A. arborescens</i>	<i>alternata</i>	Western Canada

KAS5463	<i>Triticum</i> spp. (Canada Western Prairie Spring Red)	<i>A. infectoria</i>		Western Canada
KAS5462	<i>Hordeum vulgare</i> L. (Canada Western)	<i>A. arborescens</i>		Western Canada
KAS5461	<i>Hordeum vulgare</i> L. (Canada Western)	<i>A. tenuissima</i>		Western Canada
KAS5460	<i>Hordeum vulgare</i> L. (Canada Western)	<i>A. arborescens</i>		Western Canada
KAS5459	<i>Hordeum vulgare</i> L. (Canada Western)	<i>A. arborescens</i>		Western Canada
KAS5458	<i>Hordeum vulgare</i> L. (Canada Western)	<i>A. alternata</i>		Western Canada
KAS5457	<i>Hordeum vulgare</i> L. (Canada Western)	<i>A. arborescens</i>		Western Canada
KAS5456	<i>Hordeum vulgare</i> L. (Canada Western)	<i>A. alternata</i>	<i>alternata</i>	Western Canada
KAS5455	<i>Triticum</i> spp. (Canada Western Hard Red Spring)	<i>A. infectoria</i>		Western Canada
KAS5454	<i>Triticum</i> spp. (Canada Western Hard Red Spring)	<i>A. alternata</i>		Western Canada
KAS5453	<i>Avena sativa</i> (Canada Western)	<i>A. arborescens</i>		Edmonton, Alberta
KAS5452	<i>Avena sativa</i> (Canada Western)	<i>A. alternata</i>		Edmonton, Alberta
KAS5451	<i>Avena sativa</i> (Canada Western)	<i>A. arborescens</i>	<i>alternata</i>	Edmonton, Alberta
KAS5450	<i>Triticum</i> spp. (Canada Western Amber Durum)	<i>A. tenuissima</i>	<i>alternata</i>	Corrine, Saskatchewan
KAS5449	<i>Triticum</i> spp. (Canada Western Amber Durum)	<i>A. infectoria</i>	<i>infectoria</i>	Corrine, Saskatchewan
KAS5448	<i>Triticum</i> spp. (Canada Western Amber Durum)	<i>A. tenuissima</i>	<i>alternata</i>	Corrine, Saskatchewan
KAS5447	<i>Triticum</i> spp. (Canada Western Red Winter)	<i>A. infectoria</i>		Killam, Alberta
KAS5446	<i>Triticum</i> spp. (Canada Western Red Winter)	<i>A. infectoria</i>	<i>infectoria</i>	Dunmore, Alberta
KAS5445*	<i>Triticum</i> spp.	<i>A. alternata</i>		Western Canada
KAS5444	<i>Triticum</i> spp.	<i>A. tenuissima</i>		Western Canada
KAS5443	<i>Triticum</i> spp.	<i>A. alternata</i>	<i>alternata</i>	Western Canada

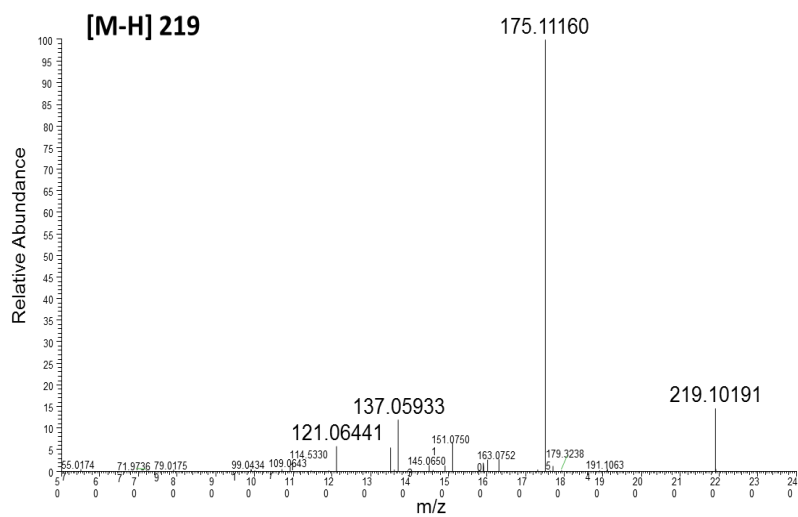
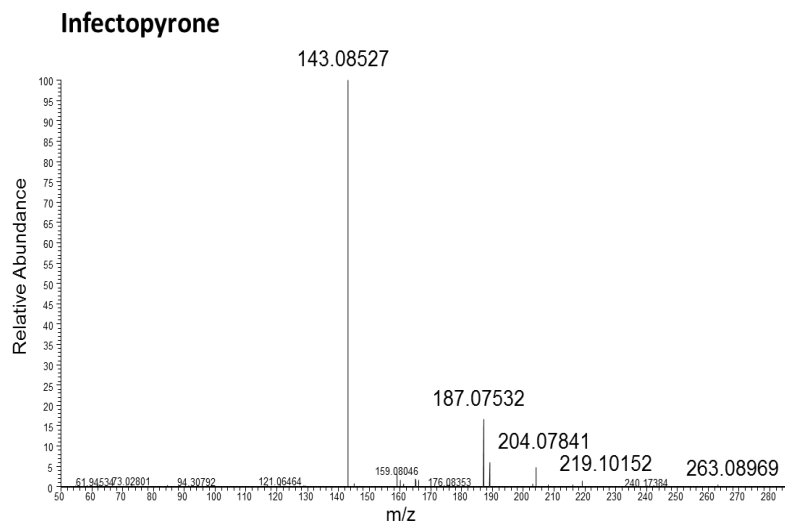


Figure 1S- ddMS² transitions of infectopyrone and 219 obtained in negative ionization mode

Appendix A2- Chapter 3 Supplementary

Table S2- List of unknown sulfoconjugated metabolites detected from the 148 *Alternaria* sp. studied showing the retention time (RT, mins) and m/z for the sulfoconjugated and corresponding free metabolites.

Metabolite	Free		Sulfoconjugated	
	RT	m/z [M-H] ⁻	RT	m/z [M-H] ⁻
C ₃₀ H ₂₂ O ₁₂	3.09	573.10278	2.89	653.05957
C ₂₇ H ₃₆ O ₆	4.97	455.24646	4.93	535.20313
C ₂₄ H ₃₅ NO ₆	4.16	432.23849	3.84	512.19440
C ₂₃ H ₃₈ O ₇	4.20	425.25400	4.00	505.20999
C ₂₄ H ₃₃ NO ₅	4.27	414.22806	4.00	494.18466
C ₂₄ H ₃₁ NO ₄	4.12	396.21790	4.52	476.17401
C ₂₄ H ₄₈ O ₃	5.49	383.35315	4.95	463.30936
C ₂₂ H ₄₄ O ₄	4.28	371.31592	4.60	451.27261
C ₂₂ H ₄₄ O ₃	5.13	355.32114	4.55	435.27768
C ₂₂ H ₄₂ O ₃	4.65	353.30539	4.73	433.26202
C ₂₁ H ₃₂ O ₄	4.14	347.22214	3.73	427.17902
C ₂₁ H ₃₀ O ₄	3.80	345.20657	3.31	425.16351
C ₂₀ H ₄₀ O ₃	5.47	327.28998	4.65	407.24637
C ₁₈ H ₃₆ O ₄	4.32	315.25461	4.02	395.21051
C ₁₈ H ₃₄ O ₄	3.74	313.23792	3.48	393.19431
C ₁₅ H ₁₂ O ₇	3.15	303.05045	3.63	383.00659
C ₁₈ H ₃₆ O ₃	5.09	299.25861	4.25	379.21527
C ₁₈ H ₃₄ O ₃	4.93	297.24301	4.12	377.20001
C ₁₅ H ₁₈ O ₆	3.26	293.10248	3.03	373.05930
C ₁₄ H ₁₄ O ₆	2.99	277.07074	2.91	357.02848
C ₁₅ H ₁₀ O ₄	3.26	253.05006	2.87	333.00731
C ₁₃ H ₁₂ O ₅	2.73	247.06038	2.57	327.01697
C ₁₄ H ₁₄ O ₄	3.24	245.08100	3.08	325.03809
C ₁₂ H ₁₀ O ₅	2.78	233.04471	2.52	313.00192
C ₁₃ H ₁₂ O ₄	3.06	231.06534	2.70	311.02258
C ₁₁ H ₁₀ O ₄	2.84	205.04947	2.66	285.00699
C ₁₀ H ₁₄ NO ₃	3.50	196.09676	2.75	276.05429
C ₁₀ H ₁₀ O ₄	2.70	193.04956	2.48	273.00748
C ₁₁ H ₁₀ O ₃	3.22	189.05452	2.78	269.01218
C ₉ H ₁₀ O ₃	2.98	165.05437	2.64	245.01186

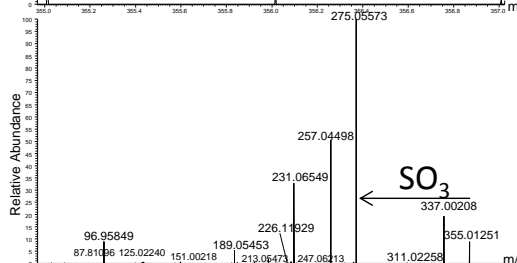
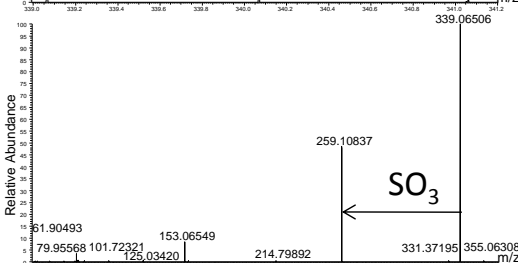
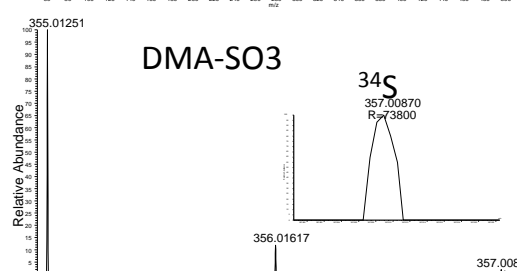
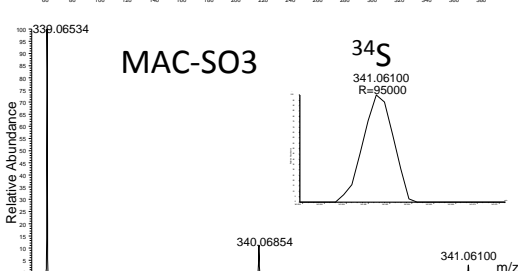
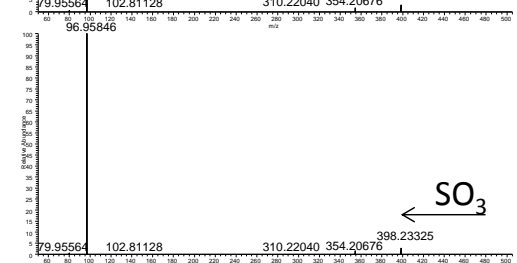
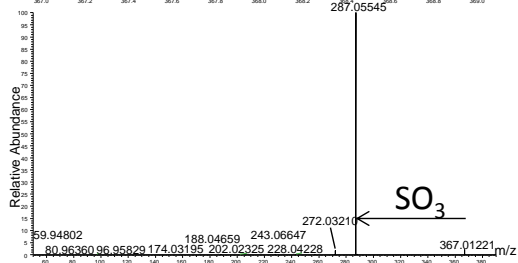
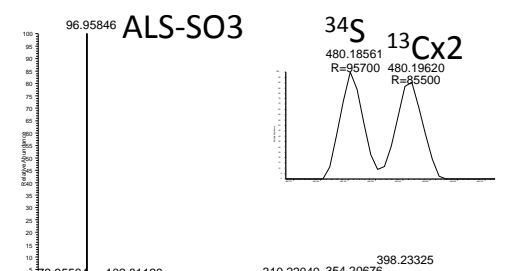
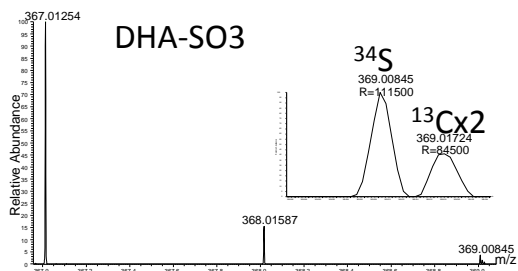
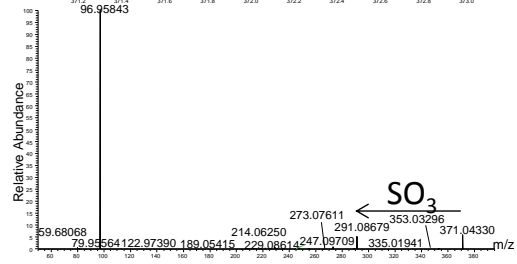
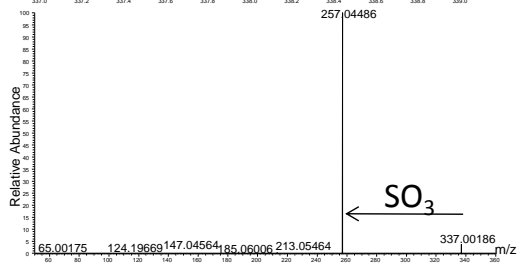
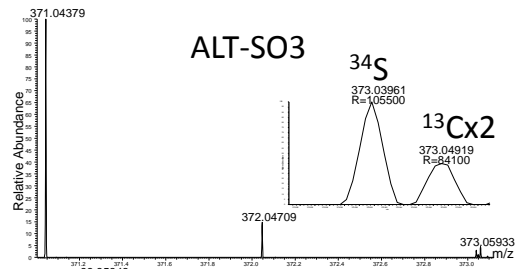
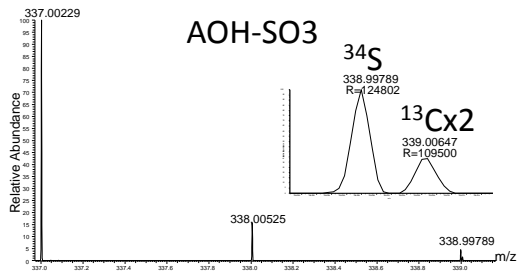


Figure 2S: HRMS data showing the ^{34}S isotope pattern along with the MS^2 data for the known sulfoconjugated AOH and five new sulfoconjugated metabolites (ALS, MAC, ALT, DHA and DMA).

Table 3S- *Fusarium* species used for enniatin analysis using product ion filtering

Culture code	Confirmed as	DAOMC Number
KAS 1907	<i>F. avenaceum</i>	
KAS 1914	<i>F. avenaceum</i>	
KAS 2925	<i>F. avenaceum</i>	235695
KAS 2926	<i>F. avenaceum</i>	235696
KAS 2927	<i>F. avenaceum</i>	235697
KAS 1912	<i>F. acuminatum</i>	
KAS 2903	<i>F. subglutinans</i>	235673

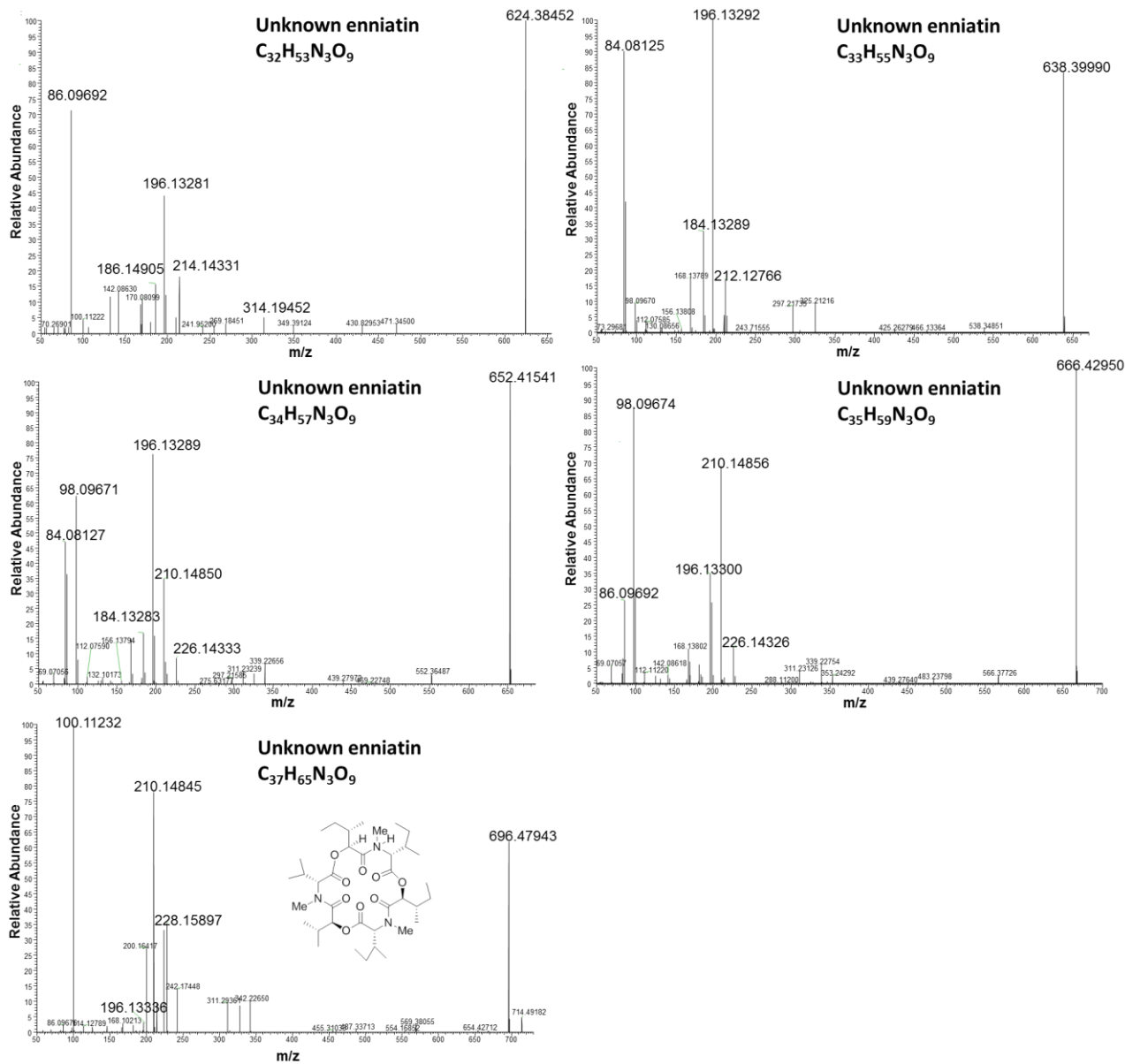


Figure 3S- MS² spectra for the unknown enniatins detected in *F. avenaceum* liquid culture extracts using product ion filtering of the 196 fragment ion. A predicted structure is provided for unknown 696 enniatin based on the observed fragments

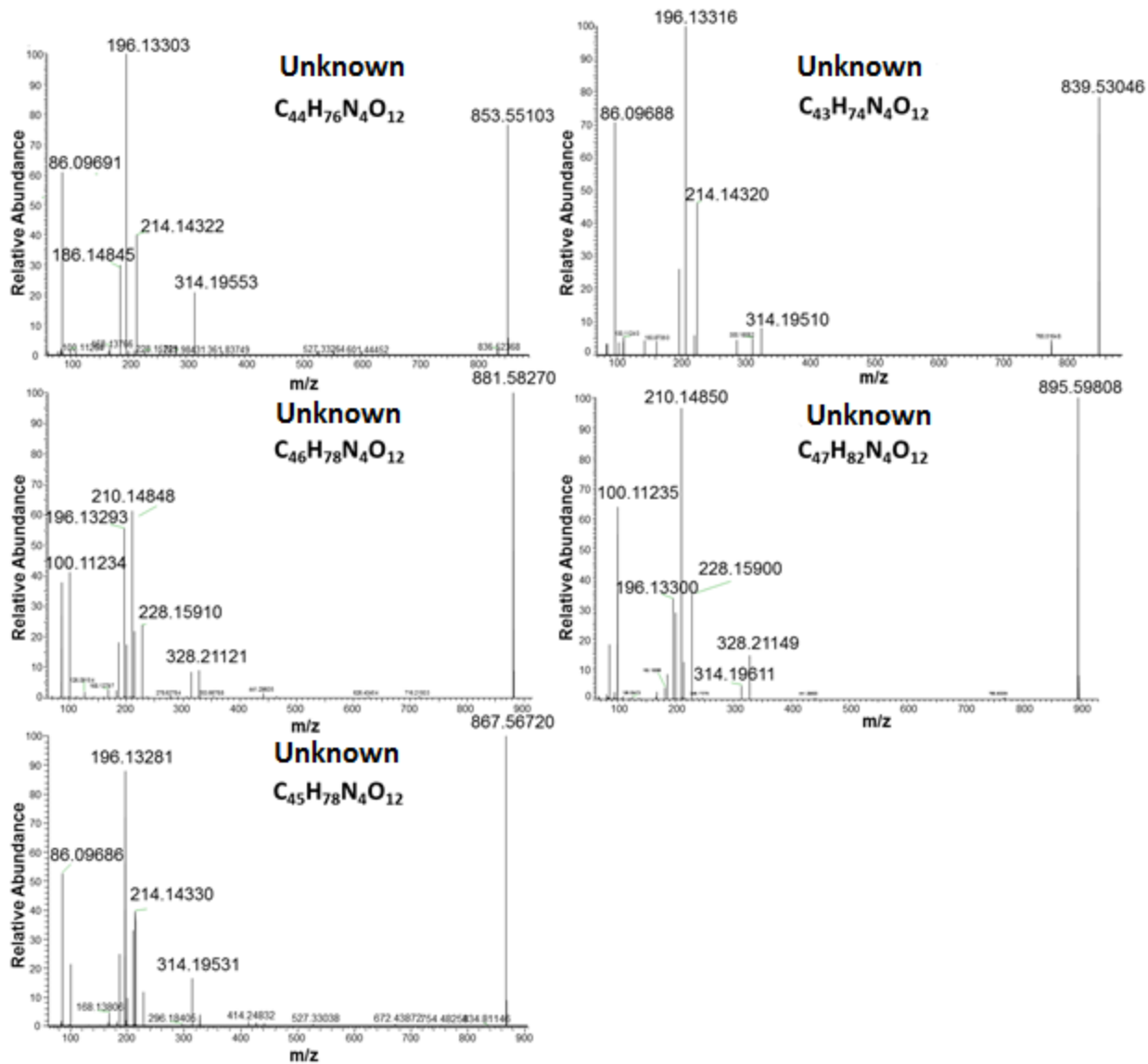


Figure 4S- MS² spectra for the unknown cyclodepsipeptides detected by product ion filtering of the 196 fragment ion

Appendix A3- Chapter 4 Supplementary

Table 4S- Primer sequences used in PCR of isolated fungal cultures from contaminated silage

Primer	Sequence (5' to 3')
ITS1	TCCGTAGGTGAACCTGCGG
ITS4	TCCTCCGCTTATTGATATGC
βtub2a	GGTAACCAAATCGGTGCTGCTTTC
βtub2b	ACCCTCAGTGTAGTGACCCTTGGC
AnF	GGATTTCGACAGCATTTCAGAACG
AnR	GATAAAACCATTGTTGTCGCGGTCG
AwF	GGGATTTCGACAGCATTTCAGAAATT
AwR	GATAAAACCATTGTTGTCGCGGTCA

Table 5S- Primer sequences used for ascomycetes and bacteria in next-generation sequencing of total silage DNA

Sample set	Sample name	Forward primer	Forward barcode	Reverse primer	Reverse barcode
Ascomycete	1-A	28S200A_1F	ataacgaa	28S476A_1R	aagatggt
Ascomycete	2-A	28S200A_1F	ataacgaa	28S476A_2R	gaggagat
Ascomycete	3-A	28S200A_1F	ataacgaa	28S476A_3R	tccgttcg
Ascomycete	4-A	28S200A_1F	ataacgaa	28S476A_4R	cattaagg
Ascomycete	5-A	28S200A_1F	ataacgaa	28S476A_17R	ctagtcac
Ascomycete	6-A	28S200A_1F	ataacgaa	28S476A_18R	gtcttcct
Ascomycete	7-A	28S200A_2F	cattaagg	28S476A_1R	aagatggt
Ascomycete	8-A	28S200A_2F	cattaagg	28S476A_2R	gaggagat
Ascomycete	9-A	28S200A_2F	cattaagg	28S476A_3R	tccgttcg
Ascomycete	10-A	28S200A_2F	cattaagg	28S476A_4R	cattaagg
Ascomycete	11-A	28S200A_2F	cattaagg	28S476A_17R	ctagtcac
Ascomycete	12-A	28S200A_2F	cattaagg	28S476A_18R	gtcttcct
Ascomycete	13-A	28S200A_3F	tggcggct	28S476A_1R	aagatggt
Ascomycete	14-A	28S200A_3F	tggcggct	28S476A_2R	gaggagat
Ascomycete	15-A	28S200A_3F	tggcggct	28S476A_3R	tccgttcg
Ascomycete	16-A	28S200A_3F	tggcggct	28S476A_4R	cattaagg
Ascomycete	17-A	28S200A_3F	tggcggct	28S476A_17R	ctagtcac
Ascomycete	18-A	28S200A_3F	tggcggct	28S476A_18R	gtcttcct
Ascomycete	19-A	28S200A_4F	gtaagcgc	28S476A_1R	aagatggt
Ascomycete	20-A	28S200A_4F	gtaagcgc	28S476A_2R	gaggagat
Ascomycete	21-A	28S200A_4F	gtaagcgc	28S476A_3R	tccgttcg

Ascomycete	22-A	28S200A_4F	gtaagcgc	28S476A_4R	cattaagg
Ascomycete	23-A	28S200A_4F	gtaagcgc	28S476A_17R	ctagtcac
Ascomycete	25-A	28S200A_5F	tccgccaa	28S476A_1R	aagatggt
Ascomycete	26-A	28S200A_5F	tccgccaa	28S476A_2R	gaggagat
Ascomycete	27-A	28S200A_5F	tccgccaa	28S476A_3R	tccgttcg
Bacteria	1-V	u518_7F	cc aag gcc	806R_5R	agttaacc
Bacteria	2-V	u518_7F	cc aag gcc	806R_6R	ccaaggcc
Bacteria	3-V	u518_7F	cc aag gcc	806R_7R	ataacgaa
Bacteria	4-V	u518_7F	cc aag gcc	806R_8R	tgacttca
Bacteria	5-V	u518_7F	cc aag gcc	806R_9R	agccacac
Bacteria	6-V	u518_7F	cc aag gcc	806R_10R	caggctta
Bacteria	7-V	u518_7F	cc aag gcc	806R_11R	cttctggg
Bacteria	8-V	u518_7F	cc aag gcc	806R_12R	gactaatc
Bacteria	9-V	u518_7F	cc aag gcc	806R_13R	gcttgatg
Bacteria	10-V	u518_7F	cc aag gcc	806R_14R	tgccggct
Bacteria	11-V	u518_7F	cc aag gcc	806R_15R	gtaagcgc
Bacteria	12-V	u518_7F	cc aag gcc	806R_16R	tccgccaa
Bacteria	13-V	u518_8F	aa gat ggt	806R_5R	agttaacc
Bacteria	14-V	u518_8F	aa gat ggt	806R_6R	ccaaggcc
Bacteria	15-V	u518_8F	aa gat ggt	806R_7R	ataacgaa
Bacteria	16-V	u518_8F	aa gat ggt	806R_8R	tgacttca
Bacteria	17-V	u518_8F	aa gat ggt	806R_9R	agccacac
Bacteria	18-V	u518_8F	aa gat ggt	806R_10R	caggctta
Bacteria	19-V	u518_8F	aa gat ggt	806R_11R	cttctggg
Bacteria	20-V	u518_8F	aa gat ggt	806R_12R	gactaatc
Bacteria	21-V	u518_8F	aa gat ggt	806R_13R	gcttgatg
Bacteria	22-V	u518_8F	aa gat ggt	806R_14R	tgccggct
Bacteria	23-V	u518_8F	aa gat ggt	806R_15R	gtaagcgc
Bacteria	25-V	u518_9F	ag tta acc	806R_5R	agttaacc
Bacteria	26-V	u518_9F	ag tta acc	806R_6R	ccaaggcc
Bacteria	27-V	u518_9F	ag tta acc	806R_7R	ataacgaa

Table 6S- Fungal secondary metabolite standards in the DIA digital archive

Metabolite	Molecular formula	Precursor m/z [M+H]	Metabolite	Molecular formula	Precursor m/z [M+H]
Mellein	C ₁₀ H ₁₀ O ₃	179.07025	Traversianal	C ₂₀ H ₂₈ O ₃	317.21110
stipitatic acid	C ₈ H ₆ O ₅	183.02878	Zearalenone	C ₁₈ H ₂₂ O ₅	319.15398
5-hydroxy culmorin	C ₁₅ H ₂₄ O ₂	237.18491	Sterigmatocystin	C ₁₈ H ₁₂ O ₆	325.07065
Viridicatin	C ₁₅ H ₁₁ NO ₂	238.08624	Aflatoxin G1	C ₁₇ H ₁₂ O ₇	329.06556
Culmorin	C ₁₅ H ₂₆ O ₂	239.20054	Aflatoxin M1	C ₁₇ H ₁₂ O ₇	329.06556
Citrinin	C ₁₃ H ₁₄ O ₅	251.09138	Aflatoxin G2	C ₁₇ H ₁₄ O ₇	331.08121
Frequintin	C ₁₄ H ₂₀ O ₄	253.14342	Altersolanol A	C ₁₆ H ₁₆ O ₈	337.09178
Walleminone	C ₁₄ H ₁₆ N ₂ O ₂	253.17982	Bostrycin	C ₁₆ H ₁₆ O ₈	337.09178
Alternariol	C ₁₄ H ₁₀ O ₅	259.06008	α -cyclopiazonic acid	C ₂₀ H ₂₀ N ₂ O ₃	337.15465
Cryptosporiopsin	C ₁₀ H ₁₀ Cl ₂ O ₄	265.00287	15-acetylDON	C ₁₇ H ₂₂ O ₇	339.14381
Verrucarol	C ₁₅ H ₂₂ O ₄	267.15907	3-acetylDON	C ₁₇ H ₂₂ O ₇	339.14381
Emodin	C ₁₅ H ₁₀ O ₅	271.06008	4',5'-bisdeoxy-dothistromin	C ₁₈ H ₁₂ O ₇	341.06556
Helminthosporin	C ₁₅ H ₁₀ O ₅	271.06008	Penicillin V	C ₁₆ H ₁₈ N ₂ O ₅ S	351.10090
Alternariol methyl ether	C ₁₅ H ₁₂ O ₅	273.07573	Griseofulvin	C ₁₇ H ₁₇ ClO ₆	353.07863
Koninginin E	C ₁₆ H ₂₆ O ₄	283.06117	Fusarenon-X	C ₁₇ H ₂₂ O ₈	355.13873
Macrosporin	C ₁₆ H ₁₂ O ₅	285.07573	4'-deoxydothistronin	C ₁₈ H ₁₀ O ₈	357.06048
Koninginin A	C ₁₆ H ₂₈ O ₄	285.20602	Brevianamide A	C ₂₁ H ₂₃ N ₅ O ₃	366.18120
Altenuene	C ₁₅ H ₁₆ O ₆	293.10195	Diacetoxyscirpenol	C ₁₉ H ₂₆ O ₇	367.17511
Phacidin	C ₁₆ H ₂₂ O ₅	295.15398	Averufin	C ₂₀ H ₁₆ O ₇	369.09686
Deoxynivalenol	C ₁₅ H ₂₀ O ₆	297.13325	Alantrypinone	C ₂₁ H ₁₆ N ₄ O ₃	373.12950
T-2 tetraol	C ₁₅ H ₂₂ O ₆	299.14890	Isomarticin	C ₁₈ H ₁₆ O ₉	377.08669
Fusarubin	C ₁₅ H ₁₄ O ₇	307.08121	3,15-aDON	C ₁₉ H ₂₄ O ₈	381.15438
Aflatoxin B1	C ₁₇ H ₁₂ O ₆	313.07065	Roquefortine C	C ₂₂ H ₂₃ N ₅ O ₂	390.19243
Nivalenol	C ₁₅ H ₂₀ O ₇	313.12816	Ochratoxin A	C ₂₀ H ₁₈ ClNO ₆	404.08952
Pyrenopherol	C ₁₆ H ₂₄ O ₆	313.16456	Neosolaniol	C ₁₉ H ₂₆ O ₈	405.14972
Aflatoxin B2	C ₁₇ H ₁₄ O ₆	315.08630	3,7,15-triacetyl-DON	C ₂₁ H ₂₆ O ₉	423.16494
HT-2 Toxin	C ₂₂ H ₃₂ O ₈	425.21698	Satratoxin H	C ₂₉ H ₃₆ O ₉	545.23811
Chaetoviridin A	C ₂₃ H ₂₅ ClO ₆	433.14123	Roridin A	C ₂₉ H ₄₀ O ₉	555.25366

Meleagrín	$C_{23}H_{23}N_5O_4$	434.18226	Ergocorninine	$C_{31}H_{39}N_5O_5$	562.30238
Kotanin	$C_{24}H_{22}O_8$	439.13874	Satratoxin F	$C_{29}H_{34}O_{10}$	565.20297
Trichoverrol A	$C_{23}H_{32}O_7$	443.20169	Satratoxin G	$C_{29}H_{36}O_{10}$	567.21753
Atranone B	$C_{25}H_{34}O_7$	447.23771	Ergocryptinine	$C_{32}H_{41}N_5O_5$	576.31803
DON-glucoside I	$C_{21}H_{30}O_{11}$	481.16586	Ergocristinine	$C_{35}H_{39}N_5O_5$	610.30238
Verrucarín J	$C_{27}H_{32}O_8$	485.21698	Penitrem A	$C_{37}H_{44}ClNO_6$	634.29298
T-2 Toxin	$C_{24}H_{34}O_9$	489.20700	Enniatin B	$C_{33}H_{57}N_3O_9$	640.41674
AAL toxin TB	$C_{25}H_{47}NO_9$	506.33234	Enniatin B1	$C_{34}H_{59}N_3O_9$	676.41034
Marticin	$C_{18}H_{16}O_9$	515.26393	Fumonisin B3	$C_{34}H_{59}NO_{13}$	690.40590
AAL toxin TA	$C_{25}H_{47}NO_{10}$	522.32726	Enniatin A1	$C_{35}H_{61}N_3O_9$	690.43000
Chaetoglobulosin A	$C_{32}H_{36}N_2O_5$	529.26968	Fumonisin B2	$C_{34}H_{59}NO_{14}$	706.40082
Chaetoglobulosin C	$C_{32}H_{36}N_2O_5$	529.26968	Fumonisin B1	$C_{34}H_{59}NO_{15}$	722.39573
Cercosporin	$C_{29}H_{26}O_{10}$	535.15987	Beauvericin	$C_{45}H_{57}N_3O_9$	806.39368
iso-Roridine E	$C_{29}H_{38}O_8$	537.24323	Stachyocin B	$C_{52}H_{70}N_2O_{11}$	899.50522
Rugulosin	$C_{30}H_{22}O_{10}$	543.12856	Stachyocin C	$C_{52}H_{70}N_2O_{11}$	899.50522

Table 7S- Fungal species isolated from each of the 26 Canadian sites

Site	<i>Aspergillus fumigatus</i>	<i>Aspergillus nidulans</i>	<i>Aspergillus welwitschiae</i>	<i>Aspergillus glaucus</i>	<i>Chaetomium globosum</i>	<i>Cladosporium sp.</i>	<i>Fusarium sp.</i>	<i>Geotrichum sp.</i>	<i>Gliocladium roseum</i>	<i>Irpex lacteus</i>	<i>Leptosphaeria</i>	<i>Monascus ruber</i>	<i>Mucor circinelloides</i>	<i>Penicillium atrovenetum</i>	<i>Myceliophthora lutea</i>	<i>Penicillium aurantiogriseum</i>	<i>Penicillium crustosum</i>	<i>Penicillium flavigeum</i>	<i>Penicillium griseofulvum</i>	<i>Penicillium nordicum</i>	<i>Penicillium paneum</i>	<i>Penicillium roqueforti</i>	<i>Penicillium rugulosum</i>	<i>Penicillium simplicissimum</i>	<i>Penicillium viridicatum</i>	<i>Pseudallescheria boydii</i>
1																										
2																										
3																										
4																										
5																										
6																										
7																										
8																										
9																										
10																										
11																										
12																										
13																										
14																										
15																										
16																										
17																										
18																										
19																										
20																										
21																										
22																										
23																										
25																										
26																										
27																										

Table 8S- Mycotoxins and secondary metabolites currently monitored by the Canadian Food Inspection Agency (CFIA) in food and feed sold in Canada[218]. Recommended guidance values are reported with an asterisk*

Secondary metabolite	Maximum level^[205]	Produced by
Deoxynivalenol (DON)	2 mg/kg in uncleaned soft wheat (humans), 5 mg/kg for cattle and poultry	<i>Fusarium graminearum</i> , <i>F. culmorum</i>
Patulin	50 µg/kg in apple juice, cider or juice blends	<i>Penicillium</i> spp., <i>Aspergillus</i> spp., <i>Byssoschlamys</i> spp.
Aflatoxin	15 µg/kg in nut and nut products (humans), 20 µg/kg animals	<i>Aspergillus flavus</i> , <i>A. parasiticus</i>
HT-2 toxin	0.1 mg/kg for cattle/poultry, 25 µg/kg for dairy animal diets	<i>Fusarium sporotrichioides</i>
Ochratoxin A (OTA)	*5 µg/kg in raw or unprocessed cereal grains (humans), 2 mg/kg swine/poultry feed	<i>Penicillium verrucosum</i> , <i>Aspergillus carbonarius</i> , <i>Aspergillus ochraceus</i>
Diacetoxyscirpenol (DAS)	*2 mg/kg swine feed, 1 mg/kg poultry feed	<i>Fusarium poae</i>
T-2 toxin	*1 mg/kg poultry feed	<i>Fusarium sporotrichioides</i> , <i>F. acuminatum</i>
Zearalenone (ZEN)	*10 mg/kg cow diets (1.5 mg/kg if other toxins present), <5 mg/kg sheep, pigs	<i>Fusarium graminearum</i> , <i>F. culmorum</i> , <i>F. equiseti</i> , <i>F. verticilloides</i>
Ergot alkaloids	*2-3 mg/kg cattle, sheep, horses, 4-6 mg/kg swine, 6-9 mg/kg chicks	<i>Claviceps</i> spp.

Table 9S- 53 unknown secondary metabolites detected in individual plug extracts

[M+H]	Molecular formula	Detected from	Silage
361.20081	C ₂₁ H ₂₈ O ₅	<i>Monascus ruber</i>	X
227.09134	C ₁₁ H ₁₄ O ₅	<i>M. ruber</i>	X
338.26880	C ₂₀ H ₃₅ NO ₃	<i>M. ruber</i>	X
341.35257	C ₂₁ H ₄₄ N ₂ O	<i>M. ruber</i> , <i>P. viridicatum</i> , <i>P. nordicum</i> , <i>P.</i>	X
303.19534	C ₁₉ H ₂₆ O ₃	<i>M. ruber</i>	X
211.14423	C ₁₁ H ₁₈ N ₂ O ₂	<i>M. ruber</i> , <i>P. roqueforti</i>	X
381.42017	C ₂₅ H ₅₄ N ₂	<i>M. ruber</i>	
369.38385	C ₂₃ H ₅₀ N ₂	<i>M. ruber</i> , <i>P. nordicum</i> , <i>P. simplicissimum</i>	
425.44641	C ₂₈ H ₄₀ O ₃	<i>M. ruber</i>	
272.12796	C ₁₆ H ₁₇ NO ₃	<i>M. ruber</i>	
398.19611	C ₂₃ H ₂₇ NO ₅	<i>M. ruber</i>	
437.26627	C ₂₆ H ₃₄ N ₃ O ₃	<i>Penicillium crustosum</i> , <i>P. paneum</i>	
481.29269		<i>P. crustosum</i> , <i>P. flavigenum</i>	
181.08601	C ₁₀ H ₁₂ O ₃	<i>P. crustosum</i>	
397.41534	C ₂₅ H ₅₂ N ₂ O	<i>P. crustosum</i>	
268.10391	C ₁₀ H ₁₃ N ₅ O ₄ ?	<i>P. crustosum</i>	X
313.23477	C ₁₆ H ₃₀ N ₃ O ₃	<i>P. crustosum</i> , <i>P. roqueforti</i>	
367.16541	C ₂₁ H ₂₂ N ₂ O ₄	<i>P. griseofulvum</i>	X
393.14188	C ₁₉ H ₂₃ NO ₈	<i>P. griseofulvum</i>	
198.12779	C ₁₄ H ₁₅ N	<i>P. griseofulvum</i>	
531.25800	C ₂₉ H ₃₈ O ₉	<i>P. paneum</i>	
515.26300	C ₂₉ H ₃₈ O ₈	<i>P. paneum</i>	
569.34503	C ₃₀ H ₄₄ N ₆ O ₅	<i>P. paneum</i>	
413.26862	C ₂₆ H ₃₆ O ₄	<i>P. paneum</i>	
251.20058	C ₁₆ H ₂₆ O ₂	<i>P. paneum</i>	
261.14853	C ₁₆ H ₂₀ O ₃	<i>P. paneum</i>	
425.28738	C ₂₀ H ₃₆ N ₆ O ₄ ?	<i>P. paneum</i> , <i>P. roqueforti</i>	
235.16924	C ₁₅ H ₂₂ O ₂	<i>P. roqueforti</i>	
157.06088	C ₆ H ₈ N ₂ O ₃	<i>P. roqueforti</i>	
471.19910	C ₂₂ H ₂₆ N ₆ O ₆	<i>P. aurantiogriseum</i>	
387.21658	C ₂₃ H ₃₀ O ₅	<i>P. aurantiogriseum</i>	
443.20392	C ₂₅ H ₃₀ O ₇	<i>P. aurantiogriseum</i>	
331.11893	C ₁₉ H ₁₄ N ₄ O ₂	<i>P. aurantiogriseum</i>	
377.16028	C ₂₀ H ₂₄ O ₇	<i>P. nordicum</i>	
267.08356	C ₁₃ H ₁₄ O ₆	<i>P. nordicum</i>	
406.17566	C ₂₃ H ₂₃ N ₃ O ₄	<i>P. nordicum</i>	
471.27109	C ₂₃ H ₃₈ N ₂ O ₈	<i>P. simplicissimum</i>	
241.14317	C ₁₃ H ₂₀ O ₄	<i>P. simplicissimum</i>	
285.28973	C ₁₇ H ₃₆ N ₂ O	<i>P. simplicissimum</i>	
313.32092	C ₁₉ H ₄₀ N ₂ O	<i>P. simplicissimum</i>	
153.05449	C ₈ H ₈ O ₃	<i>P. viridicatum</i>	
490.29016	C ₂₆ H ₃₉ N ₃ O ₆	<i>P. viridicatum</i>	
516.30585	C ₂₈ H ₄₁ N ₃ O ₆	<i>P. viridicatum</i>	

532.29980	C ₂₈ H ₄₁ N ₃ O ₇	<i>P. viridicatum</i>	
493.28030	C ₂₇ H ₄₀ O ₈	<i>P. viridicatum</i>	
558.31665	C ₃₀ H ₄₃ N ₃ O ₇	<i>P. viridicatum</i>	
379.33545	C ₂₃ H ₄₂ N ₂ O ₂	<i>P. viridicatum</i>	
374.23215	C ₂₂ H ₃₁ NO ₄	<i>P. viridicatum</i>	
273.07553	C ₁₅ H ₁₂ O ₅	<i>P. viridicatum</i>	
334.15469	C ₂₀ H ₁₉ N ₃ O ₂	<i>P. viridicatum</i>	
427.24799	C ₂₆ H ₃₄ O ₅	<i>P. flavigenum</i>	
193.08601	C ₁₁ H ₁₂ O ₃	<i>P. flavigenum</i>	
233.11729	C ₁₄ H ₁₆ O ₃	<i>P. flavigenum</i>	

Table 10S- All fungal species detected by NGS

<i>Alternaria alternata</i>	<i>Mucor circinelloides</i>
<i>Ascobolus</i> sp.	<i>Mucor plumbeus/racemosus</i>
<i>Aspergillus pseudoglaucus</i>	<i>Nigrospora</i> sp.
<i>Aspergillus fumigatus</i>	<i>Penicillium simplicissimum</i>
<i>Aspergillus welwitschiae</i>	<i>Penicillium roqueforti</i>
<i>Aspergillus</i> sp.	<i>Penicillium</i> sp.
<i>Botrytis cinerea</i>	<i>Phoma</i> sp.
<i>Candida railenensis</i>	<i>Pichia fermentans</i>
<i>Candida sake</i>	<i>Pichia membranifaciens</i>
<i>Candida</i> sp.	<i>Pithoascus</i> sp.
<i>Chaetomium globosum</i>	<i>Pseudallescheria</i> sp.
<i>Chaetomium</i> sp. 1	<i>Pseudogymnoascus destructans</i>
<i>Chaetomium</i> sp. 2	<i>Saccharomyces castellii</i>
<i>Chrysosporium chiropterorum</i>	<i>Saccharomyces cerevisiae</i>
<i>Cladosporium ramotenellum</i>	<i>Sarocladium strictum</i>
<i>Clonostachys rosea (Gliocladium)</i>	<i>Scedosporium</i> sp.
<i>Cryptococcus victoriae</i>	<i>Schizothecium</i> sp.
<i>Cryotofilobasidium macerans</i>	<i>Scopulariopsis brevicaulis</i>
<i>Debaryomyces hansenii</i>	<i>Scopulariopsis sphaerspora</i>
<i>Doratomyces</i> sp.	<i>Sordaria</i> sp.
<i>Doratomyces</i> sp.1	<i>Sphaerodes fimicola</i>
<i>Doratomyces</i> sp.2	<i>Thelebolus</i> sp.
<i>Fusarium</i> sp.	<i>Thermomyces lanuginosus</i>
<i>Fusarium avenaceum</i>	<i>Trichothecium roseum</i>
<i>Fusarium equiseti</i>	Uncultured fungus
<i>Fusarium graminearum</i>	<i>Veronaea botryosa</i>
<i>Heydenia</i> sp.	<i>Verticillium</i> sp.
<i>Hyphopichia burtonii</i>	<i>Wickerhamomyces anomalus</i>
<i>Kregervanrija fluxuum</i>	
<i>Lichtheimia ramosa</i>	

Monascus ruber
Mortierella sp.
Mrakia blollopis

*Contact author for ID confidences

Megan Kelman
Curriculum Vitae

EDUCATION

M.Sc. Candidate, Physical and Analytical Chemistry September 2014 – September 2016
Western University

Expected defense completion: August, 2016

Coursework completed:

CHEM9658Y- Graduate seminar

CHEM 4404A- Radiation and Nuclear Systems

CHEM 9604B- Radiation Induced Chemistry

B.Sc., Double Major in Chemistry and Environmental Science 2014
Western University

Relevant Coursework:

Organic chemistry, inorganic chemistry, structure elucidation, polymer chemistry, medicinal chemistry, chemistry of the environment, biostatistics, research techniques in environmental science

Advanced Diploma, Science Laboratory Technology 2011
Fanshawe College, Dean's Honor List

TECHNICAL SKILLS AND SOFTWARE EXPERIENCE

- LC-MS and metabolite elucidation and quantification
- DNA extraction, PCR and NGS
- Microscopy and fungal identification
- Microsoft Office: MS Word, MS PowerPoint, MS Excel
- Xcalibur, Mass Lynx
- MzMine
- ChemDraw and WebMO (chemical modeling)
- R, SPSS and Sigma Plot Statistical Software
- Maple (mathematical modeling)

RESEARCH EXPERIENCE

Graduate Research Assistant- Natural Products Chemistry Sept. 2014 – Sept. 2016
Agriculture and Agri-Food Canada (AAFC), London, Ontario

- Isolated and extracted fungal secondary metabolites from tomatoes, cherries, and corn silage for LC-MS analysis
- Performed statistical modelling of fungal metabolomics data through Principal Component Analysis (PCA) and biomarker discovery
- Participated in two European Commission-sponsored proficiency tests for the quantification of *Alternaria* toxins and trichothecenes in agricultural commodities
- Aided in the calibration, quality control, and routine maintenance of the mass spectrometer
- Assisted in the development of mass spectrometry instrument methods, the running of samples, and interpretation of mass spectra for collaborators and other in-house laboratories
- Organized and maintained the growing fungal culture collection

Research Assistant- Natural Products Chemistry June 2011 - May 2014
Agriculture and Agri-Food Canada (AAFC), London, Ontario

- Responsible for creating, organizing, classifying, and maintaining the culture collection of pathogenic and endophytic fungi isolated from blueberry, cranberry, corn, soybean, and grape crops
- Adapted and developed various laboratory procedures relating to chemical extraction methods, fungal isolation, molecular biology, sequencing, and proteomics
- Wrote methodologies for publishing in scientific journals, posters & presentations
- Edited graduate theses and other scientific writing from principal investigators
- Composed and presented PowerPoint presentations to project collaborators
- Maintained equipment, created a chemical inventory, and implemented laboratory quality control protocols
- Established Standard Operating Procedures (SOPs), and laboratory personnel training procedures

Research Assistant- Fungal Ecology May – December 2010
Agriculture and Agri-Food Canada (AAFC) London, Ontario

- Aided in the surveying, and identification of Corky Root Rot tomato fungi
- Assisted in the collection, organization, and interpretation of the data
- Designed various protocols and procedures pertaining to the isolation, culturing, and storing of microorganisms

TEACHING EXPERIENCE

Graduate Teaching Assistant

The University of Western Ontario

Sept. 2014 - April 2015

Sept. 2015 - April 2016

- Ran laboratory sessions for CHEM 2213 and CHEM 2223 (2 sessions weekly, or six hours/week, approximately 30 students per session) (Sept. 2015 – Present)
- Gave weekly experiment pre-laboratory lessons, and demonstrated safe and proper laboratory technique for preparing organic syntheses, various extractions, qualitative testing, and proper hazardous waste disposal
- Ran tutorial sessions for CHEM 1301 and CHEM 1302/1024 (2 sessions weekly, or four hours/week, approximately 100 students per session) (Sept. 2014 – April 2015)
 - Answered student questions regarding assigned problems, and discussed the more difficult problems with the class
 - Encouraged independent thinking and strategies for answering difficult questions
 - Organized and managed student-run study groups at Taylor and Weldon Libraries, which connected small groups of struggling students with competent first year chemistry students

OTHER LABORATORY EXPERIENCE

Teaching Assistant and Laboratory Technologist

Fanshawe College

Sept. - December 2009

- Responsible for timely preparation of media and reagents, and the setup of equipment for student laboratories
- Provided pre-lab safety talks to groups of 15-20 students in introductory biology, (BIO1016) chemistry, (CHEM1003), and microbiology (BIO3001) classes, (~1-2 hours a week)
- Supervised and aided students during the CHEM1003 laboratory session, (3x a week, 2-3 hours a session), performed health and safety inspections, and advised students on appropriate solution disposal
- Held drop-in hours for introductory biology and chemistry courses before and after laboratory sessions for both course work and laboratory write-up assistance, (5-7 hours a week)

- Calibrated and maintained laboratory instruments in good working order, kept laboratory MSDS sheets up to date, and organized a chemical inventory

PUBLICATIONS

Kelman, M.J., Renaud, J.B., Seifert, K.A., Mack, J., Sivagnanam, K., Yeung, K., Sumarah, M.W. Identification of six new *Alternaria* sulfoconjugated metabolites by high resolution neutral loss filtering. *Rapid Commun Mass Sp.* 2015, 29(19), 1805-1810

Renaud, J.B., Kelman, M.J., Qi, T., Seifert, K.A., Sumarah, M.W. Total fumonisin and AAL-toxin detection using high resolution product ion filtering with rapid polarity switching. *Rapid Commun Mass Sp.* 2015, 29(22), 2131-2139

CONFERENCE PARTICIPATION

International Mass Spectrometry Conference (IMSC) August 20-26, 2016
Metro Toronto Convention Centre, Toronto, Ontario

- Presented a poster on ‘Combining data independent acquisition-digital archiving mass spectrometry (DIA-DA-MS) with next-generation sequencing for profiling of fungal contaminated silage’ in the emerging and persistent environmental contaminants session

Gordon Research Conference- Mycotoxins and Phycotoxins June 14-19, 2015
Stonehill College, Easton MA

- Presented a poster entitled: Discovery of six new sulfoconjugated *Alternaria* metabolites by high resolution mass spectrometry with rapid semi-targeted screening based on neutral loss filtering
- Attended daily seminars given by world leaders in mycotoxin research regarding their recent cutting edge unpublished research
- Networked with other graduate students, post-doctoral fellows and researchers for future collaborative projects

Graduate Student Conference on Teaching September 2014
The University of Western Ontario

- Attended various lectures pertaining to the explanation of difficult scientific concepts and abstract ideas to students through various teaching styles

- Developed skills for dealing with difficult or disruptive students via alternative teaching styles, and key methods and strategies for ensuring a successful teaching year

Great Lakes – Saint Lawrence Mycology Workshop

April 2012

The University of Western Ontario

- Attended lectures of AAFC project coordinators, in addition to other lectures from undergraduate, graduate, and faculty members
 - Gained valuable knowledge from the current research presented by renowned mycologists and chemists in natural products chemistry
-